ARTIFICIAL AGING OF CROSSLINKED DOUBLE BASE PROPELLANTS

A THESIS SUBMITTED TO
THE GRADUATE SCHOOL OF NATURAL AND APPLIED SCIENCES
OF
THE MIDDLE EAST TECHNICAL UNIVERSITY

BY

EMRAH BAĞLAR

IN PARTIAL FULFILLMENT OF THE REQUIREMENTS
FOR
THE DEGREE OF MASTER OF SCIENCE
IN
CHEMICAL ENGINEERING

DECEMBER 2010

Approval of the thesis:

ARTIFICIAL AGING OF
CROSSLINKED DOUBLE BASE PROPELLANTS

submitted by **EMRAH BAĞLAR** in partial fulfillment of the requirements for the degree of **Master of Science in Chemical Engineering Department, Middle East Technical University** by,

Prof. Dr. Canan Özgen _____
Dean, Graduate School of **Natural and Applied Sciences**

Prof. Dr. Deniz Üner _____
Head of Department, **Chemical Engineering**

Prof. Dr. H. Önder Özbelge _____
Supervisor, **Chemical Engineering Dept., METU**

Examining Committee Members:

Prof. Dr. Ülkü Yılmazer _____
Chemical Engineering Dept., METU

Prof. Dr. H. Önder Özbelge _____
Chemical Engineering Dept., METU

Prof. Dr. Erdal Bayramlı _____
Chemistry Dept., METU

Prof. Dr. Göknur Bayram _____
Chemical Engineering Dept., METU

Burç Veral, M.Sc. _____
Propellants and Pyrotechnics Division, TÜBİTAK – SAGE

Date: December 22, 2010

I hereby declare that all information in this document has been obtained and presented in accordance with academic rules and ethical conduct. I also declare that, as required by these rules and conduct, I have fully cited and referenced all material and results that are not original to this work.

Name, Last name : Emrah Bağlar

Signature :

ABSTRACT

ARTIFICIAL AGING OF
CROSSLINKED DOUBLE BASE PROPELLANTS

Bağlar, Emrah
M.Sc., Department of Chemical Engineering
Supervisor: Prof. Dr. H. Önder Özbelge

December 2010, 132 pages

In this study, shelf life of three different crosslinked double base (XLDB) propellants stabilized with 2-nitrodiphenylamine (2-NDPA) and n-methyl-4-nitroaniline (MNA) were determined by using the stabilizer depletion method. Depletions of the stabilizers were monitored at different aging temperatures using High Performance Liquid Chromatography (HPLC). Kinetic models of pseudo zero, pseudo first, pseudo second and shifting order were used to find the best model equation that fits the experimental data. The rates of depletion of stabilizers were calculated at 45, 55 and 65°C based on the best fit kinetic models. Using the rate constants at different temperatures, rate constants at room temperature were calculated by Arrhenius equation. The activation energies and frequency factors for the depletion of 2-NDPA and MNA were obtained for all XLDB propellants. Moreover, the results were evaluated based on the NATO standard; STANAG 4117 and the propellants were found stable according to the standard. Vacuum thermal stability (VTS) tests were also conducted to evaluate the stability of XLDB propellants. The propellant that includes the stabilizer mixture of MNA and 2-NDPA was found to have less stability than the propellants that include 2-NDPA

only. However, there were rejection (puking) and migration of stabilizer derivatives for the aged samples of propellants that were stabilized with only 2-NDPA. Moreover, formation of voids and cracks were observed in block propellant samples due to excess gas generation.

Keywords: Crosslinked Double Base Propellants, Aging, Stabilizer Depletion, Vacuum Thermal Stability

ÖZ

ÇAPRAZ BAĞLI ÇİFT BAZLI ROKET YAKITLARININ
YAPAY YAŞLANDIRILMASI

Bağlar, Emrah
Yüksek Lisans, Kimya Mühendisliği Bölümü
Tez Yöneticisi: Prof. Dr. H. Önder Özbelge

Aralık 2010, 132 Sayfa

Bu çalışmada, 2-nitrodifenilamin (2-NDPA) ve n-metil-4-nitroanilin (MNA) kararlılık arttırıcıları kullanılarak üretilen üç farklı çapraz bağlı çift bazlı (XLDB) roket yakıtının raf ömürleri, kararlılık arttırıcı miktarlarındaki azalımın takip edilmesi yöntemiyle belirlenmiştir. Kararlılık arttırıcı miktarlarındaki azalım bütün yaşlandırma sıcaklıkları için Yüksek Performanslı Sıvı Kromatografisi (HPLC) kullanılarak belirlenmiştir. Deneysel verileri en iyi şekilde ifade eden kinetik model denklemleri her yakıt için ayrı ayrı bulunmuştur. Her yakıt için en iyi denklem kullanılarak, kararlılık arttırıcı miktarlarının azalım hızı 45, 55 ve 65°C olmak üzere üç farklı sıcaklıkta hesaplanmıştır. Farklı sıcaklıklarda elde edilen tepkime hızı sabitleri ve Arrhenius denklemi kullanılarak oda sıcaklığındaki tepkime hızı sabiti hesaplanmıştır. Bütün yakıtlarda 2-NDPA ve MNA kararlılık arttırıcılarının azalımı için aktivasyon enerjisi ve sıklık faktörü değerleri hesaplanmıştır. Ek olarak, sonuçlar NATO STANAG 4117 standardı temel alınarak değerlendirilmiştir ve yakıtların kararlı olduğu belirlenmiştir. Yakıtların kararlılıklarını değerlendirmek için vakum ısıl kararlılık (VTS) testleri de yapılmıştır. MNA ve 2-NDPA kararlılık arttırıcılarının ikisini de içeren yakıtın sadece 2-NDPA içeren

diğer iki yakıta göre daha kararsız olduğu saptanmıştır. Ancak, tek başına 2-NDPA içeren yakıtların yaşlandırılmış numuneleri incelendiğinde, kararlılık arttırıcı türevlerinin yakıt matrisinden dışarı atılarak yüzeye çıktığı belirlenmiştir. Ayrıca, büyük bloklar halinde yaşlandırılan yakıtlarda boşluk ve çatlak oluşumu da gözlemlenmiştir.

Anahtar Kelimeler: Çapraz Bağlı Çift Bazlı Roket Yakıtları, Yaşlanma, Kararlılık Arttırıcı, Vakum Isıl Kararlılık

To My Fiancé and My Family

ACKNOWLEDGEMENTS

I would like to express my sincere gratitude to my supervisor Prof. Dr. H. Önder Özbelge for his supervision, support, criticism, encouragements and insight throughout the research.

I would like to thank TÜBİTAK – SAGE, The Scientific and Technical Research Council of Turkey – Defense Industries Research and Development Institute, which enabled me to write this thesis.

I would also like to thank my employers Mr. Ahmet Göçmez and Mr. Burç Veral for giving me the job and for their guidance, advice and help.

The technical assistance of Mr. Serhat Varış, Mr. Volkan Kalender, Mr. H. İbrahim Tekel and Ms. Dilek Çimen are gratefully acknowledged.

Most heartfelt thanks to my parents and my sister for their trust, patience and love. Without them, this thesis would have never been completed.

Above all, I would like to express my deepest thanks to my fiancé, Nur, for her support and tolerance throughout the research and for her endless love.

TABLE OF CONTENTS

LIST OF TABLES

LIST OF FIGURES

FIGURE

LIST OF SYMBOLS

Symbol	Definition	Units
$[A]$	Concentration of Reactant A	wt. %
a	Initial concentration of Reactant A	wt. %
A	Frequency Factor in Arrhenius Equation	$days^{-1}$
E	Initial Modulus	Pa
E	Activation Energy	J/mole
e_b	Elongation at Break Stress	%
e_m	Elongation at Maximum Stress	%
k	Reaction Rate Constant	$days^{-1}$
MW	Molecular Weight	g/mole
R	Gas Constant	J/K·mole
S_b	Stress at Break	Pa
S_m	Maximum Stress	Pa
t	Time	days
T	Temperature	°K
X	Weight Fraction	wt. %

LIST OF ABBREVIATIONS

2-NDPA	2-Nitro diphenylamine
4-NDPA	4-Nitro diphenylamine
AP	Ammonium Perchlorate
BDNPA	Bis-(2,2-Dinitropropyl) Acetal
BDNPA/F	Mixture of BDNPA and BDNPF
BDNPF	Bis-(2,2-Dinitropropyl) Formal
BTTN	Butanetriol Trinitrate
ca	Crosslinking Agent
CMDB	Composite Modified Double Base
d	Diol
DAD	Diode Array Detector
DB	Double Base
di	Diisocyanate
DOA	Dioctyl Adipate
EC	Ethylcentralite
GAP	Glycidyl Azide Polymer
HFC	Heat Flow Calorimetry
HMX	Cyclotetramethylene-Tetranitramine
HPLC	High Performance Liquid Chromatography
HTPB	Hydroxyl Terminated Polybutadiene
HTPE	Hydroxyl Terminated Polyethlene
IPDI	Isophorone Diisocyanate
LC-MS	Liquid Chromatography – Mass Spectrometry
MC	Methylene Chloride
MNA	N-methyl-4-nitroaniline

MS	Mass Spectrometry
MSD	Mass Selective Detector
NATO	North Atlantic Treaty Organization
NC	Nitrocellulose
NG	Nitroglycerin
PGA	Polyethylene Glycol Adipate
RDX	Cyclotrimethylene-Trinitramine
SB	Single Base
SEC	Size Exclusion Chromatography
STANAG	Standardization Agreement
STP	Standard Conditions for Temperature and Pressure
TEA	Triethanol Amine
TMETN	Trimethylolethane Trinitrate
TMP	Trimethylol Propane
VTS	Vacuum Thermal Stability
XLDB	Crosslinked Double Base

CHAPTER 1

INTRODUCTION

1.1 SOLID ROCKET PROPELLANTS

Rocket propellants are classified as liquid and solid, when their physical states in the rocket motor are considered. In liquid propellants, fuel and oxidizer are liquid and are placed in separate tanks. Combustion takes place in a combustion chamber. In solid propellants, the propellant is solid and is case bonded within a chamber and combustion takes place on the internal surface of the grain bore. The motor case, the insulating element, the propellant, the nozzle throat and the igniter are the principle elements of a solid propellant rocket motor (Figure 1.1).

Solid propellants are stable mixtures of oxidizing and reducing ingredients which on ignition burn in a controlled manner to form predominantly very hot, low-molecular weight gases. The formation of these gases enormously increases the internal pressure and the temperature, and provides kinetic energy. These gases are released through the exhaust nozzle of the solid rocket motor and provide the thrust to fly.

Solid propellants are mainly classified as homogeneous and heterogeneous propellants. Homogeneous propellants are either single base (SB) or double base (DB). A SB propellant consists of a single compound that has both an oxidation and reduction capacity. This single compound is usually nitrocellulose (NC). DB propellants on the other hand, consist of NC and nitroglycerin (NG).

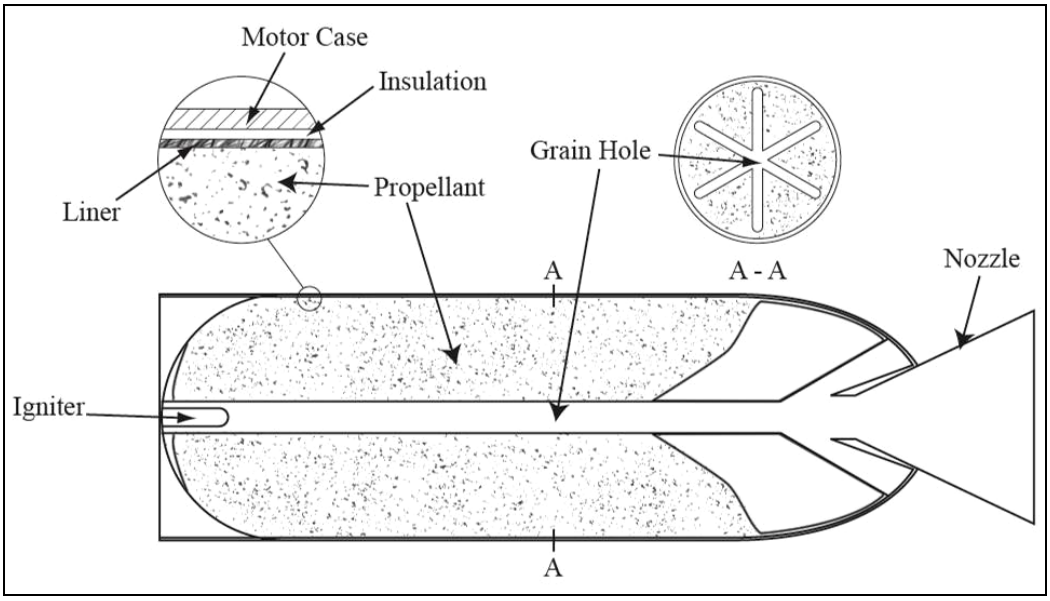

Figure 1.1 Solid Propellant Rocket Motor

Heterogeneous propellants are composite propellants that consist of an organic polymer, a solid oxidizer, and a combustible metal additive. The polymer, usually polyurethane or polybutadiene is inert and serves as a binder. The oxidizer constitutes between 60% and 90% of the mass of the propellant. Typical ingredients of a composite propellant are given in Table 1.1.

Homogeneous propellants have good mechanical properties but poor ballistic properties, and composite propellants have good ballistic properties but poor mechanical properties. Therefore, there is a need for an intermediate type of propellant that both have good mechanical and ballistic properties. These new family of propellants are called Advanced Energetic Binder Propellants.

Advanced Energetic Binder Propellants family includes all propellants composed of a nitrate ester-based energetic binder and fillers (oxidizer, metallic fuel, etc.). The binder may either be composed of an energetic polymer or an energetic plasticizer. Glycidyl Azide Polymer (GAP) is an example to an energetic polymer. Commonly used energetic plasticizers are NG, butanetriol trinitrate

(BTTN), trimethylolethane trinitrate (TMETN) and the mixture of bis-(2,2-dinitropropyl) acetal and bis-(2,2-dinitropropyl) formal (BDNPA/F).

Table 1.1 Typical Ingredients of a Composite Propellant

Ingredient	Amount	Commonly Used Kind
Polymer	10 – 20 wt. %	Hydroxyl Terminated Polybutadiene (HTPB)
Curing Agent	0.8 to 1.2 equiv. ratio	Isophorone Diisocyanate (IPDI)
Plasticizer	0 – 30 wt. %	Dioctyl Adipate (DOA)
Bonding Agent	0 – 5 wt. %	TEPANOL (Mixture of Tetraethylenepentamine, acrylonitrile and glycidol)
Crosslinker	0.07 – 0.09 equiv. ratio	Triethanol Amine (TEA)
Oxidizer	60 – 90 wt. %	Ammonium Perchlorate (AP)
Metallic Fuel	6 – 20 wt. %	Aluminum (Al)
Burning Rate Catalyst	0 – 5 wt. %	Iron (III) oxide (Fe_2O_3)

Members of the Advanced Energetic Binder Propellants family are Composite Modified Double Base (CMDB) and Crosslinked Double Base (XLDB) propellants. Among two, XLDB propellants are capable of having the highest energetic levels that are industrially feasible.

1.2 CROSSLINKED DOUBLE BASE PROPELLANTS

XLDB propellants used in the defense industry consist of a binder, a solid oxidizer and various additives. The major ingredients of XLDB binders are polymers, energetic plasticizers, non-energetic plasticizers (if necessary), curing agents and chemical stabilizers. The binder is formed by the reaction of a polyol precursor and a polyisocyanate curing agent, plasticized by an energetic plasticizer, and crosslinked by NC. The major ingredients of XLDB propellants are given in Table 1.2.

Table 1.2 The Major Ingredients of XLDB Propellants

Ingredient	Commonly Used Kind
Polymers	Polyesters, Polyethers, Polycaprolactones
Curing Agents	Polyisocyanates
Energetic Plasticizers	NG, BTTN, TMETN and BDNPA/F
Crosslinker	NC
Oxidizer	Cyclotrimethylene-Trinitramine (RDX), Cyclotetramethylene-Tetranitramine (HMX) and Ammonium Perchlorate (AP)
Burning Rate Catalyst	Lead and Copper Salts
Stabilizers	2-Nitro Diphenylamine (2-NDPA), N-Methyl –4-Nitroaniline (MNA) and Resorcinol Derivatives

The binder is the elastomeric matrix that carries the oxidizer and the other additives. It is the continuous phase of a propellant and it serves a variety of functions. In addition to binding the oxidizer and the other additives together, it serves as the main source of fuel for the propellant. Utilization of nitrate-ester plasticizers and nitrocellulose crosslinker in XLDB propellant binders make this

propellant family more advanced when compared to composite propellants [1]. However, the nitrate esters are chemically unstable and they decompose in ambient conditions. Therefore aging is a crucial problem in XLDB propellants.

1.3 MECHANICAL PROPERTIES OF XLDB PROPELLANTS

Propellant binder binds together the oxidizer and the other additives to form a rubbery material that is capable of withstanding the strains produced by the thermal and mechanical stresses. Therefore, mechanical properties of the propellant are seriously affected by the binder [2].

Generally, propellants are used in case-bonded configurations in the rocket motor. Solid propellant grains, in case-bonded configuration, are subjected to a variety of stresses and strains during manufacture, transportation, storage and utilization. Because of the differential thermal expansion between the propellant and the case material and the temperature gradients during curing and cooling, stresses and strains are formed. Hence, a propellant grain should have sufficient tensile strength and elongation to withstand these stresses and strains [3]. XLDB propellants exhibit good levels of elongation and satisfactory stress. Consequently, they are well-suited for the production of case-bonded grains [1].

Mechanical properties of solid propellants are generally determined by uniaxial tensile testing. During the test, the propellant is subjected to a tensile force from one end while keeping the other end stationary. Eventually, a typical stress-strain curve for the propellant is obtained. An example of such curve is given in Figure 1.2.

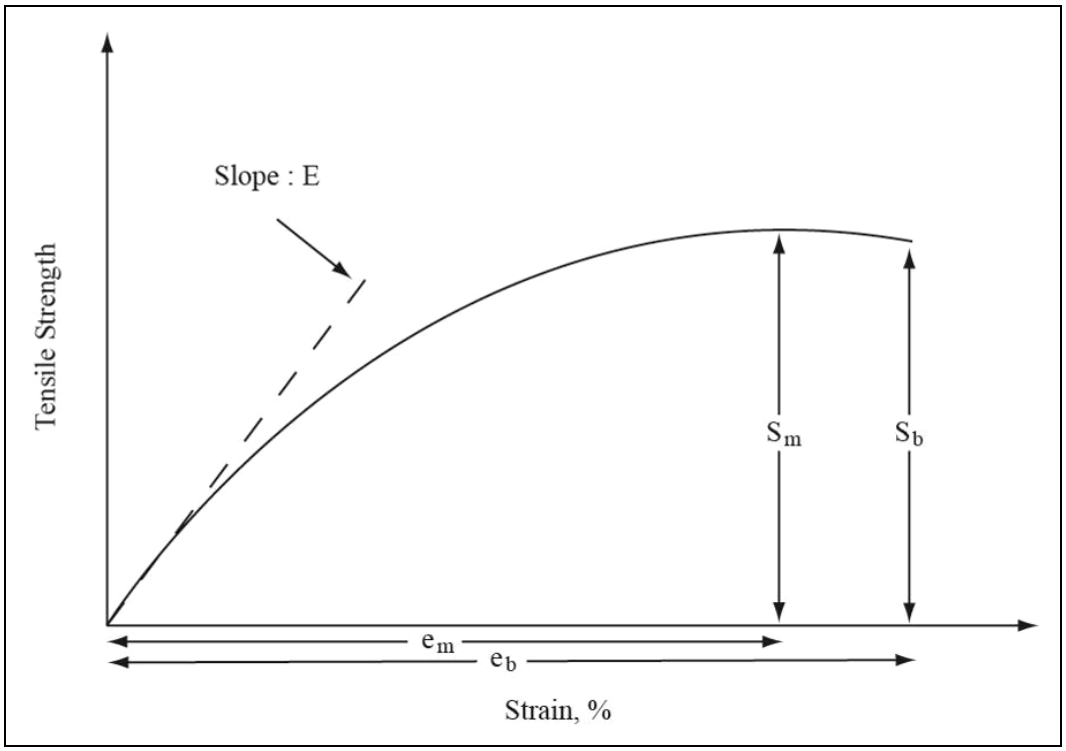

Figure 1.2 Typical Stress-Strain Diagram

The properties that can be collected from the stress-strain curve are the *initial modulus* (E), *maximum stress* (S_m), and *break stress* (S_b), *elongation at maximum stress* (e_m) and *elongation at break* (e_b). E is an important indicator of the stiffness of the propellant and it is obtained from the initial slope of the stress-strain curve. Stress is the amount of unit force loaded on the unit cross sectional area of the specimen. Strain is the ratio of total elongation to the initial length of the specimen. Generally, the quantities S_m and e_m are taken into account when evaluating the results of a mechanical test. Since the propellant is mechanically unstable beyond the strains greater than elongation at maximum stress, *break stress* and *elongation at break* are not normally used.

The mechanical properties of a propellant depend mainly on the tensile properties of the binder matrix and the nature of the interface between the binder and the solid particles.

1.3.1 Influence of Binder on Mechanical Properties

The polyurethane binder of XLDB propellants is formed with the curing reaction. A polyol precursor, containing hydroxyl functional groups, reacts with a curing agent to form the polyurethane matrix. The precursor is usually a diol with an average functionality of 2 and the curing agent is usually a diisocyanate. The polyurethane formation reaction can be illustrated as follows [4].

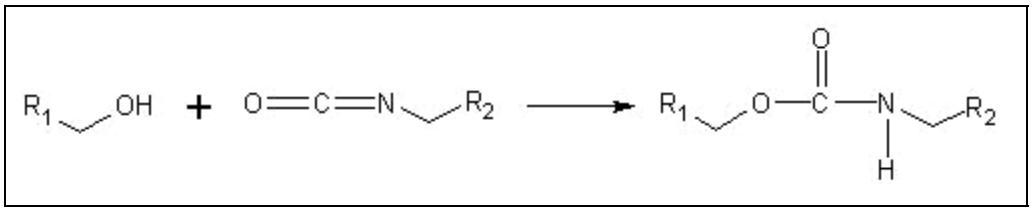

Figure 1.3 Polyurethane Formation Reaction

Due to the highly unsaturated -N=C=O group, the isocyanates are very reactive with a wide range of compounds. Especially the compounds containing a hydrogen atom connected to oxygen react under suitable conditions. Alcohols are the most reactive ones among this class of compounds. Moreover, the polyurethane reactions are known to be very sensitive to any moisture either in the reactants or in the reaction medium. Isocyanates react with water and some side reactions may occur. Possible side reactions of isocyanate with water are given in Figure 1.4 [5].

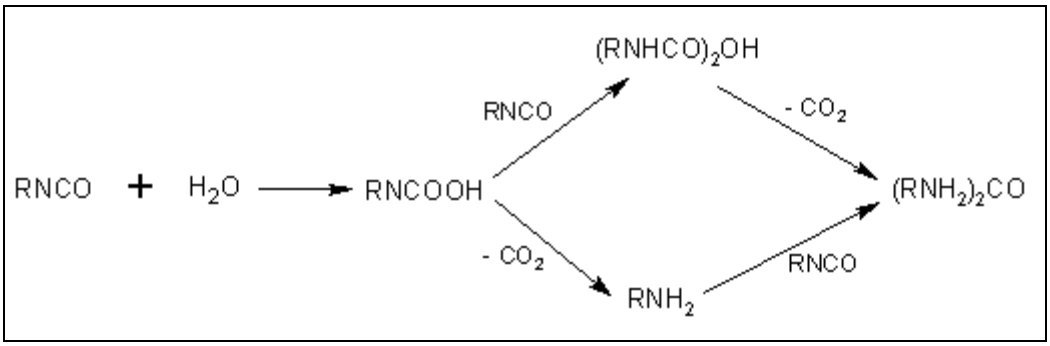

Figure 1.4 Side Reactions of Isocyanates with Water

The polyurethane formation reaction yields a linear polyurethane chain if a crosslinking agent is not used. Conventional crosslinking agents, frequently used for the manufacture of composite propellants, are triols, such as trimethylol propane (TMP) and triethanol amine (TEA). However, the use of these agents is prohibited with energetic binders due to their chemical incompatibility with nitrate esters [1]. NC and tri-functional isocyanates are generally preferred in the production of XLDB propellants. NC is a polymer that is obtained by nitrating cellulose with nitric acid. The hydroxyl groups of cellulose turn into nitro groups by nitration; however, the nitration is partial and still some hydroxyl groups are present in NC. Therefore, it is considered as a polyol crosslinking agent. The structure of NC is given in Figure 1.5.

Since the crosslinking agents are different, the formation of the crosslinked polymeric binder is slightly different from the one that is given by Klager et al. [2] for the composite propellant binders. The resulting crosslinked polymeric chain is a bit complicated, but a simple scheme of the formation of the crosslinked polymeric binder can be illustrated as in Figure 1.6. Note that NC is shown as a straight line and the nitro groups and ether linkages are not shown.

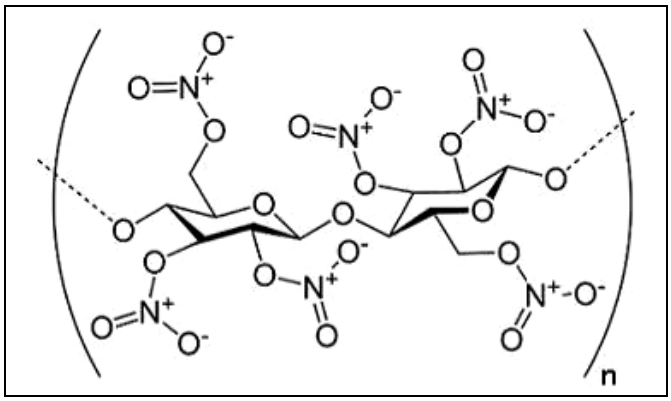

Figure 1.5 Chemical Structure of Nitrocellulose

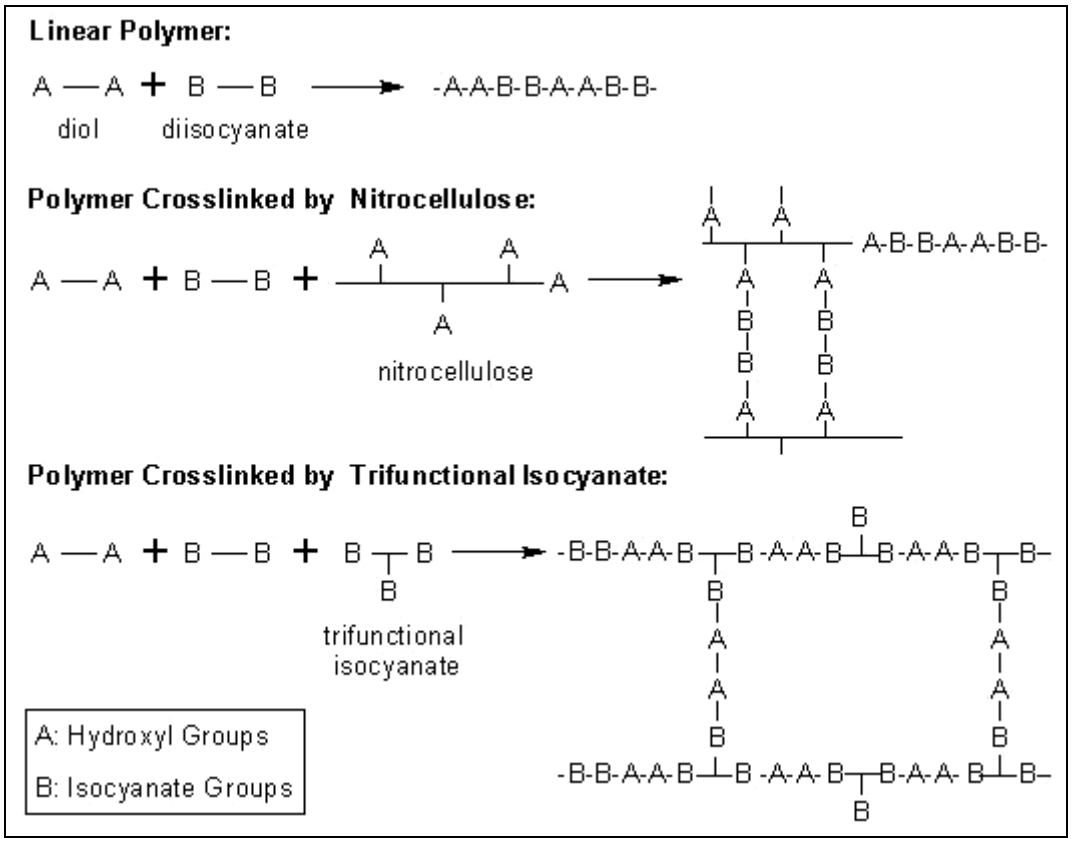

Figure 1.6 Crosslinked Polyurethane Binder

The NCO/OH ratio, which is also known as isocyanate index or R value, is an important parameter governing the crosslink density and molecular weight of polyurethanes. NCO/OH ratio is defined as the ratio of the number of isocyanate groups (or isocyanate equivalents) to the number of hydroxyl groups (or hydroxyl equivalents):

$$\frac{NCO}{OH} = \frac{(f_{di} / MW_{di})(X_{di})}{(f_d / MW_d)(X_d) + (f_{ca} / MW_{ca})(X_{ca})} \tag{1.1}$$

where f is the functionality, MW is the molecular weight and X is the weight fraction, and subscripts d, di, and ca denote the diol, diisocyanate and crosslinking agent, respectively. NCO/OH ratio is a very important parameter and a useful tool for controlling the physical and mechanical properties of propellants [3]. For higher values of NCO/OH, the propellant tends to be harder with low elongation and high tensile strength. For NCO/OH ratios slightly greater than the stoichiometry, the crosslinking density of a polyurethane binder is optimal [1].

Crosslinking density of polyurethane binders decrease when plasticizing level of the binder increases; it drops significantly when the plasticizer to polymer ratio is close to 3. When the molecular weight of the precursor increases, crosslinking density again decreases. Whereas, incorporation of polyols with high molecular weights (NC, acetobutyrate), as crosslinking agents, improve the crosslinking density, and lead to a greater elasticity due to the large average chain length between branch units. For simple systems, when crosslinking density of the binder increases, its mechanical properties also increase [1].

The polymers possessing two functional groups are called telechelic polymers. Molecular weight and molecular weight distributions are of great importance in telechelic polymers [6]. Telechelic polymers with narrow molecular weight distributions tend to cure faster than the telechelic polymers with broad molecular weight distributions. Moreover, it is known that the latter forms a binder that has a lower elongation at break [7]. Functionality, which is defined as the ratio

of the molecular weight to equivalent weight, of a telechelic precursor has great influence on the mechanical properties of the uncured mixture and the cured propellant.

1.3.2 Influence of Solids on Mechanical Properties

In all composite structures, the mechanical properties depend on the interactions between the binder and fillers. Fillers act as reinforcing elements that divide the load together with the binder matrix. Addition of rigid filler particles increases the modulus of an elastomer, provided the elastomer wets the filler or adheres to the filler. However, if the adhesion is excessive, then the elastic properties are lost; this causes in embrittlement and cracking, which further causes an increase in the burning surface. Also, if the adhesion is poor, then dewetting occurs; this causes the degradation of mechanical properties and cavity formation. All these lead to uncontrolled burning of the propellant, which is undesirable [8].

On the other hand, the addition of fillers decreases the elongations. Moreover, the loading capabilities of binders are limited, and these limits particularly depend on the nature of the polymer, the plasticizer content and the nature of the fillers [1].

The solid filler particles commonly used in XLDB propellants are oxidizer, burning rate modifier, curing catalysts and stabilizers. If the amount of solid particles, for example oxidizer and burning rate catalyst, is increased, the thrust and the burning rate of the propellant enhance; however, the mechanical and rheological properties deteriorate. For high levels of solid loading, elongation of the propellant decreases; on the other hand, modulus and tensile strength of the cured mixture and the viscosity of the uncured mixture increase. Since the hardness and modulus of the solid particles are higher than the binder matrix, the changes in mechanical properties can be referred to the decrease of the fraction of the binder matrix at high solid loading [9].

1.4 AGING PROPERTIES OF XLDB PROPELLANTS

Aging is the deterioration of the properties of the solid propellants in time due to the nature of the propellant and the environmental conditions (e.g. temperature, humidity). For XLDB propellants, this aging translates into the evolution of chemical and/or physicochemical characteristics. These evolutions generally lead to changes in the ballistic properties (burning rate, calorimetric value, etc.), mechanical properties (modulus, tensile strength, etc.) and the safety behavior of the propellant. Major consequences related to these evolutions are summarized in Table 1.3 [1].

Table 1.3 Consequences of Aging on the Properties of XLDB Propellants

Type of Evolution	Nature of the Evolution	Consequences and Properties Affected
Chemical	Decomposition of nitrate esters	• Chemical Stability (consumption of stabilizer) ➢ Risk of ignition • Physical Integrity (cracks) ➢ Operational safety
	Polymer network: rupture of chains, creation of links	• Crosslinking density ➢ Mechanical properties
Physicochemical	Mobility of the energetic plasticizer: migration, exudation, volatilization	• Composition of the material ➢ Mechanical properties ➢ Ballistic properties ➢ Explosive properties
	Binder charge adhesion	➢ Mechanical properties
	Crystallization of the plasticizer	➢ Mechanical properties ➢ Explosive properties

XLDB propellants are rich in nitrate ester ingredients. NC and energetic plasticizers are unstable nitrate-ester compounds. Nitrate-esters decompose and produce oxides of nitrogen. These, especially NO_2, are very reactive and capable of catalyzing a series of exothermic reactions, which are responsible for the self-ignition of propellants [10]. During storage, self-ignition can cause devastating accidents; therefore, it is essential that the autocatalytic reactions be prevented.

The decomposition of nitrate esters is slow in ambient conditions; however, the decomposition becomes autocatalytic at higher temperatures. Initiation reaction gives rise to the formation of free radicals:

$$RONO_2 \rightarrow RO_2\bullet + NO_2\bullet$$

The free radicals attack the nitrate esters that are not yet decomposed; this is followed by successive secondary reactions producing gaseous products such as CO, N_2, and mainly nitrogen oxides, NO and NO_2 [1]. The degradation of nitrate esters is complicated, because many reactions are superimposed on each other. Secondary reactions of degradation products with oxygen and water further complicate the degradation path. Nitrogen oxides react with water, in the presence of humidity, to form reactive nitrous acid (HNO_2) and nitric acid (HNO_3) that further deteriorates the stability [11].

Nitrate ester decomposition reaction is the main mechanism that affects the aging of nitrate ester containing propellants; however it is not the only one. Migration is another mechanism that seriously affects the chemical life of propellants. The plasticizers, which have relatively low molecular weight and are liquid at room temperature, may migrate due to low boiling point and concentration differences in the propellant matrix. They migrate into the materials that are in contact with the propellant in the rocket motor (inhibitor, liner, etc.). The localized depletion of the plasticizer causes a hardening of the propellant and changes in the ductility and sensitivity of the propellant.

Other additives such as burn rate catalysts may also migrate due to concentration differences. Migration of the plasticizer and the additives can be

prevented by using the materials in contact equilibrated to the propellant. If the type and the concentration of the plasticizer and the additives in the contact material are matched to the ones in the propellant, the concentration differences are eliminated; hence, the possibility of migration is minimized.

Oxidation of the binder is another aging mechanism. Binder is vulnerable to oxidation because of the unsaturated double bonds in its molecular structure. Changes in the mechanical properties of the propellant are directly related with the total amount of oxidation. Crosslinking density and the density of the propellant increase with oxidation; this causes a lower tensile strength and a higher modulus and hardness.

The bond between the binder and the energetic components may also deteriorate and this type of aging results in gaps inside the propellant; the mechanical and ballistic properties deteriorate and the sensitivity of the propellant increases.

As a result of nitrate ester decomposition, some gaseous products are released into the propellant. These products are soluble in the propellant through which they diffuse to atmosphere. The gases exert a pressure when the rate of the generation is greater than the rate of diffusion. This pressure may cause a physical breakdown of the material such as cracks and vacuum holes, particularly in the case of thick propellant grains. The terms *critical pressure* and *critical diameter* are defined respectively as the pressure and the diameter above which the physical breakdown occurs. The critical diameter may be experimentally obtained by subjecting propellant cubes of different sizes to high temperatures, and by detecting the occurrence of cracks and vacuum holes with X-Rays. The critical edge length is obtained by determining the largest cube that exhibits no degradation [1].

1.4.1 Stabilization of XLDB Propellants

Since nitrate-esters are unstable compounds, they have to be stabilized with stabilizers. Stabilizers react with oxides of nitrogen at a faster rate than the

propellant itself, thus they stop the acid-catalyzed ester hydrolysis. Stabilizers usually have a benzene nucleus, which is capable of fixing the nitrogen oxides by substitution [12]. The decomposition reaction is controlled when stabilizers are utilized in the propellant formulations.

An uncontrolled nitrate ester decomposition reaction could have serious disadvantages. Since the decomposition is exothermic, there could be a risk of ignition of the propellant. As stated above, when the decomposition rate of gas generation is greater than the rate of gas diffusion, there could be a risk of gas cracking. Moreover, the available energy of the propellant would decrease [12]. Therefore, the selection of the stabilizer and controlling the amount of the stabilizer in the propellant is of great importance.

The stabilizers generally used in XLDB propellants that contain no ammonium perchlorate are 2-NDPA and MNA. When ammonium perchlorate is present in the formulation, recorcinol and derivatives of recorcinol combined with 2-NDPA are efficiently used [1]. Chemical structures of 2-NDPA and MNA are given in Figure 1.7.

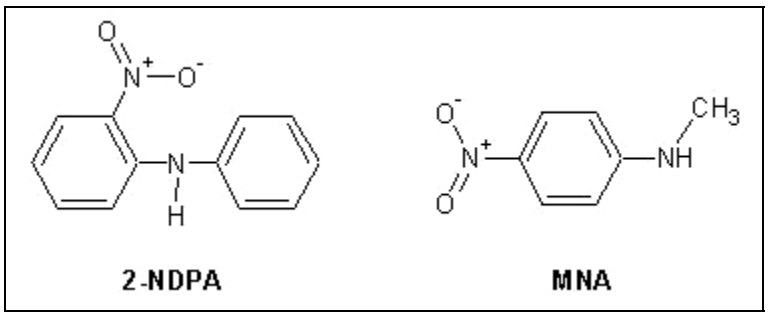

Figure 1.7 Chemical Structures of 2-NDPA and MNA

As stabilizers react with the nitrogen oxides, the number of reactive sites on the stabilizer molecules available for addition of nitrogen oxides decreases. During the reactions the original stabilizers are consumed and a number of derivatives are

formed. These may themselves also act as stabilizers. However, eventually acids can form, which can lead to hydrolysis and deterioration of the stability.

Stabilizer reactions are successive nitrosation and nitration reactions in which a portion of nitrogen dioxides are removed and chemically fixed by the stabilizers. The type of reactions of 2-NDPA and MNA are given in Figure 1.8.

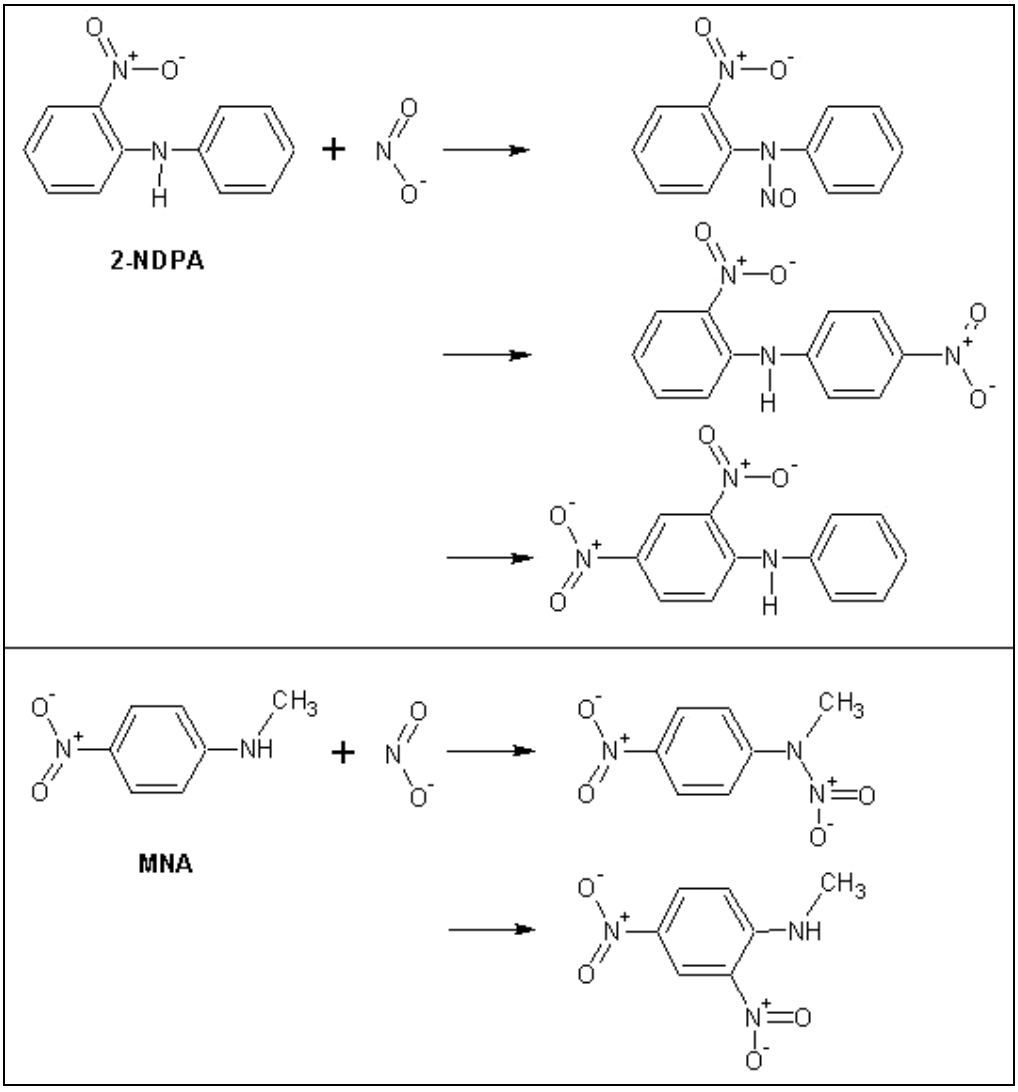

Figure 1.8 Reaction Types of 2-NDPA and MNA with Oxides of Nitrogen

For 2NDPA, the first derivative is n-nitroso 2NDPA. This further rearranges into di-nitrated diphenylamines, mostly 2, 4'-dintirodiphenyl amine. This compound can then react with additional nitrogen oxides, forming higher nitrated derivatives. The first derivative of MNA, on the other hand, is NO-MNA.

Just as the decomposition of nitrate esters, the stabilizer reactions are also complicated; hence, the chemical processes taking place throughout the aging of the propellant are not known in all details. Moreover, the chemical stability of the propellant binder may be affected by the ingredients of the binder and the nature of the fillers and the additives.

1.4.2 Influence of Binder on Aging

Increase of energetic plasticizer content of the propellant generally results in a faster consumption of the stabilizers. The polyurethane binders plasticized with energetic nitrate esters usually present a lower chemical stability. Besides, chemical stability is influenced by the nature of the polyisocyanates; in general, the aromatic polyisocyanates give a slightly better chemical stability. In addition, nature of the polymer influences the stability; precursors rich in ether functions lead less chemical stability [1].

Nitrogen oxides react directly with the polymeric chains or with traces of humidity present in the propellant to produce chemical species which are particularly aggressive toward the polymers. This may lead to cutting by acid hydrolysis. Depolymerization occurs as a result, causing a decrease of the Young's modulus of the propellant [12].

If the crosslinking is not entirely completed at the end of the curing phase, mechanical aging may occur during the storage of the propellant. A slight hardening, caused by the continuation of the polymerization, may evolve. Moreover, formation of secondary products due to the presence of impurities or humidity may have an influence on the kinetics of self decomposition of nitrate esters [1].

1.4.3 Influence of Fillers on Aging

The oxidizers, RDX and HMX are nitramines and they are chemically stable. They do not take part in the degradation of the propellant significantly. Ammonium perchlorate, on the other hand, modifies the decomposition mechanisms of the nitrate esters and the interaction mechanisms of the nitrogen oxides with the stabilizers. This is expressed by a lower consumption of the stabilizer and lower gaseous emissions [1].

The presence of the other additives, especially ballistic modifiers, causes modifications in the decomposition kinetics. Besides, the resistance of the propellant to cracks caused by aging depends on the presence of these ingredients.

1.4.4 Kinetics of Aging Reaction

The kinetics of the stabilizer depletion reaction is of great importance, since it gives important information about the service life of a propellant. Propellants are subjected to accelerated aging at elevated temperatures and the kinetic behavior of the depletion is observed. Reaction rate constants are obtained for different temperatures and parameters in Arrhenius equation are calculated. Using these, reaction rate constant at room temperature; hence the chemical life of the propellant is obtained.

The stabilizer depletion reaction may exhibit a pseudo zero or pseudo first order kinetics. The reaction order can be determined from the experimental data generated. For a pseudo zero order reaction the following applies:

$$-\frac{d[A]}{dt} = k_0 a \tag{1.2}$$

where [*A*] is the concentration of the reactant A, *a* is the initial concentration of A and k_0 is the rate constant. By rearranging and integrating this equation for the amount converted, *x*, after time *t*, the following is obtained:

$$\frac{x}{a} = k_0 t \tag{1.3}$$

When *x/a* is plotted against *t*, a straight line should be obtained conforming that the reaction is pseudo zero order. The rate constant, k_0 could be obtained from the slope of this line.

For a pseudo first order reaction the following applies:

$$-\frac{d[A]}{dt} = k_1[A] \tag{1.4}$$

By rearranging and integrating this equation for the amount converted, *x*, after time *t*, the following is obtained:

$$\ln(\frac{a}{a-x}) = k_1 t \tag{1.5}$$

When ln(*a/a-x*) is plotted against *t*, a straight line should be obtained conforming that the reaction is pseudo first order. The rate constant, k_1 could be obtained from the slope of this line.

Plots for pseudo zero and pseudo first order are compared and the plot that best fits a straight line is selected. The rate constant for each temperature is determined from the slope of the plot of the best linear fit. Sometimes the plots may be nonlinear or a discontinuity may be noted due to the complexity of the reactions. Hence, the depletion reaction may exhibit a pseudo second order or shifting order kinetics. For a pseudo second order reaction the following could be assumed:

$$-\frac{d[A]}{dt} = k_2[A]^2 \tag{1.6}$$

By rearranging and integrating this equation for the amount converted, *x*, after time *t*, the following is obtained:

$$\frac{x}{a(a-x)} = k_2 t \tag{1.7}$$

When *x/[a(a-x)]* is plotted against *t*, a straight line should be obtained conforming that the reaction is pseudo second order. The rate constant, k_2 could be obtained from the slope of this line.

It is possible that the consumption of a stabilizer may exhibit a reaction of shifting order, where the experimental data is well evaluated by a first-order reaction at high concentrations of the stabilizer, but by a zero-order reaction at low concentrations during the final phase of the propellant life time. In this case the following could be assumed:

$$-\frac{d[A]}{dt} = k_0 + k_1[A] \tag{1.8}$$

By rearranging and integrating, the following is obtained:

$$[A] = -\frac{k_0}{k_1} + \left[\frac{k_0}{k_1} + a\right]\exp[-k_1 \cdot t] \tag{1.9}$$

Equation 1.9 can be solved for k_0 and k_1, by the least squares fit method using Mathematical software like MathCAD, MatLAB or Mathematica. This method is commonly used to find the line that best fits a set of data. The sum of the squares of the distances from the individual data points to the line itself is referred as the “Least squares”. A least squares fit finds the smallest possible sum.

After a series of rate constants for different temperatures is obtained, the variation of k with temperature is determined by the Arrhenius equation:

$$k = Ae^{-\frac{E}{RT}} \tag{1.10}$$

where E is the activation energy (J/mole), A is the frequency factor, R is the gas constant (8.3143 J/K·mole) and T is temperature (K). After rearranging:

$$\ln k = \ln A - \frac{E}{RT} \tag{1.11}$$

The value of the activation energy could be determined by plotting ln$k$ versus 1/T and determining the slope of the line. Frequency factor is determined from the intersection of the line with y-axis. Using the Arrhenius parameters, the rate constant for the stabilizer depletion, is estimated for any specified temperature. By this means, the chemical life of the propellant could be determined if the minimum allowable final amount of stabilizer, in other words the maximum allowable amount of stabilizer depletion, is known.

1.5 DETERMINATION OF THE CHEMICAL LIFE

Aging studies are carried out mainly in two different ways; normal aging and artificial aging. In normal aging, the propellant is aged at room temperature in storage conditions. The chemical life is determined by surveillance for many years. The changes in the properties of the propellant are observed and this method gives accurate results. However, this technique is not the primary method in determining the chemical life of a propellant, since it gives results late.

Artificial aging, on the other hand, is an accelerated aging technique in which the propellant is stored at elevated temperatures and the changes in the

properties are observed for a shorter period of time. This technique gives results quickly and it is used more preferably to estimate the chemical life. However, the results may not be as accurate as the results of normal aging, since some physical and chemical reactions that do not occur at room temperature may take place at elevated temperatures.

There are various methods for determining the aging of solid propellants. These methods generally differ for DB propellants and composite propellants.

Chemical life of composite propellants is determined by observing the changes in their mechanical properties, e.g. modulus and stress, with aging. In special cases, estimation of chemical life as characterized by the ballistic properties is desirable. The propellant is aged at elevated temperatures and the rate of change of the property is determined for each temperature. Then, the dependence of rate constant on temperature is obtained using Arrhenius equation (Eq. 1.10).

SB and DB propellants include high amounts of nitrate esters and as stated before nitrate ester decompose readily. Therefore methods in which the determination of the decomposition products is effective are generally used in these propellants. For example, “Stability Test at 120°C” is a test in which a propellant sample is placed in a test tube inside a temperature-regulated enclosure, and the rate of nitrogen dioxide output of the propellant sample is measured. A methyl purple reactive paper is placed in the tube and the color of the paper changes in the presence of nitrogen oxides. This change of color indicates the first release of nitrous vapors that are not trapped by the stabilizer. However, the test takes place at 120°C and it is a very high temperature that is not related with to the normal storage temperature of the propellant. Therefore, the results of this test may not be directly related to the chemical life of the propellant; but they give a reference value which is a characteristic of the composition [12].

Determination of the stabilizer depletion or the stabilizer reaction products during storage at elevated temperatures is a modern and preferred method in the aging studies of nitrate ester containing solid propellants. The stabilizers and derivatives are determined quantitatively generally by High Performance Liquid Chromatography (HPLC), and the rate of the chemical decomposition is estimated by calculating the rate of the depletion reaction of the stabilizers or the rate of the

formation reaction of stabilizer derivatives. The kinetics of the stabilizer reactions are obtained from the equations and with the method presented in Section 1.4.4. HPLC is usually combined with Mass Spectrometry for the confirmation of the chemicals that are determined with the detector.

1.6 AIM OF THIS STUDY

The aim of this study was to use 2-NDPA with and without MNA in three newly developed XLDB propellant formulations that include BDNPA/F with and without BTTN, and evaluate the effects of MNA and BTTN on aging properties of the propellants. In order to achieve this aim, the kinetics of stabilizer depletion reaction were investigated during the aging period of XLDB propellants, and activation parameters and chemical life were determined by means of Liquid Chromatography – Mass Spectrometry (LC-MS) analysis. A further aim was to determine the stability of the propellants by vacuum stability tests and compare the results of two test methods.

CHAPTER 2

LITERATURE SURVEY

2.1 CHEMICAL STABILITY TESTING METHODS

All solid propellant rocket motors have a storage life. At the end of this life, the safe operation of the motor can not be guaranteed. Therefore, it is crucial to predict the extent to which the propellant will degrade over time. In order to do that, the type of aging mechanisms and the relative rates of these mechanisms at various temperatures should be determined.

Aging mechanisms of solid propellants differ based on their constituents. For example, DB propellants composed of high amounts of nitrate ester ingredients will degrade very differently than composite propellants based on ammonium perchlorate-loaded polybutadiene binders. Moreover, aging and degradation of propellants occur together with a series of phenomena such as gas generation, heat generation or decrease of primary stabilizer concentration. Therefore, the variety of the mechanisms and these phenomena should be considered in the propellant stability judgment and the estimation of the chemical life.

Since the beginning of the chemical stability concerns, various methods have been developed for stability monitoring of propellants. These methods include stability monitoring both immediately after the production of the propellant and under storage. The earlier chemical stability tests were so-called heat tests performed at temperatures up to 132°C. Urbanski [13] gives the most widely-used

test methods based on various parameters, which are summarized by Brook et al. (Table 2.1).

Table 2.1 Most Widely-Used Stability Tests [13]

Test	*T*, °C	Time of Test	Based on	Indicator
Abel Heat	65	10-30 min.	Gas Emission	KI Starch Paper
Methyl Violet	120	40 min.	Gas Emission	Methyl Violet Paper
Dutch	105	72 hr.	Weight Loss	Weight Loss of Sample
Surveillance	80	150 hr.	Gas Emission	Brown Fumes
Small Vessel	100	5 days	Weight Loss	Weight Loss of Sample
NATO	65	60 or 120 days	Stabilizer Consumption	Loss in Stabilizer Determined by Spectroscopy or Gas-Liquid Chromatography
Woolwich	80	3 weeks	Stabilizer Consumption	Loss in Stabilizer Determined by Gas-Liquid Chromatography

In tests based on gas emission, the time until visible amounts of nitrogen oxides appear (time-to-fume) is measured. By measuring the time-to-fume at different temperatures, time-to-fume at normal storage temperatures can be estimated. This is an old high temperature test.

Monitoring the weight loss, while storing the propellant at elevated temperatures is generally used for NC-based (single or double base) propellants.

Monitoring the change in molecular weight distribution of the NC by size exclusion chromatography (SEC) is another method used for NC-based propellants. Determination of the viscosity of the NC is another method.

Measurement of the heat flow from the exothermal decomposition reactions by microcalorimetry (MCA) and determination of stabilizer and degradation products by HPLC are more modern methods generally used today. By measuring the stabilizer consumption at different temperatures, the time for stabilizer consumption at normal storage temperatures can be estimated. The values are than used in kinetic models.

For composite propellants, on the other hand, observation of the mechanical or ballistic properties is the most common method used for the determination of chemical stability. The rate of change of a property is determined for different temperatures and the chemical life is estimated for normal storage temperature in this method. Determination of the stabilizer consumption is also used for this kind of propellants, since they may contain stabilizers.

There are lots of studies in the literature [14 – 29] based on these methods. The methods have been evolved with the developments in technology and with the use of new kinds of propellants. The studies can be examined in three parts based on the type of the propellant whose chemical stability is monitored.

2.2 AGING STUDIES OF NC-BASED PROPELLANTS

SB (NC) and DB (NC + NG) propellants contain high amounts of unstable nitrate esters. The binding energy of the CO-NO_2 bond of nitrate esters is very low (155 kJ/mol) when compared to the binding energy of a typical C-H bond (414 kJ/mol) [14]. Splitting of CO-NO_2 bond produces the very reactive NO_2 radical. This strong oxidizing agent reacts with the cellulose backbone of the NC in SB propellants. First of all, ring-opening and oxidative-radical consecutive reactions occur. Stable molecular units split off and the polymer chain is separated through the decomposition of at least one chain element. According to Bohn and Volk [14], this results in the reduction of mean molar masses, M_n, M_w and M_z, of the NC, whereby the mechanical properties are changed.

Bohn and Volk [14] studied aging behavior of four DB rocket propellants and a SB gun propellant between 50 – 90°C and 40 – 110°C, respectively. These propellants were tested to find out stabilizer consumption, molar mass degradation and heat generation, which were respectively measured by HPLC, GPC and MCA. The Arrhenius parameters of the reactions were determined. Heat production was measured as a function of temperature and the influence of pre-aging was investigated. The results showed that the heat production values increase as the primary stabilizer content decreases; however, as the conversion products of the stabilizer have also stabilizing effects, no very high values are obtained after 32 days of pre-aging at 80°C. The experimental data of molar mass degradation were described by a kinetic model based on statistical chain scission. The consumption of the stabilizers 2-NDPA and DPA were investigated in the rocket propellant and in the gun propellant, respectively. The experimental data of the stabilizer decrease were described by a first order reaction.

In another study, Lindblom et al. [15] attempted to analyze the amount of DPA and its three first derivatives in a SB propellant using infrared spectroscopy and chemometrics. Partial least squares calibration of the infrared spectroscopic profiles of the stabilizer and its derivatives in the propellant against their respective quantities (determined by HPLC) was tested to find out whether the quantitative determination of the remaining shelf life of the propellant was possible. They showed that the method can be used to monitor the amount of stabilizer in unknown samples at least down to the lower allowed limit of 0.2% DPA, but with less accuracy than with HPLC.

Jelisavac and Filipovic [16] used HPLC to investigate the kinetic model for the consumption of stabilizer (DPA) in a SB gun propellant. The SB gun propellant, containing about 99 % NC and 1 % DPA, was subjected to artificial aging at 100, 90, 80 and 60 ºC for times necessary for the complete consumption of the stabilizer. The stabilizer content in the aged propellant samples was measured by reverse-phase HPLC. They verified a model that assumes a reaction of shifting order for the consumption of DPA. It was found that the experimental data were well evaluated by a first-order reaction at high concentrations of diphenylamine in the propellant, but by a zero-order reaction at low concentrations during the final

phase of the propellant life time. The kinetic parameters of the model, which permit the calculation of the time up to complete consumption of DPA, were determined. The results were compared with kinetic data obtained using a widely accepted model which combines the first and zero-order reactions, designated as an "exponential and linear" model. All comparisons gave satisfactory agreement.

In another study, Jelisavac and Filipovic [17] developed a reversed-phase HPLC method for identification, separation and quantitative determination of DPA, N-nitroso-DPA, 2-NDPA and 4-NDPA contents in the same single-base gun propellant during storage, until their levels become undetectable. These compounds were determined during a storage period of 168 hours at 100°C using the developed, successfully verified HPLC method.

Volk [18] studied the determination of the shelf life of several DB propellants with the same composition differing only in the stabilizer. While stored at various temperatures between 65 and 90°C, the propellants were aged artificially to the onset of autocatalytic decomposition. A correlation between the temperature and the storage period was established for the results obtained at the respective temperatures. Studies were carried out on the chromatographic analysis of stabilizer reaction products of the type occurring in particular in propellants with DPA, 2-NDPA, Acardite I, Acardite II, and Ethyl Centralite (EC) as a result of storage at elevated temperatures.

Volk [18] showed in his study that continuing aging of the propellant gives rise to stabilizer reaction products which are quite characteristic of the respective aging condition, and these reaction products may be used as a criterion for different stages of aging within the shelf life of solid propellants. Derivatives of 2-NDPA at different stages of aging at 90°C are given in Table 2.2 as an example.

Table 2.2 Decomposition Reaction Products of 2-NDPA (Double Base Propellant Stored at 90°C)

Time of Aging, days	Derivative
1	Dinitrodiphenylamines
2	Trinitrodiphenylamines
14	Tetranitrodiphenylamine
23	Pentanitrodiphenylamine
27	Hexanitrodiphenylamine and picric acid

In another study on DB propellants, Volk and Wunsch [19] used gel permeation chromatography to determine the molecular weight distribution of NC in a DB propellant containing 47.5% NC, 39.8% NG and 1.9% 2-NDPA. Propellant samples were aged at temperatures between 60 and 90°C for different lengths of time. They obtained a linear relationship between temperature and depolymerization. Moreover, they used HPLC to determine the chemical life of the propellant and measured tensile strength and strain at break to determine the drop in mechanical properties. They showed that the relationship between temperature and depolymerization corresponds with the stabilizer depletion rate and the deterioration of the mechanical properties.

Volk et al. [20] aimed to show similar relationship between the chemical aging and molecular weight degradation and mechanical property deterioration of DB propellants. They stored two different DB propellants at temperatures between 60 and 90°C, and showed that the decomposition of NC determines not only the decreasing of stabilizer and molecular weight but also a significant part of the deterioration of the mechanical properties.

In another study, a cast double base (CDB) propellant containing the stabilizer mixture of MNA and 2-NDPA was aged at 80 and 90°C by Bellerby and Sammour [21]. They used HPLC to monitor the depletion of the stabilizers and formation of the derivatives. They showed that MNA is converted almost entirely

into N-nitroso-MNA during the early aging stages, and 2-NDPA reacts more slowly to give both N-nitroso and C-nitro derivatives.

In a recent study, Bixon and Lopez [22] used stabilizer depletion method to compare three different stabilizers, namely Akardite II (1-Methyl-3,3-Di-phenylurea), EC and DPA, in three different SB propellant formulations. They stored the propellants at elevated temperatures between 50 and 80°C at standard humidity and 75% relative humidity. They showed that predicted lifetimes of the propellants stabilized with Akardite II and EC were much longer than those with DPA. They also showed that Akardite II is longer lasting than EC, which in turn longer lasting than DPA.

Pettersson and Eldsater [23] used heat flow calorimetry (HFC) to determine the stability of three different formulations of DB propellants stabilized with Centralite I and mixture of Centralite I, Centralite II and DPA. The propellants were aged at elevated temperatures between 45 and 80°C. They determined the instability of the propellants from the deviations in the Arrhenius plots. They showed in this recent study that HFC is a good method in the determination of stability of DB propellants.

2.3 AGING STUDIES OF COMPOSITE PROPELLANTS

Stability of composite propellants is studied generally by monitoring the change in mechanical and/or ballistic properties. Different methods such as weight loss, determination of plasticizer migration by HPLC, sol-gel analysis and stabilizer depletion are also used.

Hocaoğlu et al. [24] studied the aging behavior of HTPB/AP-based composite solid propellants as a function of crosslink density, which is predominantly determined by the NCO/OH ratio and the molar ratio of triol to diol (triol/diol ratio). For this purpose, 16 different propellant samples with four different NCO/OH ratios between 0.81 and 0.85 and four different triol/diol ratios between 0.07 and 0.13 were subjected to accelerated aging at 65°C for 300 days.

The mechanical properties of the propellants were monitored during aging. They concluded that the results of this parametric investigation can readily be used in the design of composite propellants.

Judge [25] investigated the aging kinetics and mechanisms of a composite propellant by monitoring propellant samples during prolonged storage at elevated temperatures. He compared mechanisms for propellant samples confined with air and samples that are unconfined. He showed that for samples confined under air during aging, oxidative crosslinking of the propellant binder was the main degradation mechanism over time. However, for the unconfined samples plasticizer loss was the significant aging mechanism. Moreover he showed that ambient humidity had a significant but reversible effect on mechanical properties. He derived Arrhenius mathematical relationships to ascertain the extent to which aging was accelerated by increased propellant temperature. He argued that there are essentially no degradation reactions occurring in a sealed rocket motor during accelerated aging at elevated temperature, and since holding the motor at an elevated temperature reproduces the state at which the grain was cured, this procedure may actually reduce grain stress and prevent cohesive failure of the binder. In light of this, he concluded that it can be argued that the common practice of high temperature accelerated aging of solid propellant motors is counter-productive.

Fletcher and Comfort [26] compared service life test results for gas generation, stabilizer depletion and mechanical and ballistic property stability for two Hydroxyl Terminated Polyethlene (HTPE) propellants with DB and XLDB propellants. The propellant was stabilized with MNA and 2-NDPA and stored at elevated temperatures between 25 and 74°C. They monitored the depletion of the MNA stabilizer and determined the depletion rate for several temperatures. Based on these rates, they calculated the Arrhenius activation energy as 26 to 29 kcal/mole for both HTPE propellants. They concluded that this value is the same as the activation energy for MNA depletion in DB and XLDB propellants, and these propellants and the two HTPE propellants are aging by the same mechanism and their service lives are comparable. They also monitored the changes in mechanical and ballistic properties of the propellant.

In a recent study, Sridhar et al. [27] stored a composite propellant at 55, 60 and 70°C at 50% constant relative humidity. They have conducted tension test, scanning electron microscopy (SEM) and stress relaxation test to monitor the mechanical property changes; burning rate and heat of combustion tests to monitor ballistic property changes. They used the results of these tests to evaluate the stability of the propellant.

2.4 AGING STUDIES OF ADVANCED ENERGETIC BINDER PROPELLANTS

Available studies on CMDB and XLDB propellants are limited in the open literature, since most of the information is classified. Although being the last developed solid propellant type, the studies on the advanced energetic binder propellant family date back to 1970s.

In a study published in 1976, Doall and Juhasz [28] used HPLC to quantitatively determine 2-NDPA and its derivatives in a CMDB propellant. The analysis was performed using a mobile phase of 20% methylene chloride / 80% cyclohexane and a 1-m Corasil II column. An internal standard 2, 4 dinitrotoluene was used to obtain quantitative results with a relative standard deviation of less than 1%. They concluded that liquid chromatography is an effective method to determine 2-NDPA in CMDB propellants.

In a more recent study in 1989, Asthana et al. [29] investigated the stability of a crosslinked CMDB propellant stabilized with 2-NDPA and carbamite with and without resorcinol. The propellant samples were confined in aluminum foil and stored in 70, 80 and 100°C. Many different tests including Abel Heat Test, Methyl Violet Test, vacuum stability, autoignition tests and stabilizer depletion were conducted. They used an alcohol-water mixture as the mobile phase and a C-8 column in HPLC analyses. They have obtained comparable results with DB propellants in heat tests. Autoignition tests revealed shelf life of 27.1 and 157 years at 40 and 30°C, respectively. On the other hand, stabilizer depletion tests revealed

shelf life of 6-9 and 26-42 years at 40 and 30°C, respectively. They calculated the activation energy as 33 kCal/mol, which corresponds to the energy required for cleavage of RO-NO_2 bonds in nitric esters. Hence, they concluded that the rate determining step during the aging of CMDB propellants is the decomposition of nitric esters.

CHAPTER 3

EXPERIMENTAL

3.1 MATERIALS USED

Stability of three XLDB propellants with different formulations was studied by artificial aging. The general formulation of the propellants is given in Table 3.1. The percentages are given in intervals due to confidentiality. All the propellants were recently developed and manufactured in TÜBİTAK – SAGE in a successfully completed "Technology Development" project.

Table 3.1 General Formulation of the XLDB Propellants in This Study

Ingredient	Material Used	Percentage
Polymer	(PEG-1000) or (Polyethylene Glycol Adipate, PGA)	5 – 10 %
Curing Agent	(HMDI) or (Desmodur N-3200)	1 – 2 %
Energetic Plasticizer	(BDNPA/F) or (BDNPA/F + BTTN)	20 – 30 %
Crosslinker	(NC)	0.50 – 2 %
Oxidizer	(HMX) or (RDX)	50 – 60 %
Stabilizer	(2-NDPA) or (2-NDPA + MNA)	1.25 %
Others	TPB, CB, ZrC, $PbCO_3$	3 – 4 %

The most important ingredients that affect the stability are the nitrate esters; nitrocellulose (NC) and energetic plasticizers, and the stabilizers. Exact materials used in all propellants are given in Table 3.2.

Table 3.2 Nitrate Esters and Stabilizers Used in XLDB Propellants

Propellant	**Ingredient**		
	Energetic Plasticizer	Crosslinker	Stabilizer
XLDB-1	BDNPA/F	NC (2 %)	2-NDPA (1.25 %)
XLDB-2	BDNPA/F + BTTN	NC (2 %)	2-NDPA (1.25 %)
XLDB-3	BDNPA/F	NC (2 %)	2-NDPA (0.5 %) + MNA (0.75 %)

3.1.1 Energetic Plasticizers

The energetic plasticizers, BDNPA/F and BTTN were purchased from Copperhead Chemical Company, USA. BDNPA/F is a 1:1 mixture of Bis-(2,2-Dinitropropyl) Acetal (BDNPA) and Bis-(2,2-Dinitropropyl) Formal (BDNPF). The molecular formulas of BDNPA and BDNPF are given in Figure 3.1. Properties of BDNPA/F are given in Table 3.3.

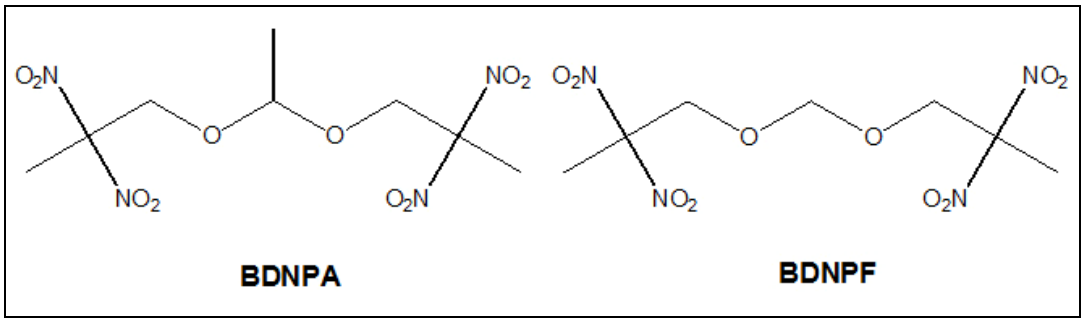

Figure 3.1 Molecular Formula of BDNPA/F

Table 3.3 Properties of BDNPA/F

Property	Specification	TÜBİTAK - SAGE
Appearance	Deep Brown Liquid	Deep Brown Liquid
BDNPA Content, wt. %	45 to 55	48.7
BDNPF Content, wt. %	45 to 55	48.8
Water Content, wt. %	Max. 0.05	0.006
Density, g/ml, 25°C	1.383 to 1.397	1.391
Stabilizer Content, DPA, wt. %	0.08 to 0.18	0.13
Freezing Point, °C	15	-
Boiling Point, °C	125	-

Molecular formula of BTTN is given in Figure 3.2. Properties of BTTN are given in Table 3.4.

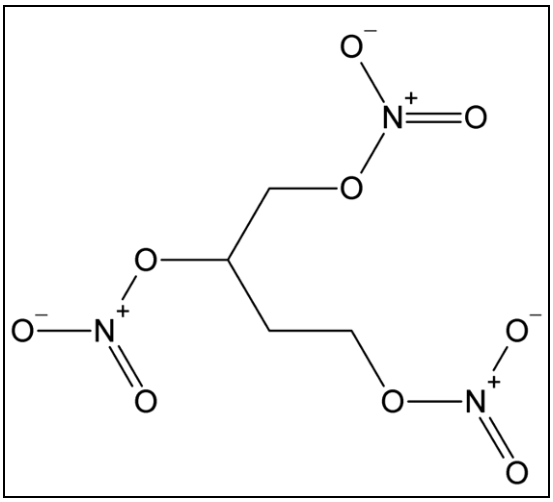

Figure 3.2 Molecular Formula of BTTN

Table 3.4 Properties of BTTN

Property	Specification	TÜBİTAK - SAGE
Appearance	Light Brown Liquid	Light Brown Liquid
% Nitrogen	16.9 to 17.6	17.2
Acidity/Alkalinity	Max. 0.002 %	0.001 NA_2CO_3
Water Content, wt. %	Max. 0.5	0.4
Density, g/ml, 25°C	1.52	1.52
Freezing Point, °C	- 27	-

3.1.2 Crosslinker

The crosslinker used in the XLDB propellant formulations in this study is "Collodium Wolle" grade NC. It was purchased from MKEK, Mechanical and Chemical Industry Corporation, Turkey. The molecular formula of NC is given in Introduction Section in Figure 1.5. The properties are given in Table 3.5.

Table 3.5 Properties of Nitrocellulose ("Collodium Wolle" Grade)

Property	Specification
Appearance	White, Cotton-Like Powder
% Nitrogen	12.20
Solubility in Ethyl Alcohol, %	3.96
Matter Insoluble in Acetone, %	0.26
Ash, wt. %	0.18
Moisture, wt. %	26.20
Density (packed), g/ml	Max. 1.67

3.1.3 Stabilizers

The stabilizers 2-NDPA and MNA were purchased from Sigma-Aldrich Chemicals. The molecular formulas of these stabilizers are given in Introduction Section in Figure 1.7. Properties of 2-NDPA are given in Table 3.6. Properties of MNA are given in Table 3.7.

Table 3.6 Properties of 2-NDPA

Property	Specification
Appearance	Red to Orange Crystals
Assay, %	98
Melting Point, °C	74 – 76
Vapor Density (vs. air)	10.7

Table 3.7 Properties of MNA

Property	Specification
Appearance	Yellow Powder
Assay, %	97

3.2 INSTRUMENTS USED

3.2.1 Vacuum Stability Tests

In order to evaluate the vacuum stability of XLDB propellant samples STABIL – Vacuum Stability Tester of OZM Research (Czech Republic) was used. The instrument is shown in Figure 3.3.

Figure 3.3 STABIL – Vacuum Stability Tester

Vacuum stability tester is used for measuring chemical stability and compatibility of energetic materials, detecting volume of gases evolved from

heated samples by pressure transducers. The instrument is equipped with sensitive electronic pressure transducers, communication with PC for direct control and continuous data acquisition, analysis and archiving.

The apparatus complies with requirements of STANAG 4556 – "Explosives, Vacuum Stability Tests". It can also be used with minor modifications for other customer-defined tests. Chemical instability of energetic materials due to presence of destabilizing impurities, incompatibility with surrounding materials or aging can be discovered by vacuum stability tests.

3.2.2 LC-MS Analysis

In determination of residual stabilizer in aged propellants, Agilent 1000 Series LC-MS Instrument was used. The analyses were done in TÜBİTAK – ATAL (Ankara Test and Analysis Laboratory). The instrument is shown in Figure 3.4.

Figure 3.4 Agilent 1000 Series LC-MS Instrument

The instrument consists of a binary pump equipped with a micro-degasser, a column compartment, a well-plate auto sampler equipped with an automation

interface, a well-plate handler, which is the sample storing device, a diode-array detector (DAD) and a mass selective detector (MSD), based on quadrupole ion trap technology.

In this study, reverse-phase chromatography technique was used. The column was a Waters Spherisorb C18 column (4.6 X 250 mm, 5 μm) at an analysis temperature of 25°C. The mobile phase was a mixture of water, acetonitrile and glacial acetic acid. Chromatographic conditions are given in Table 3.8.

Table 3.8 Chromatographic Conditions

Column :	Waters Spherisorb C18 column (4.6 mm X 250 mm, 5 μm)
Temperature :	25°C
Mobile Phase :	A: Water with 1% glacial acetic acid 5% acetonitrile (%40) B: Acetonitrile with 1% glacial acetic acid 5% H_2O (%60)
Flow Rate :	0.6 mL /min
DAD :	261 nm (2-NDPA) and 395 nm (MNA)
Injection Volume :	20 μL

Mass detector provides increased reliability and it shortens the time of analysis. Mass detector conditions are given in Table 3.9.

Table 3.9 Mass Detector Conditions

Dry Gas Flow Rate :	8 L/min
Nebulizer Pressure :	30 psig
Dry Gas Temperature :	325 °C
Capillary Voltage (V) :	3000(+) ; 3000(-)

3.3 EXPERIMENTAL PROCEDURE

3.3.1 Manufacture of Propellants

XLDB propellants were manufactured by the following general procedure:

- Precursor polymer and crosslinker were dissolved in energetic plasticizer in the presence of acetone and heat,
- Stabilizers, other additives and oxidizer were added to the mixture,
- Curing agent was added to the mixture,
- Resulting paste was mixed under vacuum,
- The propellant paste was poured into mold before the end of pot-life,
- The propellant was cured at an elevated temperature.

3.3.2 Preparation of Propellant Samples

Propellant blocks of 12cm×12cm×15cm were aged at 65°C and small samples of approximately 10 to 15 cm^3 were aged in ovens held at constant temperatures of 45, 55 and 65°C for 120 days. All samples were wrapped in aluminum foil. 3-4 grams of samples were taken for LC-MS analyses every 30 days.

3.3.3 Vacuum Thermal Stability Tests

Vacuum Thermal Stability (VTS) tests were conducted with the un-aged samples. The following procedure was carried out:

- 5 grams of samples from each propellant were prepared by cutting the propellant into small pieces of 4 mm × 4 mm × 2 mm,
- These samples were placed into test tubes that comply with STANAG 4556, and pressure transducers were placed on the top of the tubes,
- A light film of a lubricant is used to ensure a good airtight connection,
- The tubes were evacuated by a vacuum pump until the pressure was reduced to 6.7 mbar,
- The tubes were heated for 48 hours at 100°C,
- The volumes of the gas released from the samples were calculated based on STANAG 4556.

3.3.4 LC-MS Analyses

The analyses of aged samples were done every 30 days. The following procedure was carried out for extraction:

- Take 0.1 gram samples from each propellant for every aging temperature,
- Cut the samples into pieces of 1 – 2 mm^3,
- Add 25 mL of acetonitrile,
- Mix for 4 hours at room temperature,
- Add 10 mL of 2% dry $CaCl_2$,
- Wait for 1 hour at room temperature,
- Wait for all night at 5°C,

- Centrifuge for 10 minutes at 5000 rpm,
- Pass from 0.45 µm filter and inject onto the system.

Stock standards were prepared: 1 mg/mL 2-NDPA in acetonitrile and 1 mg/mL MNA in acetonitrile.

Calibration standards were then prepared using the stock standards: 1 – 5 µg/mL 2-NDPA in acetonitrile and 1 – 5 µg/mL MNA in acetonitrile. Calibration curves were then plotted by injecting the standards of known concentration onto the system and collecting the absorbance versus concentration data for every stabilizer and for both DAD and MSD in every single analysis. Calibration curve for the analysis of 2-NDPA in DAD is given in Figure 3.5.

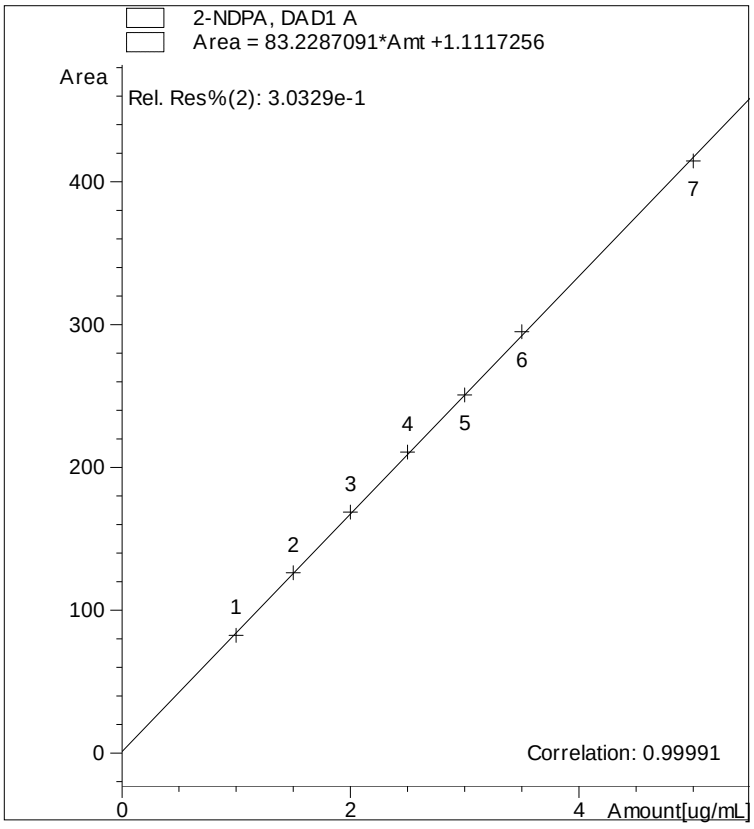

Figure 3.5 Calibration Curve for the Analysis of 2-NDPA in DAD

Standard chromatograms for DAD analyses are given in Figure 3.6 and standard chromatograms for MSD analyses are given in Figure 3.7.

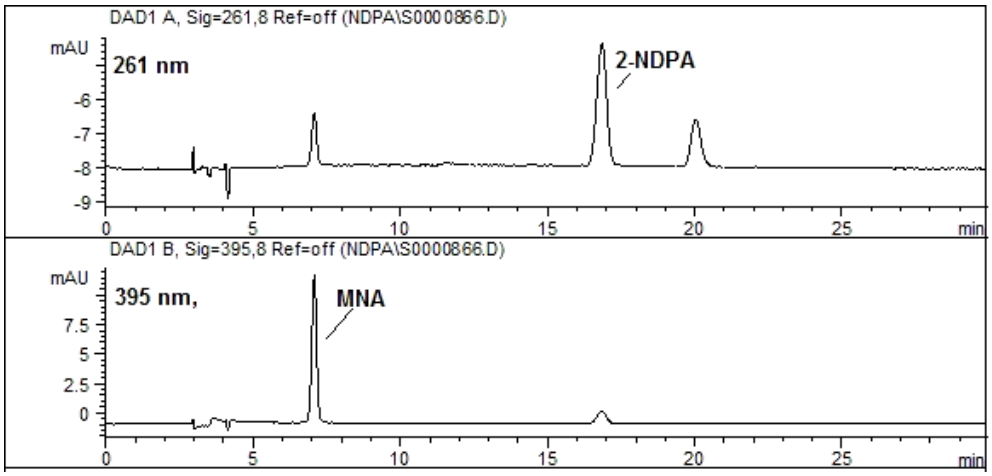

Figure 3.6 Standard Chromatograms of 2-NDPA (261 nm) and MNA (395 nm) for DAD Analyses

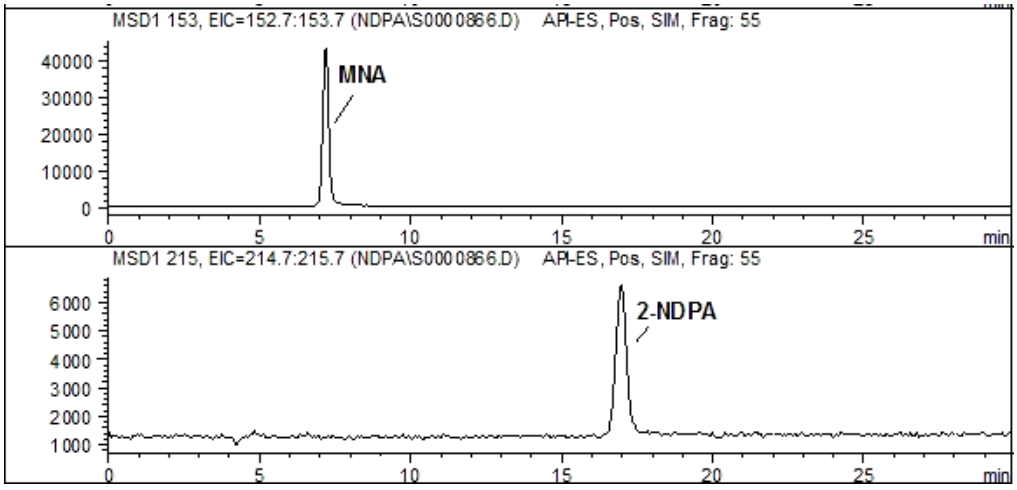

Figure 3.7 Standard Chromatograms of 2-NDPA and MNA for MSD Analyses

3.4 EVALUATION OF THE CHROMATOGRAMS

Chromatograms for the DAD analyses of XLDB-3 aged for 120 days at 65°C is given in Figure 3.8. The area under the peak for the stabilizer is calculated and then the concentration of the stabilizer in the sample is found.

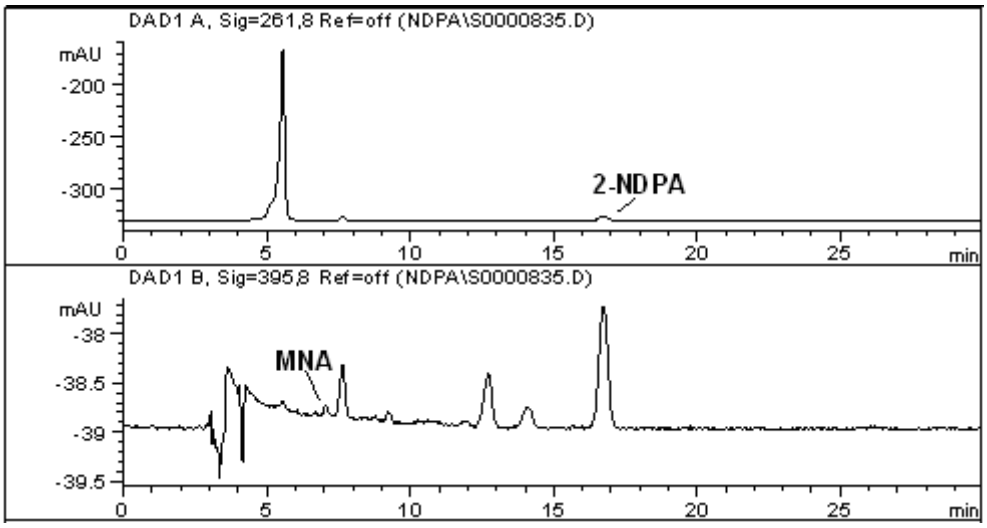

Figure 3.8 Chromatograms for DAD Analyses of XLDB-3 aged for 120 days at 65°C

Chromatograms for the MSD analyses of XLDB-3 aged for 120 days at 65°C is given in Figure 3.9. These chromatograms supply the DAD data and provide reliability.

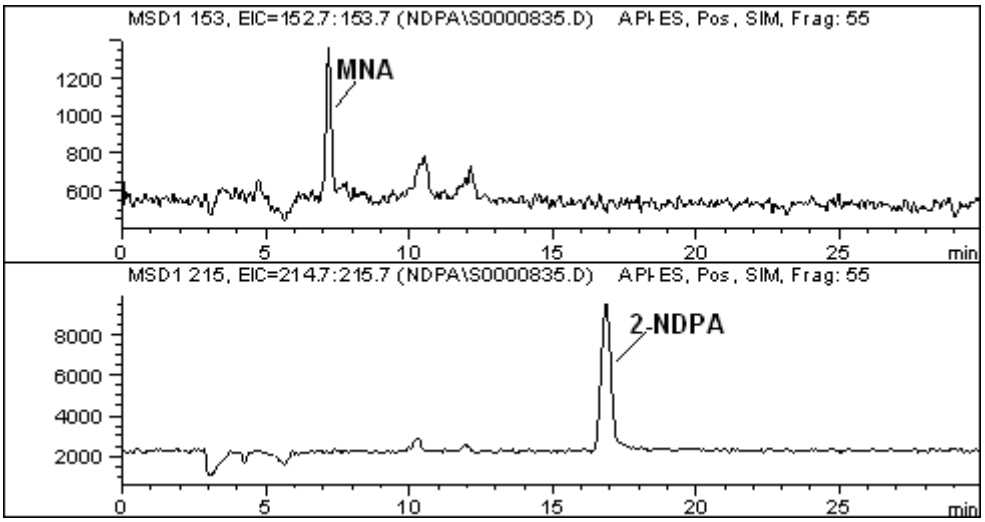

Figure 3.9 Chromatograms for MSD Analyses of XLDB-3 aged for 120 days at 65°C

On a reverse-phase column, the higher and more polar components leave the column first. Therefore, 2-NDPA and MNA will leave the column after the derivatives. That means higher the derivative, shorter the retention time. On the other hand at different wavelengths, different resolutions are obtained.

In order to determine which peak represents which derivative, the retention times must be obtained using standard chromatograms of stabilizer derivatives. A sample chromatogram of DPA and derivatives on a Reverse-Phase column is given in Figure 3.10 by Lindblom, T. [11].

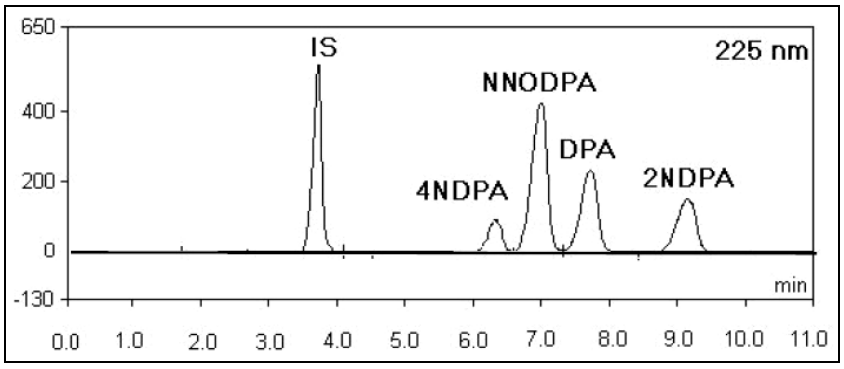

Figure 3.10 Chromatogram of DPA and Derivatives on a Reverse-Phase Column [11]

CHAPTER 4

RESULTS AND DISCUSSION

4.1 VACUUM THERMAL STABILITY TESTS

Vacuum stability instrument, Stabil, calculates the volume of gas evolved from the propellant samples by using a pressure transducer that converts the voltmeter readings into pressure. The following formula is used in the calculation;

$$V = \left[V_c + V_t - \frac{m}{d} \right] \times \left[\frac{P_2 \times 273}{273 + t_2} - \frac{P_1 \times 273}{273 + t_1} \right] \times \frac{1}{1.013}$$

where: V = volume of gas liberated from the sample (cm^3, at STP)
V_c = volume of the transducer and adapter (cm^3)
V_t = volume of the heating tube (cm^3)
m = mass of the sample (g)
d = density of the sample (g/cm^3)
P_1 = calculated pressure at the beginning of the test (bar)
P_2 = calculated pressure at the end of the test (bar)
t_1 = room temperature at the beginning of the test (°C)
t_2 = room temperature at the end of the test (°C).

Gas pressure versus time graphs were plotted and the values for the volume of the gas evolved were calculated by the software of the instrument. Graphs are

given in Appendix A and results in volume of gas per gram of sample (ml/g) are given in Table 4.1 for all propellants. For comparison, the results of Asthana et al [29] for a double base (DB) and a CMDB propellant are given in the table.

Table 4.1 Results of Vacuum Stability Tests

Propellant:	**XLDB-1**	**XLDB-2**	**XLDB-3**
Evolved Gas, ml/g (48 hours at 100°C)	1.50	1.50	2.62
	DB	**CMDB**	
Evolved Gas, ml/g (40 hours at 90°C) [29]	1.84	2.40	

Although aging time and temperature in Asthana's [29] experiments are slightly different, the stability values can be used as a comparison. Asthana et al. accept the stability of DB propellants as the criterion of stability of CMDB propellants; therefore, these values can also be accepted as the criterion of stability of XLDB propellants. It is seen from the table that XLDB-1 is slightly less stable than the DB propellant; however XLDB-1 is more stable than the CMDB propellant.

XLDB-2 propellant has the same formulation with XLDB-1 except that the former contains the additional energetic plasticizer, BTTN (See Table 3.2). Although BTTN contains methylene chloride (MC) in its formulation, the gas generation values do not differ for two propellants.

XLDB-3 has the same formulation with XLDB-1, differing only in the stabilizer content. XLDB-3 contains 0.75% of MNA and 0.50% of 2-NDPA, whereas XLDB-1 contains 1.25% of 2-NDPA only. It is known from the literature that MNA reacts with the oxides of nitrogen more preferentially than the 2-NDPA; hence its concentration decreases by 90% (relative) before any appreciable loss of 2NDPA is observed [21]. From Table 4.1 it is seen that XLDB-3 is more stable

than XLDB-2; however, it is less stable than XLDB-1. Hence, it can be argued that higher reactivity of MNA does not always make it a better stabilizer over 2-NDPA when they are used together.

It should be noted that the manufacturing process of XLDB propellants involve the addition of inert solvent, acetone. Acetone is used to dissolve the NC, which is not very soluble in BDNPA/F and BTTN. Acetone is removed during the manufacture of the propellant by mixing the propellant mixture at high temperature and under vacuum. However, there is a trade-off between the temperature and the pot-life of the propellant. Since the curing of the polyurethane structure accelerates at higher temperatures, the pot-life decreases. This restricts the manufacture of the propellant. Also, at low mixing temperatures, it takes more time to remove the acetone. The pot-life of the XLDB propellants developed in this work is limited to 60 minutes due to the requirements of the TÜBİTAK-SAGE Project. Hence, in any case, a small amount of acetone is trapped in the propellant binder matrix, and this causes XLDB propellants to have higher gas generation values. This should be considered when evaluating the vacuum stability of these propellants.

4.2 LC-MS ANALYSES

4.2.1 Depletion of Stabilizers

The concentrations of the stabilizers in all propellants were measured periodically during aging. The chromatograms for DAD and MSD analyses are given in Appendix B. The concentration values of 2-NDPA and MNA with respect to time of storage at 45, 55 and 65°C are given in Appendix C. Stabilizer concentrations versus time graphs at all temperatures were plotted using the data. Figure 4.1 is a plot of 2-NDPA concentration (mass of stabilizer per total mass of propellant) versus aging time at three temperatures for XLDB-1 propellant.

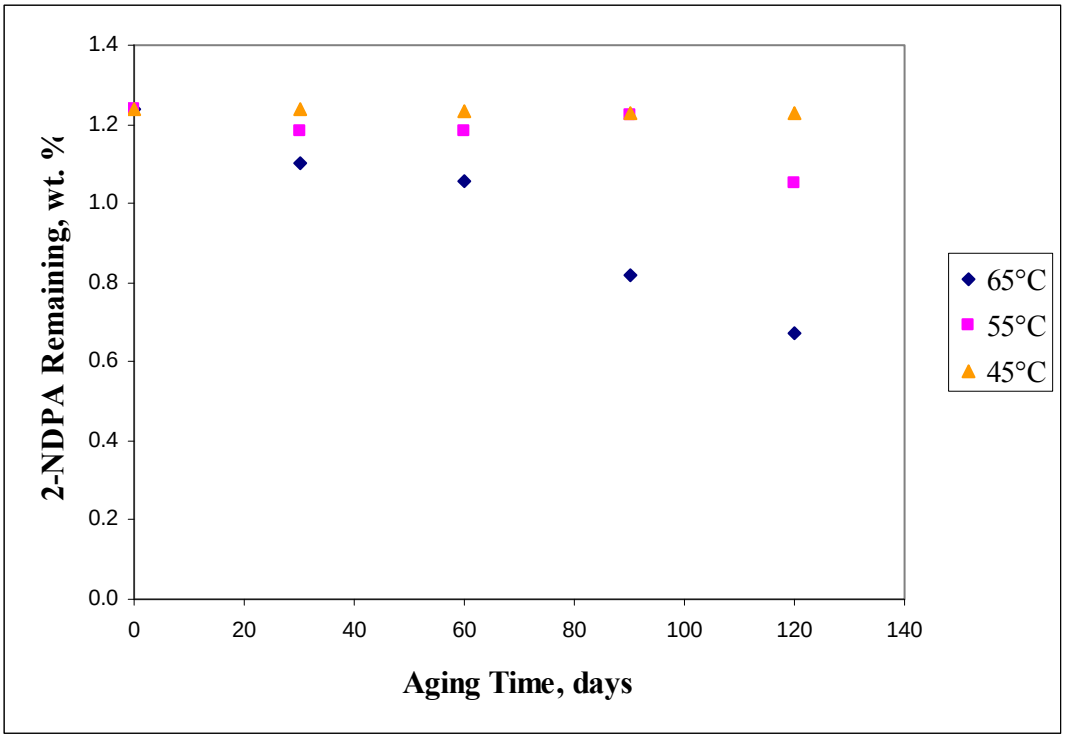

Figure 4.1 Depletion of 2-NDPA in XLDB-1 Propellant Samples

XLDB-1 contains 1.25% of 2-NDPA in its formulation. The experimentally determined amount for the unaged sample is 1.239%. From Figure 4.1 it is seen that the depletion rate decreases as the aging temperature decreases. Moreover, there is no measurable decrease in 2-NDPA content during the aging period for the sample aged at 45°C. The residual 2-NDPA content was measured as 0.672% for the sample aged at 65°C for 120 days. For the sample aged at 55°C, the residual 2-NDPA content was measured as 1.049%. It is seen from the figure that for 90 days of aging at 55°C the residual 2-NDPA content is very close to the initial content. This may be caused from experimental errors or from the nature of the stabilizer reactions. It is known that the reactions of stabilizers with degradation products can be reversible [30].

2-NDPA concentration versus aging time plot for XLDB-2 is given in Figure 4.2. XLDB-2 contains 1.25% of 2-NDPA in its formulation. The experimentally determined amount for the unaged sample is 1.243%.

From the figure, it is seen that there is no significant decrease in 2-NDPA content for the sample aged at 45°C. The residual 2-NDPA content was measured as 0.507% for the sample aged at 65°C and 1.127% for the sample aged at 55°C, after 120 days. Just like XLDB-1, similar signs of possible reversible reactions are seen for XLDB-2 samples aged at 45 and 55°C.

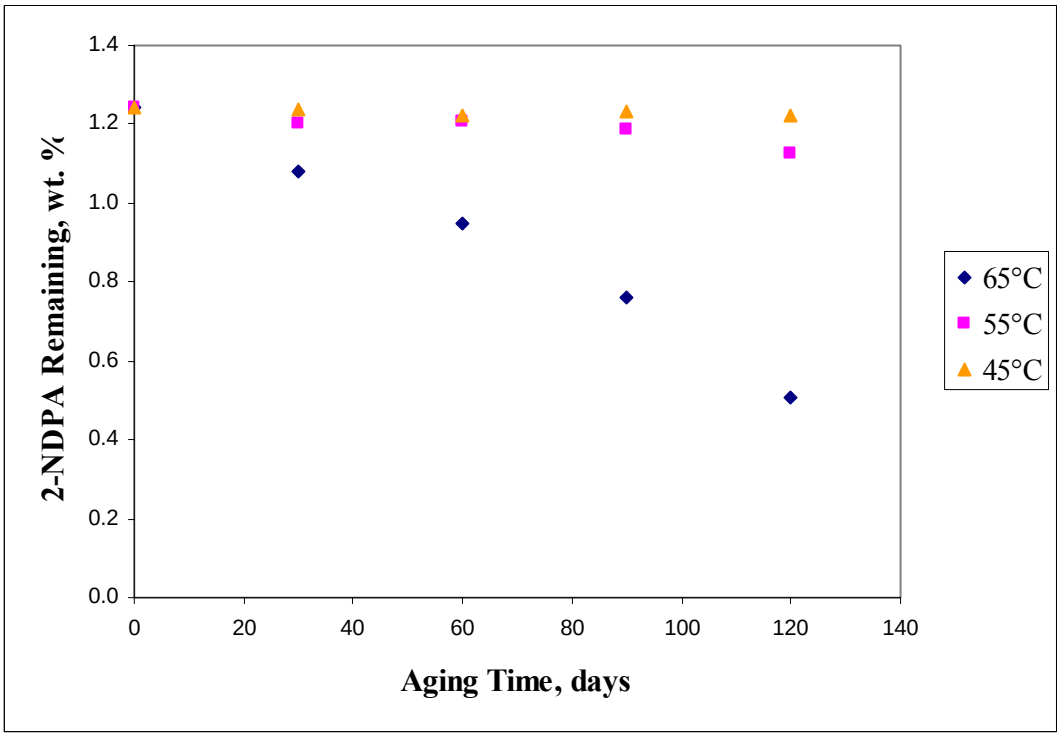

Figure 4.2 Depletion of 2-NDPA in XLDB-2 Propellant Samples

XLDB-3 propellant formulation contains the stabilizer mixture of MNA and 2-NDPA. The initial concentrations of MNA and 2-NDPA were measured as 0.730% and 0.550%, respectively. The stabilizer reactions are complicated again in this case. However, it is known from the literature that MNA reacts with the degradation products more readily than 2-NDPA and its concentration decreases by about 90% (relative) before any appreciable loss of 2NDPA is observed [21]. For the sample aged at 65°C, the residual MNA and 2-NDPA contents were measured as 0.170% and 0.453%. It is seen that 77% of MNA was consumed, on the other

hand, only 18% of 2-NDPA was consumed during aging for 120 days at 65°C. The consumption values of 2-NDPA are smaller for lower temperatures; 10% at 55°C and 7% at 45°C. Therefore, in evaluating the stability of XLDB-3, which contains both MNA and 2-NDPA, the depletion of MNA is taken into account. Hence, concentration of MNA versus aging time plot is given in Figure 4.3.

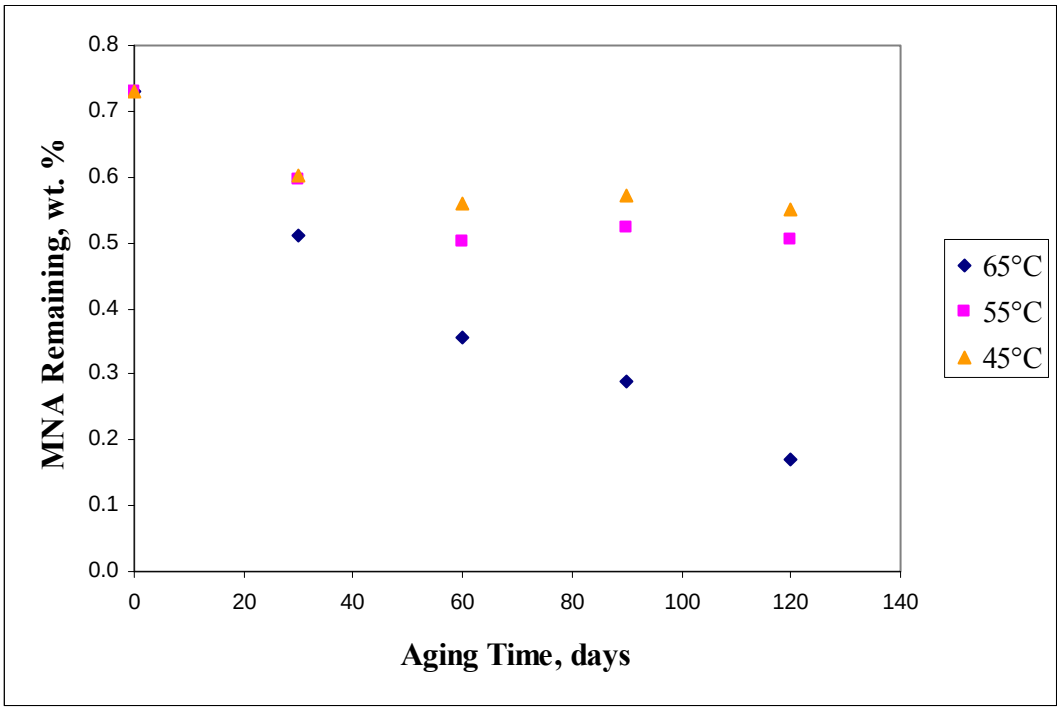

Figure 4.3 Depletion of MNA in XLDB-3 Propellant Samples

It is seen from Figure 4.3 that the nature of MNA depletion reaction at 65°C is likely to be linear. For the samples aged at lower temperatures, the nature of the depletion reaction is more likely to be polynomial. For these temperatures, the concentration drops slightly for the first 60 days of aging, then it increases slightly until the end of the aging period. It is obvious that at low temperatures reversible reactions take place. Furthermore, complicated trans-nitrosation reactions between the stabilizers and stabilizer derivatives could also be taking place.

The depletion of 2-NDPA in XLDB-3 is given in Figure 4.4 as comparison with the depletion of MNA. It is easily seen that there is no significant change in the concentration of 2-NDPA even after 120 days at 65°C.

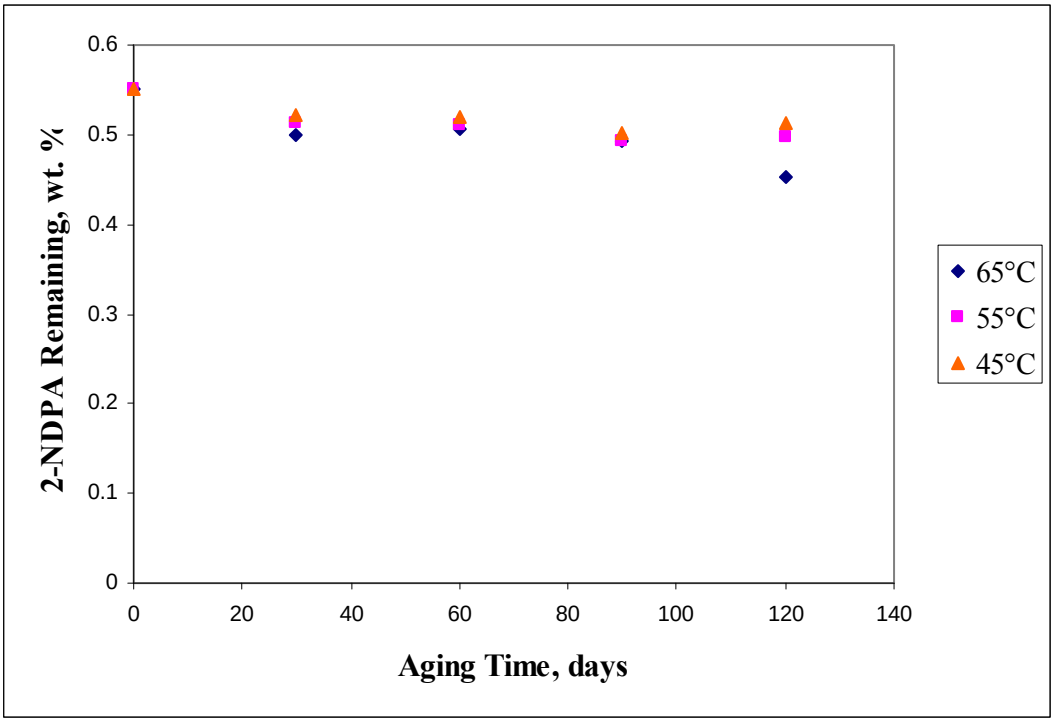

Figure 4.4 Depletion of 2-NDPA in XLDB-3 Propellant Samples

4.2.2 Determination of Rate Constants and Best-Fit Kinetic Models

The experimental data is used to plot *x/a*, *ln(a/a-x)* and *x/[a(a-x)]* against time, *t*, to determine the reaction rate constants for pseudo zero, pseudo first and pseudo second order reactions, respectively (See Equation 1.3, Equation 1.5 and Equation 1.7). Here, *x* is the amount of stabilizer converted at time *t*, and *a* is the initial concentration of the stabilizer in wt %. Pseudo reaction kinetics assume that the concentrations of the reactants other than the stabilizer (nitrate esters, etc.) are constant as the reaction proceeds; hence, the reactions depend on the concentration

of only one reactant (stabilizer). Another assumption is that the aging mechanisms (the reactions taking place) are the same for both low and high temperatures; only the reaction rate differs.

Linear fits are drawn to all kinetic plots and the formulas of the lines are obtained using MS EXCELL. The slope of each line gives the reaction rate constant. Also the R^2, coefficient of determination, values of the lines are obtained and this way the plot with the higher R^2 value is determined as the best fit.

The plots for XLDB-1 sample aged at 65°C are given in Figure 4.5, 4.6 and 4.7, respectively for pseudo zero, pseudo first and pseudo second orders. From the figures it is seen that the plot for the pseudo zero order reaction has an R^2 value of 0.9592, which is greater than the one for pseudo first order reaction; 0.9287 and pseudo second order reaction; 0.8856. Therefore, the depletion of 2-NDPA at 65°C is more likely a pseudo zero order reaction for XLDB-1 propellant, and the reaction rate constant is 0.0036 $days^{-1}$ at this temperature.

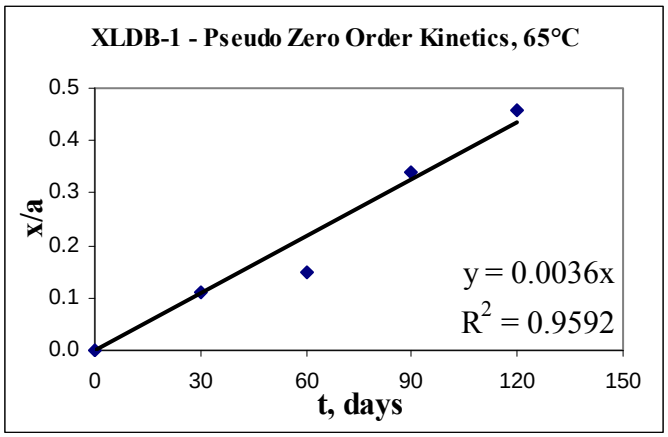

Figure 4.5 Determination of Reaction Rate for the Pseudo Zero Order Depletion of 2-NDPA at 65°C for XLDB-1 Propellant

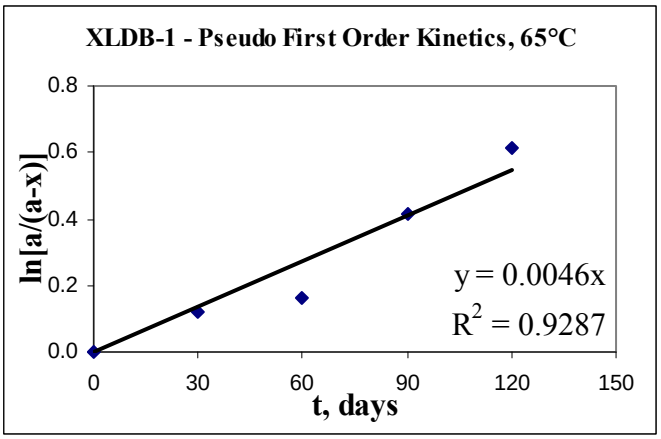

Figure 4.6 Determination of Reaction Rate for the Pseudo First Order Depletion of 2-NDPA at 65°C for XLDB-1 Propellant

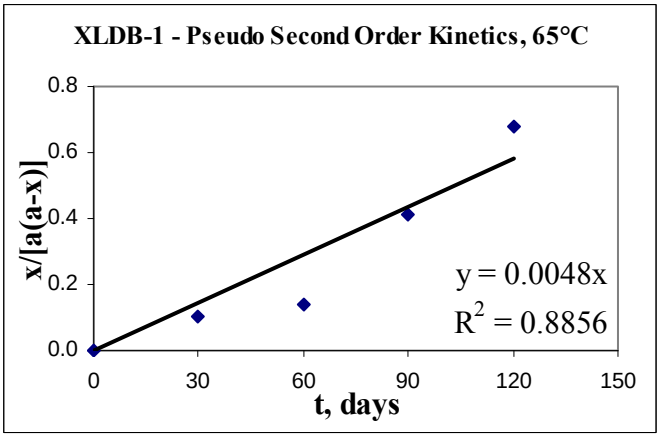

Figure 4.7 Determination of Reaction Rate for the Pseudo Second Order Depletion of 2-NDPA at 65°C for XLDB-1 Propellant

By the same way, plots for pseudo zero, pseudo first and pseudo second order reaction kinetic models for all propellants at all temperatures were plotted. The plots are given in Appendix D. The R^2 values for kinetic model estimations at all aging temperatures are given in Table 4.2. The values written in bold are the greatest values for the corresponding propellant and aging temperature.

Table 4.2 Coefficients of Determination for Kinetic Model Estimations for the Stabilizer Depletion Reaction at Different Temperatures

Propellant		Coefficient of Determination, R^2		
		Pseudo Zero Order	Pseudo First Order	Pseudo Second Order
XLDB-1*	45°C	**0.9905**	0.9902	0.990
	55°C	**0.517**	0.5163	0.515
	65°C	**0.9592**	0.9287	0.8856
XLDB-2*	45°C	**0.4416**	0.4394	0.4373
	55°C	**0.8479**	0.8431	0.8377
	65°C	**0.9815**	0.9196	0.826
XLDB-3**	45°C	0.4967	0.5298	**0.5632**
	55°C	0.6011	0.6313	**0.6564**
	65°C	0.9352	**0.9848**	0.8854

* Depletion of 2-NDPA

** Depletion of MNA

It is seen from Table 4.2 that for XLDB-1 and XLDB-2 propellants the best kinetic model is Pseudo Zero Order kinetic model. However, for XLDB-3 propellant; therefore for the depletion reaction of MNA, the best kinetic model is questionable. It seems that at 65°C the reaction is best described by a Pseudo First Order kinetic model; but at low temperatures, Pseudo Second Order kinetic model provides better estimation. From Figure 4.3 it is obviously seen that the nature of the depletion reaction of MNA is likely to be polynomial at low temperatures. Hence, it is reasonable that the reaction is better expressed by Pseudo Second Order kinetic model, which is a polynomial model. However, at 65°C Pseudo First Order kinetic model, which is an exponential model, gives better estimation. Therefore, a combined model, in which a reaction of shifting order expresses the depletion of MNA, could be the best model in this case. Equation 1.9 represents this kind of a model, where the experimental data are well evaluated by a first-

order reaction at high concentrations of the stabilizer in the propellant, but by a zero-order reaction at low concentrations during the final phase of the propellant life time. Equation 1.9 was solved for k_0 and k_1, by the least squares fit method using the Mathematical software MathCAD. The function called "expfit" was used with refined initial guesses 0.135, -0.012 and 0.595 for (k_0/k_1+a), $-k_1$ and $-k_0/k_1$, respectively. (Third parameter guess is -0.595 for the reaction at 65°C.) The output from the software is given in Appendix E. The resulting coefficients of determination for the kinetic model for all temperatures are given in Table 4.3.

Table 4.3 Coefficients of Determination for Shifting Order Kinetic Model Estimation for the Depletion of MNA at Different Temperatures

Propellant		**Coefficient of Determination, R^2**
		Shifting Order Kinetics
XLDB-3**	45°C	0.990
	55°C	0.968
	65°C	0.993

** Depletion of MNA

When the values for XLDB-3 in Table 4.2 and in Table 4.3 are compared, it is clearly seen that the best model for the depletion of MNA in this propellant is the Shifting Order kinetics model at all temperatures. Therefore the rate constants for the MNA depletion reaction should be calculated based on this model.

Since the best kinetic models for all stabilizer depletion reactions are selected, the reaction rate constants can be calculated. Rate constants for the depletion of 2-NDPA in XLDB-1 and XLDB-2 propellants were calculated in MS EXCELL using the above stated method; on the other hand the rate constant for the depletion of MNA in XLDB-3 was calculated in MathCAD using the least squares fit method for shifting order kinetic model. Reaction rate constants obtained are given in Table 4.4. Rate constants for the depletion of MNA for pseudo first order

kinetic model were also calculated using MS EXCELL, since according to NATO STANAG 4527: "*When it is not clear which line is the best fit, first order kinetics shall be used in the determination of the chemical life of the propellant.*" [33]. In the case of XLDB-3 propellant, the relation between temperature and the rate constants for the shifting order model are quite complicated (See Table 4.4). Therefore, it shall be proper to consider the pseudo first order kinetic model in the calculation of the chemical life of this propellant.

Table 4.4 Rate Constants for the Stabilizer Depletion Reaction for All Propellants at Different Temperatures

Propellant	**Reaction Rate Constant, *k* days^{-1}**			**Kinetics of the Depletion Reaction**
	45°C	55°C	65°C	
XLDB-1*	8×10^{-5}	9×10^{-4}	3.6×10^{-3}	Pseudo Zero Order
XLDB-2*	1×10^{-4}	7×10^{-4}	4.6×10^{-3}	Pseudo Zero Order
XLDB-3**	k_0: -0.026	k_0: -0.017	k_0: 5.9×10^{-6}	Shifting Order
	k_1: 0.047	k_1: 0.034	k_1: 0.011	
	2.9×10^{-3}	3.8×10^{-3}	1.2×10^{-2}	Pseudo First Order

* Depletion of 2-NDPA

** Depletion of MNA

Note that at 45 and 55°C the shifting order reaction model results in an equilibrium reaction in which the forward reaction is in first order and the backward reaction is in zero order. The negative sign in front of k_0 values for 45 and 55°C denotes that the zero order part of the shifting order reaction is reverse for the corresponding aging temperatures. It is also seen from the table that the reaction rate constants of the shifting order kinetic model are inversely dependent on the temperature. This is because this model is a combined kinetic model that assumes well evaluation of the experimental data by a first-order reaction at high

concentrations of the stabilizer in the propellant, but by a zero-order reaction at low concentrations during the final phase of the propellant life time.

4.2.3 Fitting Kinetic Model Equations to Experimental Data

The best-fit kinetic models for the stabilizer depletion reactions for every propellant were determined in Section 4.2.2 above. The corresponding model equations for the stabilizer concentrations are given in Table 4.5. Note that pseudo first order kinetic model is also included for XLDB-3 propellant.

Table 4.5 Kinetic Model Equations for the Depletion of Stabilizers

Propellant	**Stabilizer Concentration, *[A]* wt %.**	**Kinetics of the Depletion Reaction**
XLDB-1*	$a - k_0 \cdot a \cdot t$	Pseudo Zero Order
XLDB-2*		
XLDB-3**	$-\frac{k_0}{k_1} + \left[\frac{k_0}{k_1} + a\right] \exp[-k_1 \cdot t]$	Shifting Order
	$\exp(\ln a - k_1 \cdot t)$	Pseudo First Order

* Depletion of 2-NDPA

** Depletion of MNA

Using the calculated reaction rate constants in corresponding model equations the residual stabilizer contents were determined through the aging period for every temperature. The model equations were plotted on the same graph with the experimental data for a visual observation of the fits. Figure 4.8 shows the depletion of 2-NDPA in XLDB-1 propellant; both experimental data and model

equation. The coefficients of determination for the model equations are also shown in the figure. These values show the quality of the correlation between the model and the experimental data. They were calculated using MathCAD. The software outputs are given in Appendix E.

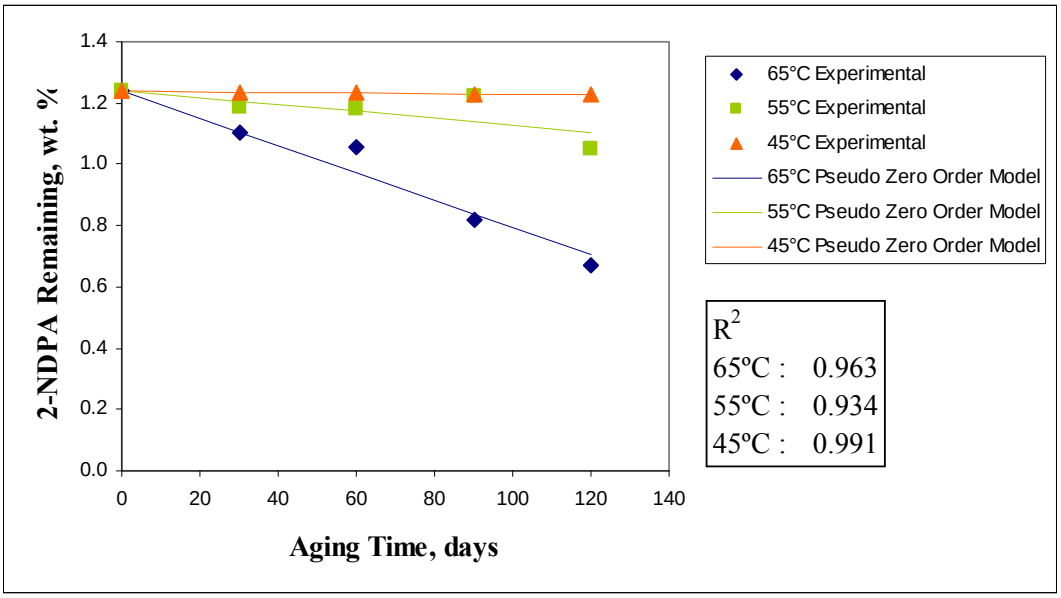

Figure 4.8 Depletion of 2-NDPA in XLDB-1 Propellant Samples – Description by a Pseudo Zero Order Model

Figure 4.9 shows the depletion of 2-NDPA in XLDB-2 propellant; both experimental data and model equation. The coefficients of determination for the model equation are also shown in the figure.

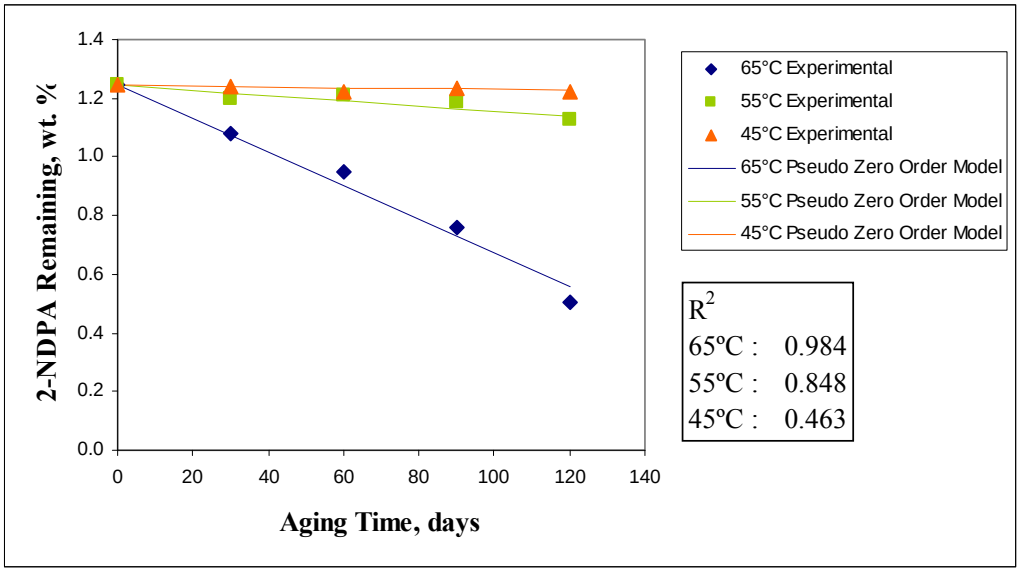

Figure 4.9 Depletion of 2-NDPA in XLDB-2 Propellant Samples – Description by a Pseudo Zero Order Model

Both experimental data and model equation are shown in Figure 4.10 for the depletion of MNA in XLDB-3 propellant. The coefficients of determination for the model equation are also shown in the figure.

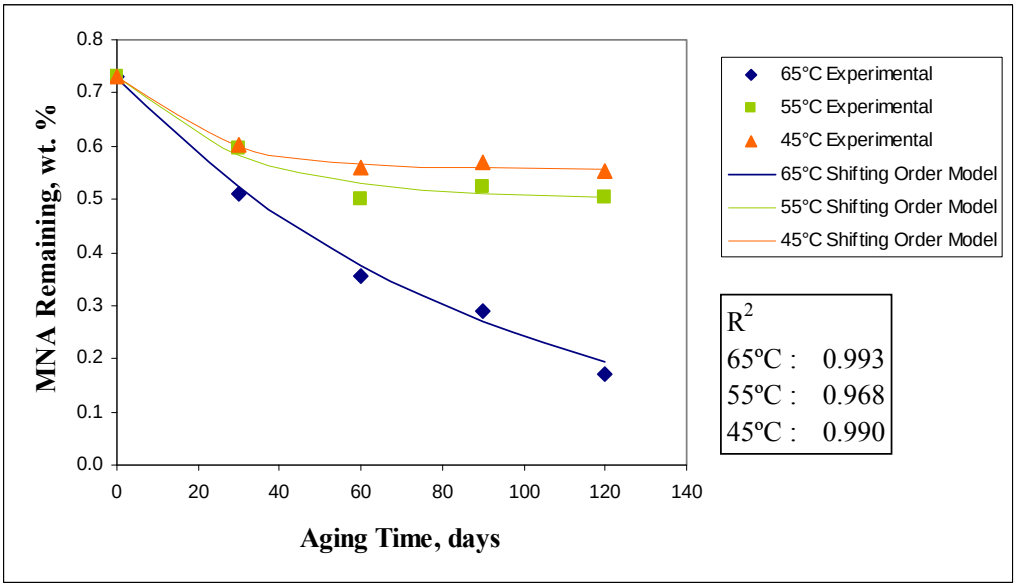

Figure 4.10 Depletion of MNA in XLDB-3 Propellant Samples – Description by a Shifting Order Model

It is seen from Figure 4.10 that at low temperatures the concentration of the stabilizer, MNA, reaches a limiting value at the final stages of aging period. This means that at low temperatures the stabilizer will never be exhausted theoretically; the weight percent of the remaining MNA will never drop under a certain value.

Pseudo first order model fit for the depletion of MNA in XLDB-3 propellant is shown in Figure 4.11, together with the experimental data. The coefficients of determination for the pseudo first order model equation are also shown in the figure.

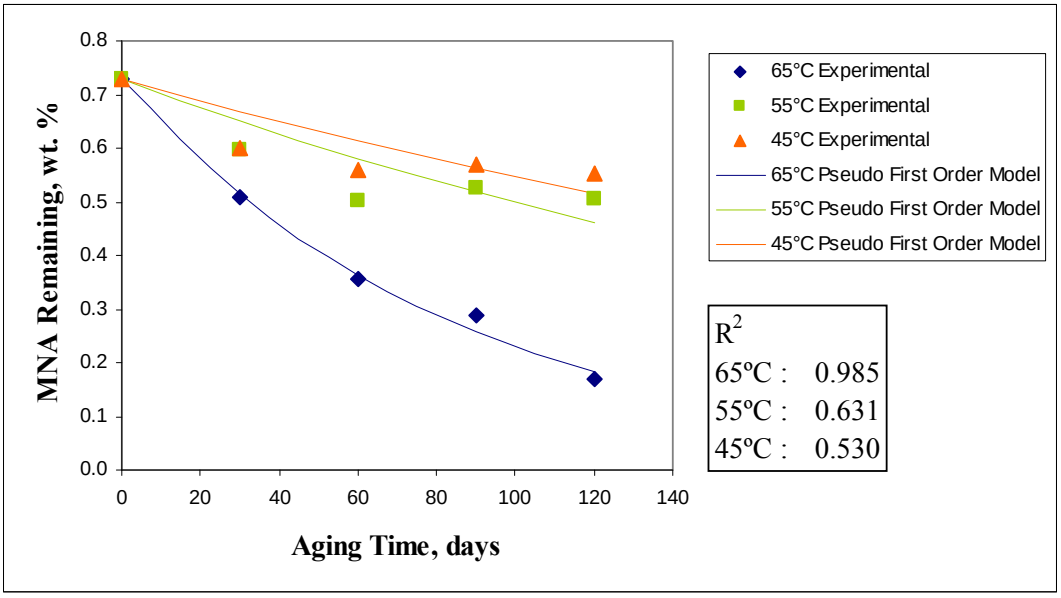

Figure 4.11 Depletion of MNA in XLDB-3 Propellant Samples – Description by a Pseudo First Order Model

It is seen from Figure 4.11 that the pseudo first order model gives good estimation of the depletion reaction at 65°C. However, at low temperatures, 45 and 55°C, the model produces poor results.

4.2.4 Determination of Arrhenius Parameters

After obtaining a series of rate constants at different temperatures, the variation of the rate constant with temperature is determined by the Arrhenius equation. By using Equation 1.11, plotting *lnk* versus *1/T*, and determining the slope of the line, *-E/R*, the value for the activation energy was determined. The plot for the depletion of 2-NDPA in XLDB-1 propellant is given in Figure 4.12. From the figure it is seen that the slope of the line, *-E/R*, is calculated as -20,527, and the intercept, *lnA*, was calculated as 55.234. Hence, the activation energy, *E*, was calculated as 170,668 J/mol, and the frequency factor, *A*, was calculated as 9.72×10^{23} $days^{-1}$.

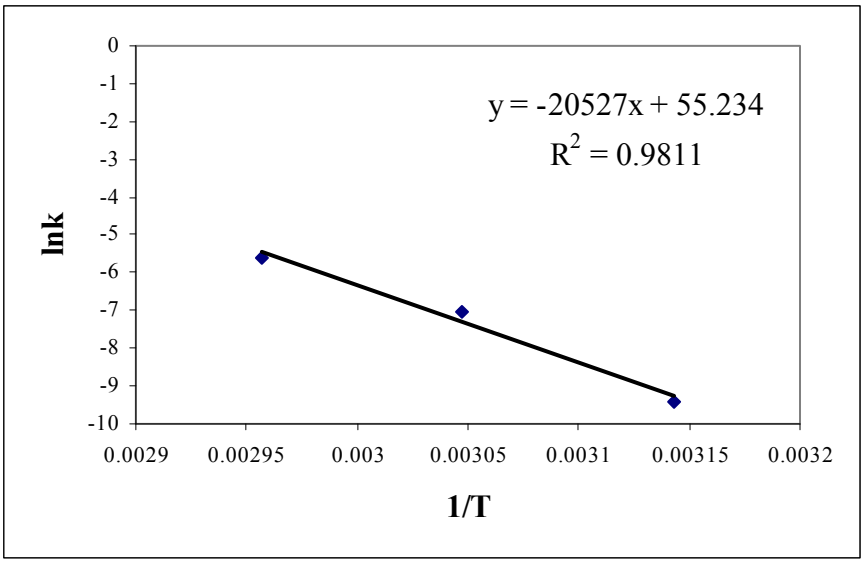

Figure 4.12 Determination of Arrhenius Parameters for the Depletion of 2-NDPA in XLDB-1

Using the rate constants given in Table 4.4, the kinetic parameters, namely activation energy and frequency factor, were obtained for all propellants, using the same way. The values are given in Table 4.6. Arrhenius plots are given in

Appendix F. Note that kinetic parameters for the pseudo first order kinetic model were calculated for the depletion of MNA in XLDB-3 propellant.

Using the kinetic parameters in Arrhenius equation (Equation 1.10) the reaction rate constants at room temperature (23°C) were calculated. These values are also given in Table 4.6. Note that the parameters are for the depletion of 2-NDPA for the first two propellants and for the depletion of MNA for the third propellant. It is seen from the table that the parameters are very close for the first two propellants. The rate constants for the depletion of 2-NDPA in these propellants are nearly the same.

Table 4.6 Arrhenius Parameters and Rate Constants for the Stabilizer Depletion Reaction for All Propellants

Propellant	E, J/mole	A, $days^{-1}$	k at 23°C, $days^{-1}$
XLDB-1*	170,668	9.72×10^{23}	7.42×10^{-7}
XLDB-2*	171,208	1.28×10^{24}	7.81×10^{-7}
XLDB-3**	61,596	3.26×10^{7}	4.40×10^{-4}

* Depletion of 2-NDPA

** Depletion of MNA

From Table 4.6, it is also seen that the rate of depletion of MNA in XLDB-3 is greater than the rate of depletion of 2-NDPA in first two propellants. Lower activation energy for the depletion of MNA shows that this stabilizer reacts with the degradation products more readily than the stabilizer 2-NDPA.

4.2.5 Evaluation of Chemical Life

When evaluating the stability and shelf life of propellants based on stabilizer depletion, criteria related with the rate of depletion of the stabilizer or with the amount of residual stabilizer could be used. Usually, these criteria are limits of acceptance such as a maximum allowable depletion rate or a minimum amount of residual stabilizer for the safe usage of the propellant up to a certain time. Moreover, the chemical life of a propellant could be determined by calculating the time to reach any specified level of stabilizer depletion at a particular temperature using kinetic equations.

For single base (SB) propellants containing DPA, limits of acceptance are given in NATO STANAG 4117 [31]; Satisfactory chemical stability for a period of storage of 10 years requires that either one of the following to be satisfied:

1. After the heating period of 60 days at 65°C the decrease in DPA level must not exceed **0.3%** and the minimum level found by analysis must be **0.6%**.
2. After the heating period of 120 days at 65°C the decrease in DPA level must not exceed **0.5%** and the minimum level found by analysis must be **0.3%**.

As an assumption, these limits could be used to determine the stability of DB and XLDB propellants containing 2-NDPA, which is one of the first derivatives of DPA. The decrease in 2-NDPA level and the remaining 2-NDPA amounts for XLDB-1 and XLDB-2 propellants aged for 60 days and 120 days at 65°C are given in Table 4.7.

It is seen from the table that all XLDB-1 and XLDB-2 satisfy the criterion 1. Although the amount of remaining stabilizer is greater than 0.3%, the decrease in 2-NDPA exceed 0.5% for these propellants.

Table 4.7 Decrease in 2-NDPA and Remaining 2-NDPA for the Propellants Aged at 65°C

Propellant	Aged for 60 days		Aged for 120 days	
	Decrease in 2-NDPA	Remaining 2-NDPA	Decrease in 2-NDPA	Remaining 2-NDPA
XLDB-1	0.18	1.06	0.57	0.67
XLDB-2	0.29	0.95	0.74	0.51

According to the results given in Table 4.7, two propellants have a minimum shelf life of 10 years; however, the fact that XLDB-1 and XLDB-2 do not satisfy criterion 2 of STANAG 4117 makes this results questionable. It is obvious that criterion 1 could be satisfied by changing the initial stabilizer content; however, criterion 2 is independent of the initial content and it is a better indication of stability.

The limits of acceptance given in STANAG 4117 could be used to estimate the chemical life of the propellants; the time for residual 2-NDPA to reach 0.3% or the time for 0.5% decrease in 2-NDPA level at room temperature can be calculated. Another criteria used in many studies in the literature [19, 29 and 32] is more reasonable and suitable for the propellants in this study; for a satisfactory chemical stability of 2-NDPA containing propellants the stabilizer level must not decrease below the half of the initial level. Using the kinetic data given above, the chemical lives of all propellants were calculated for storage at 23°C. The results are given in Table 4.8. It is obvious that the values in Table 4.8 are very high and unreasonable. It should be noted that if the first two criterion are considered, the chemical life could be altered by controlling the initial amount of 2-NDPA.

Table 4.8 Chemical Lives of 2-NDPA Containing Propellants for Storage at 23°C and for Different Limits of Acceptance – Pseudo Zero Order Kinetics

	Chemical Life at 23°C, Years		
Limit of Acceptance:	**0.3% 2-NDPA Remaining**	**0.5% Decrease in 2-NDPA**	**Half life of 2-NDPA**
XLDB-1	2798	1490	1846
XLDB-2	2661	1411	1754

The chemical life of XLDB-3 should be determined based on the depletion of MNA, which reacts with the degradation products more readily than 2-NDPA as stated above. In the literature [26], minimum allowable level of remaining MNA is given as 0.1%. This value and "the half life of the stabilizer" could be used as limits of acceptance for the satisfactory chemical life of XLDB-3. Using the pseudo first order kinetic data obtained for the depletion of MNA in XLDB-3, the chemical life of the propellant was calculated for storage at 23°C. The results are given in Table 4.9.

Table 4.9 Chemical Life of XLDB-3 for Storage at 23°C and for Different Limits of Acceptance – Pseudo First Order Kinetics

	Chemical Life at 23°C, Years	
Limit of Acceptance:	**0.1% MNA Remaining**	**Half life of MNA**
XLDB-3	12	4

It is seen from the table that the chemical life of XLDB-3 is quite shorter than the chemical lives of XLDB propellants containing 2-NDPA. However, 12 years at 23°C for 0.1% MNA remaining is a very reasonable value. It should be noted that the initial level of MNA in XLDB-3 is 0.73%, and the chemical life of

this propellant could be increased by using higher amounts of MNA at the beginning. However the amount should be limited to a certain value since the mechanical and ballistic properties deteriorate above certain values of this additive.

The values for the chemical life of XLDB propellants containing 2-NDPA are not comparable with the value for XLDB-3. Sometimes, as in this case, calculating the chemical life does not make sense. Therefore, the stability of the propellants should be compared by comparing the reaction rates for the depletion of the stabilizer. For example, Andrade et al. [34] compared the activation energy and frequency factor value for the pseudo first order depletion of 2-NDPA in a DB propellant with the values for the depletion of DPA in different SB propellants. Since the reaction rate at a certain temperature can be calculated using the activation energy and the frequency factor, this is same as comparing the reaction rates for the depletion.

The comparison of the activation energies, frequency factors and reaction rate constants at 23°C of XLDB propellants with the literature [16, 19, 26, 29, and 34] can be seen in Table 4.10. Note that the values for XLDB-3 were calculated using the pseudo first order model estimation. The activation energy values are given in kcal/mol for comparison. The reaction rate constants of the literature propellants are calculated using the given activation energy and frequency factor values.

From Table 4.10, it is seen that the activation energy values of XLDB propellants are comparable with the literature [16, 19, 26, 29, and 34]. Only the activation energy for XLDB-3 is quite different. Lower activation energy means less variation of the reaction rate constant with temperature. It also means lower activation barrier so the reactants can form products at a faster rate. Therefore, it means less stable propellant. However, for XLDB-3, lower activation energy does not mean less stability, because XLDB-3 contains both MNA and 2-NDPA and MNA reacts with the degradation products more readily than 2-NDPA. The stability of the propellant increases when the stabilizers MNA and 2-NDPA are used together, as in the case of XLDB-3.

Table 4.10 Comparison of the Kinetic Parameters of XLDB Propellants with the Parameters of SB, DB, CMDB and HTPE Propellants in Literature

Propellant	E, kcal/mole	A, $days^{-1}$	k at 23°C, $days^{-1}$
XLDB-1*	41	9.72×10^{23}	7.42×10^{-7}
XLDB-2*	41	1.28×10^{24}	7.81×10^{-7}
XLDB-3**	15	3.26×10^{7}	4.40×10^{-4}
SB-1 [16] ***	31	7.82×10^{12}	1.79×10^{-10}
SB-2 [34] ***	32	10^{22}	5.08×10^{-2}
SB-3 [34] ***	31	10^{18}	1.15×10^{-5}
DB-1 [34] *	29	10^{16}	2.96×10^{-6}
DB-2 [19] *	34	-	-
CMDB [29] *	32	-	-
HTPE [26] **	29	2.42×10^{7}	9.35×10^{-15}

* Depletion of 2-NDPA

** Depletion of MNA

*** Depletion of DPA

The reaction rate constant for the depletion of MNA in XLDB-3 is the second largest of the rate constants for all propellants. The largest one is for the depletion of DPA in SB-2 propellant. Although the activation energy for SB-2 propellant, 32 kcal/mol, is not very small, the rate constant is large because the frequency factor is very large.

Higher activation energy means higher activation barrier so the reactants form products at a slower rate. Rate constants for XLDB-1 and XLDB-2 are very close and they are lower than the rate constants for the other XLDB propellants. It is seen from the table that XLDB-1 and XLDB-2 have the highest values of activation energy.

A value of 33 kcal/mol for the activation energy corresponds to the energy required for cleavage of $RO\text{-}NO_2$ bonds in nitric esters [29]. Hence, the rate

determining step during the aging of the propellants that have activation energies near 33 kcal/mol is the decomposition of nitric esters.

Reaction rate constant for the XLDB propellants that contain 2-NDPA are smaller than the rate constants for the SB-2, SB-3 and DB-1 propellants. On the other hand SB-1 propellant has a smaller reaction rate constant. It could be concluded that XLDB propellants that contain 2-NDPA are more stable than the DB-1 propellant of Andrade et al. [34] and have comparable stability with SB propellants that contain DPA. XLDB-3 propellant, which contains MNA, has a higher reaction rate constant than the HTPE propellant. Hence, XLDB-3 propellant is less stable than the HTPE propellant. HTPE propellant is a composite propellant and it has lower nitrate ester content than the SB, DB and XLDB propellants.

Nitrate ester degradation might be the main aging mechanism for XLDB propellants; however, it is not the only one. Migration, gas formation and others may also affect the properties of the aged propellant. Visual inspection of the aged propellants might give ideas about the stability. Pictures of XLDB-1 propellant samples aged for 120 days at 45, 55 and 65ºC are given in Figure 4.13.

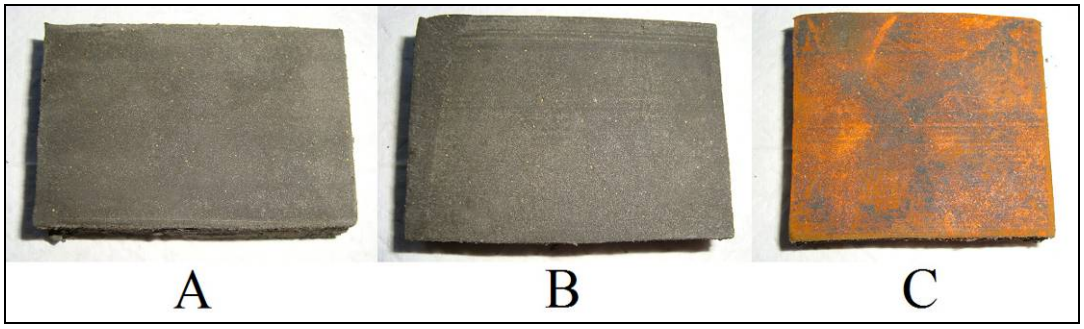

Figure 4.13 XLDB-1 Aged for 120 days at (A) 45°C, (B) 55°C and (C) 65°C

It is seen from Figure 4.13 that there is no visual change in propellant samples aged at 45 and 55ºC. However, the rejection (puking) and migration of a substance or substances in propellant sample aged at 65ºC is clearly seen. These are most probably the derivatives of 2-NDPA. It is found by FTIR that they have the same functional groups with 2-NDPA. Therefore, it is reasonable that this

substance or substances are high molecular weight derivatives of 2-NDPA, which are not soluble in the propellant matrix. The FTIR plots for 2-NDPA and migrated unknown substance/s are given in Appendix G.

Pictures of XLDB-2 propellant samples aged for 120 days at 45, 55 and 65ºC are given in Figure 4.14. It is seen that the sample aged at 45ºC shows no signs of visual change. However, there are signs of rejection and migration for the samples aged at 55 and 65ºC. The migration is very low for the sample aged at 55ºC and very high for the sample aged at 65ºC.

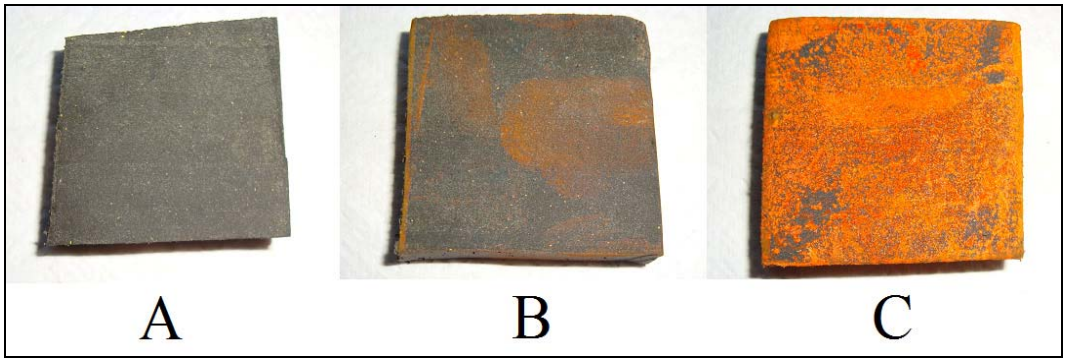

Figure 4.14 XLDB-2 Aged for 120 days at (A) 45°C, (B) 55°C and (C) 65°C

As stated above, the only difference in XLDB-1 and XLDB-2 propellants is that the latter contains additional plasticizer, BTTN. Therefore, XLDB-2 having more rejection and migration can be explained as the rejected substances have less solubility in BTTN or BTTN accelerates the degradation of the propellant and the formation of these substances. Table 4.7 shows that the depletion of 2-NDPA in XLDB-2 propellant is higher than the depletion of this stabilizer in XLDB-1 propellant. Hence, it is reasonable that the formation of stabilizer derivatives in XLDB-2 propellant is higher. Therefore, it could be expressed that although the calculated rate constants for the depletion of 2-NDPA are very close for the two propellants (See Table 4.10), XLDB-2 is less stable than XLDB-1.

On the other hand, it is seen from Table 4.4 that the reaction rate constants for XLDB-2 at 45 and 65ºC are higher than the ones for XLDB-1, but the rate

constant for XLDB-2 at 55ºC is lower than the one for XLDB-1. This may be caused by experimental errors in the determination of 2-NDPA by HPLC; the derivatives of 2-NDPA may be accounted in the calculation of the remaining 2-NDPA in XLDB-2 sample aged at 55ºC. Alternatively, the substance that migrates may be 2-NDPA itself.

Pictures of XLDB-3 propellant samples aged for 120 days at 45, 55 and 65ºC are given in Figure 4.15. It is seen from the figure that there are no signs of rejection or migration or any other visual change for XLDB-3. This propellant, containing the combination of 2-NDPA and MNA as stabilizer, may also be expressed as more stable than XLDB-1 and XLDB-2 propellants. It is seen that derivatives of MNA did not migrate during aging. Using 2-NDPA together with MNA definitely increases the stability of a propellant.

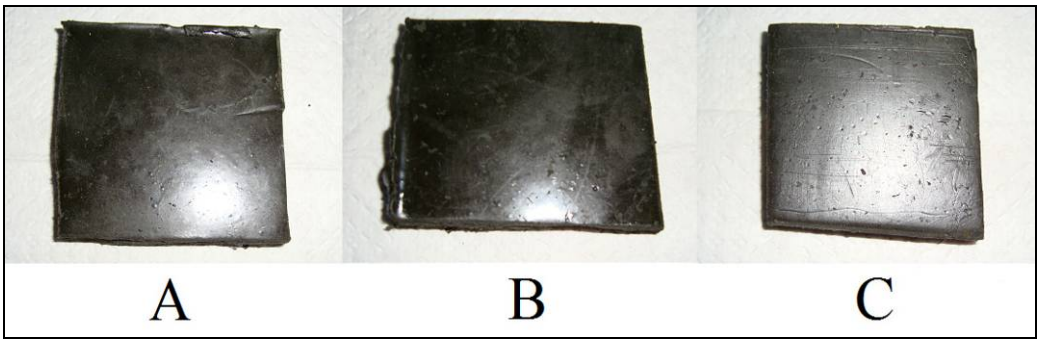

Figure 4.15 XLDB-3 Aged for 120 days at (A) 45°C, (B) 55°C and (C) 65°C

XLDB-1 and XLDB-2 propellant blocks of about 12 cm × 12 cm × 15 cm were also aged at 65°C. The pictures of aged XLDB-1 propellant block are given in Figure 4.16.

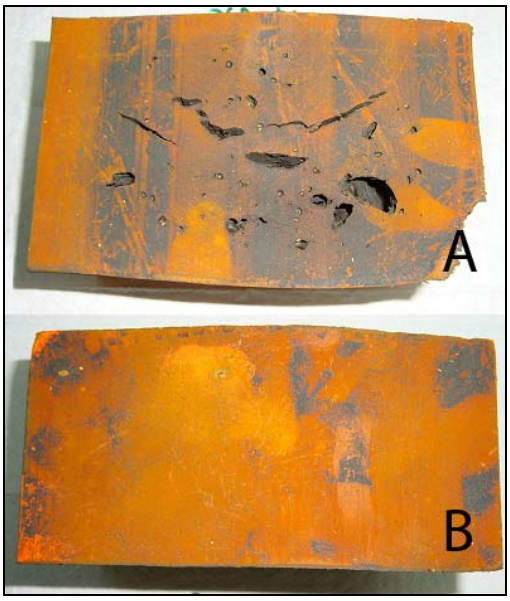

Figure 4.16 XLDB-1 Propellant Block Aged at 65°C for 120 days; (A) Cross-Section (B) Outer Surface

It is seen from the figure that there are cracks and void formation due to excess gas generation. This means that the kinetics of the gas generation is greater than the rate of diffusion of the gases to the atmosphere. Moreover, the rejection and migration of the stabilizer and/or its derivatives is clearly seen.

The pictures of XLDB-2 propellant block are given in Figure 4.17. It is seen from the figure that there are cracks and voids in aged XLDB-2 propellant block. Just like for XLDB-1, the kinetics of the gas generation is again greater than the rate of diffusion of these gases. The number and the size of the cracks and holes in XLDB-2 propellant block are very close to the ones in XLDB-1 propellant. On the other hand, the amount of migration is larger in XLDB-2 than in XLDB-1. Also the rejected particles in XLDB-2 propellant block are larger in size.

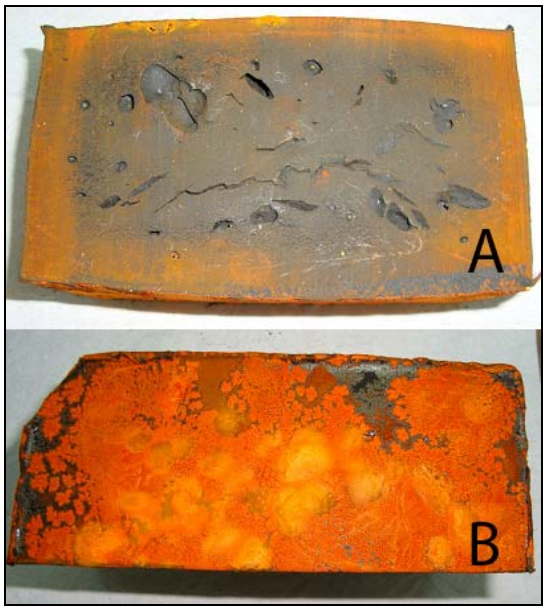

Figure 4.17 XLDB-2 Propellant Block Aged at 65°C for 120 days;
(A) Cross-Section (B) Outer Surface

It could be concluded that XLDB-1 and XLDB-2 propellants have similar stability when the block samples are examined visually for physical changes.

CHAPTER 5

CONCLUSIONS

Vacuum thermal stability and stabilizer depletion methods are extensively applied to estimate the chemical stability and shelf life of nitrate ester containing double-base propellants. However, there is limited information on the shelf life of XLDB propellants and the most effective method is still undecided.

In this study, the stability of three different XLDB propellants stabilized with 2-NDPA and MNA were determined by vacuum thermal stability tests. Comparable stability data with the literature [29] has been obtained. It has been found that the stability of XLDB-1 and XLDB-2 are the same, and it is higher than the stability of XLDB-3. Using the energetic plasticizers BTTN and BDNPA/F together in XLDB-2 did not change the stability when compared with XLDB-1, which includes BDNPA/F only. The gas generation value of 2.62 ml/g for XLDB-3 is higher than the value of 1.50 ml/g for the other two propellants. Hence XLDB-3 has lower stability than the other XLDB propellants based on the VTS tests. Using MNA together with 2-NDPA did not increase the stability of XLDB-3; hence, MNA, which is more reactive, is not always considered as a better stabilizer over 2-NDPA when they are used together.

Shelf lives of the XLDB propellants were determined by using the stabilizer depletion method. The depletion of stabilizers was monitored by HPLC and experimental data were recorded for three elevated aging temperatures, 45, 55 and 65°C. Kinetic models of pseudo zero, pseudo first, pseudo second and shifting order were used to find the best model equation that fits the experimental data. Coefficient of determination values (R^2) were used to select the best fit. It was

found that pseudo zero order kinetic model describes the depletion of 2-NDPA in XLDB-1 and XLDB-2 propellants best; on the other hand, shifting order kinetic model describes the depletion of MNA in XLDB-3 propellant best. However, pseudo first order kinetic model was used to determine the chemical life of XLDB-3 propellant, since kinetic parameters of the shifting order model were complicated and unreasonable.

The rates of depletion of stabilizers were calculated at three temperatures. The reaction rate constants were also calculated based on the kinetic models. Using the rate constants at different temperatures rate constant for the stabilizer depletion reaction at room temperature (at storage conditions) was calculated using Arrhenius equation. The activation energy and frequency factor for the depletion reaction of 2-NDPA and MNA were obtained for all XLDB propellants. The results were comparable with the literature [16, 19, 26, 29, and 34]. Moreover, the results were evaluated based on the NATO standard; STANAG 4117 and all XLDB propellants were found to satisfy the requirement of a minimum shelf life of 10 years.

Calculation of the chemical life of the propellants revealed unreasonable results due to very low reaction rate constants. However, the kinetic data obtained were comparable with the literature data for double and SB propellants containing 2-NDPA and DPA, respectively. Moreover, the chemical life of XLDB-3, which contains both 2-NDPA and MNA, was calculated as 12 years at 23°C. This value is reasonable and comparable with the data in literature [26].

Rejection (puking) and migration of derivatives of the stabilizer, which are not soluble in the propellant matrix, was observed in XLDB-1 and XLDB-2 samples aged at 65°C. Formation of voids and cracks due to gas generation was also observed in the block samples of XLDB-1 and XLDB-2 aged at 65°C. However, it should be kept in mind that some reactions may occur at elevated temperatures; which otherwise would not take place at storage conditions.

CHAPTER 6

RECOMMENDATIONS

As a recommendation, in order to fully understand the aging mechanism in XLDB propellants,

- Increased number of elevated temperatures (e.g. 30 – 80°C) can be used as aging temperatures,
- Detailed analysis of the stabilizer derivatives can be done (Formation and depletion of the derivates can be monitored),
- Vacuum Thermal Stability of an unstabilized propellant can be evaluated,
- Migration and gas fissuring in an unstabilized propellant can be inspected after accelerated aging,
- Change in other properties (e.g. mechanical, ballistic, etc.) can be monitored throughout artificial aging.

Surveillance of the rocket motor as a whole throughout the aging period would give the most realistic results for the property changes and chemical life of the propellant.

REFERENCES

1. Couturier, R., *Advanced Energetic Binder Propellants*, In A. Davenas (Ed.), Solid Rocket Propulsion Technology, pp. 477-524, Pergamon Press, 1993.

2. Klager, K., Wrightson, J.M., *Recent Advances in Solid Propellant Binder Chemistry*, Mechanics and Chemistry of Solid Propellants, Pergamon Press, 1970.

3. Manjari, R., Somasundaran, U.I., Joseph, V.C., Sriram, T., *Structure-property relationship of HTPB-based propellants. II. Formulation tailoring for better mechanical properties*, Journal of Applied Polymer Science, Volume 48, Issue 2, pp. 279-289, 2003.

4. Cunliffe, A.V., Farey, M., Davis, A., Wright, J., *Kinetics of the reaction of isophorone di-isocyanate with mono-alcohols*, Polymer, Volume 26, pp. 301-306, 1985.

5. Saunders, J.H., Frisch, K.C., *Polyurethanes Chemistry and Technology*, Robert E. Krieger Publishing Company, p.73, 1978

6. Goethals, E.J., *Telechelic Polymers: Synthesis and Applications* CRC Press, Boca Raton, FL, 1989.

7. Entelis, S.G., Evreinov, V.V., and Gorshkov, A.V., *Functionality and molecular weight distribution of Telechelic polymers*, Advances in Polymer Science, Volume 76, pp. 129-175, 1986.

8. Sairiala, M.E., *Composite Propellant Aging; SEM and Chemical Examinations*, Paper presented at the meeting of Insensitive Munitions – The Effect of Aging upon Lifecycle Workshop, Helsinki, Finland, May 2005.

9. Göçmez, A., Erişken, C., Yılmazer, Ü., Pekel, F., Özkar, S., *Mechanical and Burning Properties of Highly Loaded Composite Propellants*, Journal of Applied Polymer Science, vol. 67, pp. 1457-1464, 1998.

10. Verneker, V.R.P., Kishore, K., *Mechanism of Thermal Decomposition of Double Base Propellants*, Propellants Explosives Pyrotechnics, Volume 8, p. 77, 1983.

11. Lindblom, T., *Reactions in the System Nitro-cellulose/Diphenylamine with Special Reference to the Formation of a Stabilizing Product Bonded to Nitro-cellulose*, Comprehensive Summaries of Uppsala Dissertations from the Faculty of Science and Technology, Acta Universitatis Upsaliensis, Uppsala, 2004.

12. Austruy, H., *Double Base Propellants*, In A. Davenas (Ed.), Solid Rocket Propulsion Technology, pp. 369-413, Pergamon Press, 1993.

13. Urbanski, T., *Chemistry and Technology of Explosives, Volume 4*, Pergamon Press, 1984.

14. Bohn, M.A., Volk, F., *Aging Properties of Propellants Investigated by Heat Generation, Stabilizer Consumption and Molar Mass Degradation*, Propellants Explosives Pyrotechnics, Volume 17, p. 171-178, 1992.

15. Lindblom, T., Christy, A.A., Libnao, F.O., *Quantitative determination of stabilizer in a single base propellant by chemometric analysis of Fourier transform infrared spectra*, Chemometrics and Intelligent Laboratory Systems, Volume 29, pp. 243-254, 1995

16. Jelisavac, L., Filipovic, M., *A kinetic model for the consumption of stabilizer in single base gun propellants*, Journal of the Serbian Chemical Society, Volume 67 (2), pp.103-109, 2002

17. Jelisavac, L., Filipovic, M., *Determination of Diphenylamine and its Mono-Derivatives in Single-Base Gun Propellants During Aging by High Performance Liquid Chromatography*, Chromatographia, Volume 55, pp.239-241, 2002

18. Volk, F., *Determining the Shelflife of Solid Propellants*, Propellants and Explosives, Volume 1, pp.59-65, 1976

19. Volk, F., Wunsch, G*., Determination of the Decomposition Behavior of Double Base Propellants at Low Temperatures*, Propellants Explosives Pyrotechnics, Volume 10, p. 181-186, 1985

20. Volk, F., Bohn, M.A., Wunsch, G*., Determination of Chemical and Mechanical Properties of Double Base Propellants During Aging*, Propellants Explosives Pyrotechnics, Volume 12, p. 81-87, 1987

21. Bellerby, J.M., Sammour, M.H., *Stabilizer Reactions in Cast Double Base Rocket Propellants. Part: 1 HPLC Determination of Stabilizer and Their Derivatives in a Propellant Containing the Stabilizer Mixture pNMA and 2-NDPA Aged at 80°C and 90°C*, Propellants Explosives Pyrotechnics, Vol. 16, pp.235-239, 1991

22. Bixon, E.R., Lopez, L., *Stabilizer Comparison for Single Base Propellant Formulations*, 37th International Annual Conference of ICT, June 27 -June 30, 2006, Karlsruhe, Federal Republic of Germany

23. Pettersson, M.L., Eldsater, C., *Stability Study of Smokeless Propellants of up to 60 Years of Age as Measured by Heat Flow Calorimetry*, 37th International Annual Conference of ICT, June 27 - June 30, 2006, Karlsruhe, Federal Republic of Germany

24. Hocaoğlu, Ö., Özbelge, T., Pekel, F., Özkar, S., *Aging of HTPB/AP-Based Composite Solid Propellants, Depending on the NCO/OH and Triol/Diol Ratios*, Journal of Applied Polymer Science, Vol. 79, pp. 959-964, 2001

25. Judge, M.D., *An Investigation of Composite Propellant Accelerated Aging Mechanisms and Kinetics*, Propellants Explosives Pyrotechnics, Volume 28, pp. 114-119, 2003

26. Fletcher, W.G., Comfort, T.F., *Updates on HTPE Propellant Service Life*, ATK Tactical Systems Company, Allegany Ballistics Laboratory Rocket Center, 2005

27. Sridhar, B.T.N., Ravichandran, K., Nagappa, R., 37th International Annual Conference of ICT, June 27 - June 30, 2006, Karlsruhe, Federal Republic of Germany

28. Doall, J.O., Juhasz, A. A., *Determination of 2-NDPA in a Composite Modified Double Base Propellant by HPLC*, Analytical Chemistry, Vol. 48, No: 13, November, 1976

29. Asthana, S.N., Divekar, C. N., *Singh, H., Studies on Thermal Stability, Autoignition and Stabilizer Depletion for Shelf Life of CMDB Propellants*, Journal of Hazardous Materials, Vol. 21, pp. 35-46, 1989

30. Bellerby, J.M., Sammour, M. H., *Stabilizer Reactions in Cast Double Base Rocket Propellants. Part: II: Formation and Subsequent Reactions of N-Nitroso Derivatives of para-Nitro-N-methylaniline and 2-Nitro-diphenylamine in Mixed Stabilizer Propellants Aged at 80°C and 90°C*, Propellants Explosives Pyrotechnics, Vol. 16, pp. 273-278, 1991

31. NATO STANAG 4117 - Explosives, Stability Test Procedures and Requirements for Propellants Stabilized with DPA, EC or Mixtures of Both

32. Raha, K.C., Adhav, S.S., Bhide, N.M., Yewale, A.D., Gupta, G.K., Karir, J.S., *Thermal Stability and Shelf-life of High Energy Fuel for Torpedoes*, Defence Science Journal, Vol. 52, No. 2, pp. 165-171, 2002

33. NATO STANAG 4527 - Explosive, Chemical Stability, Nitrocellulose Based Propellants, Procedure for Assessment of Chemical Life and Temperature Dependence of Stabilizer Consumption Rates

34. Andrade, J., Iha, K., "Rocco, J.A.F.F., Franco, G.P., Moreira, E.D., Suarez-Iha, M.E.V., *Estudo da cinética de consumo do estabilizante 2NDPA no propelente base dupla*, Ecl. Quím., Vol. 32(4), pp. 7-12, 2007, São Paulo

APPENDIX A

VACUUM THERMAL STABILITY TEST RESULTS

The volume of gas evolved from XLDB propellant samples was measured by a pressure transducer that converts the voltmeter readings into pressure by the vacuum thermal stability instrument (STABIL). Gas pressures versus time graphs are given below in Figure A.1, Figure A.2 and Figure A.3, respectively for XLDB-1, XLDB-2 and XLDB-3. The values for the volume of the gas evolved are calculated by the software of the instrument and are also given in the figures.

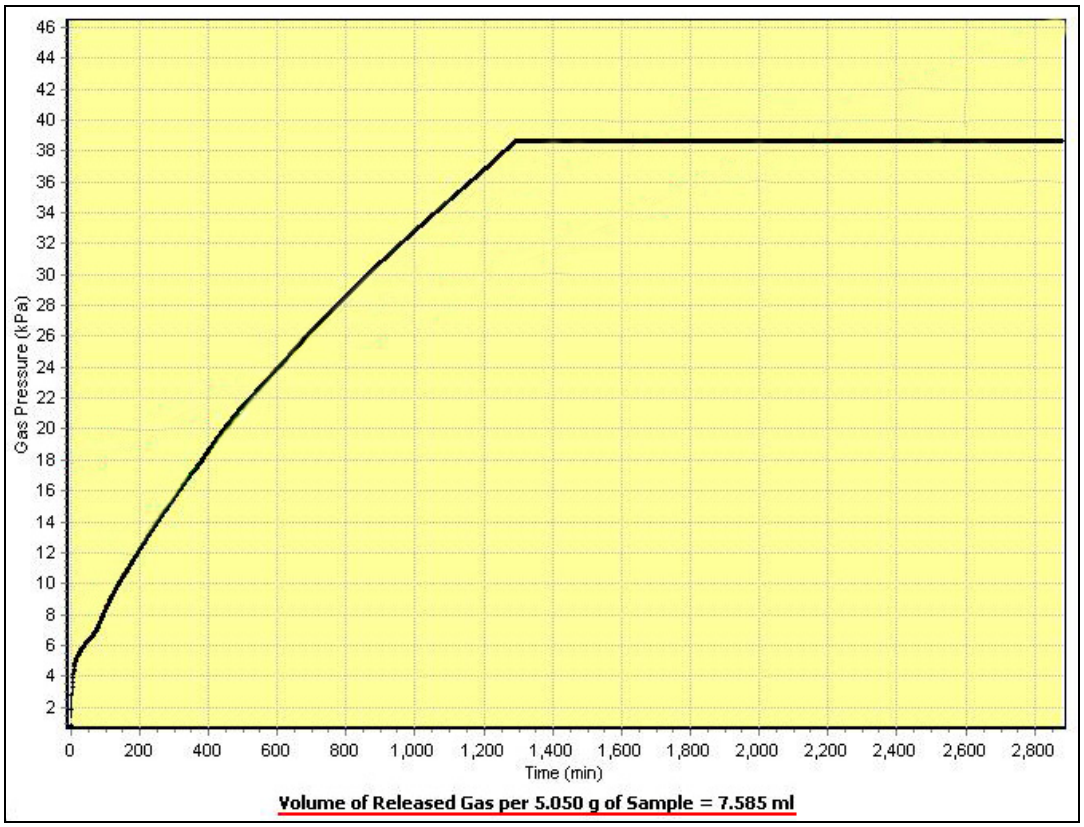

Figure A.1 Vacuum Thermal Stability Test Result for XLDB-1

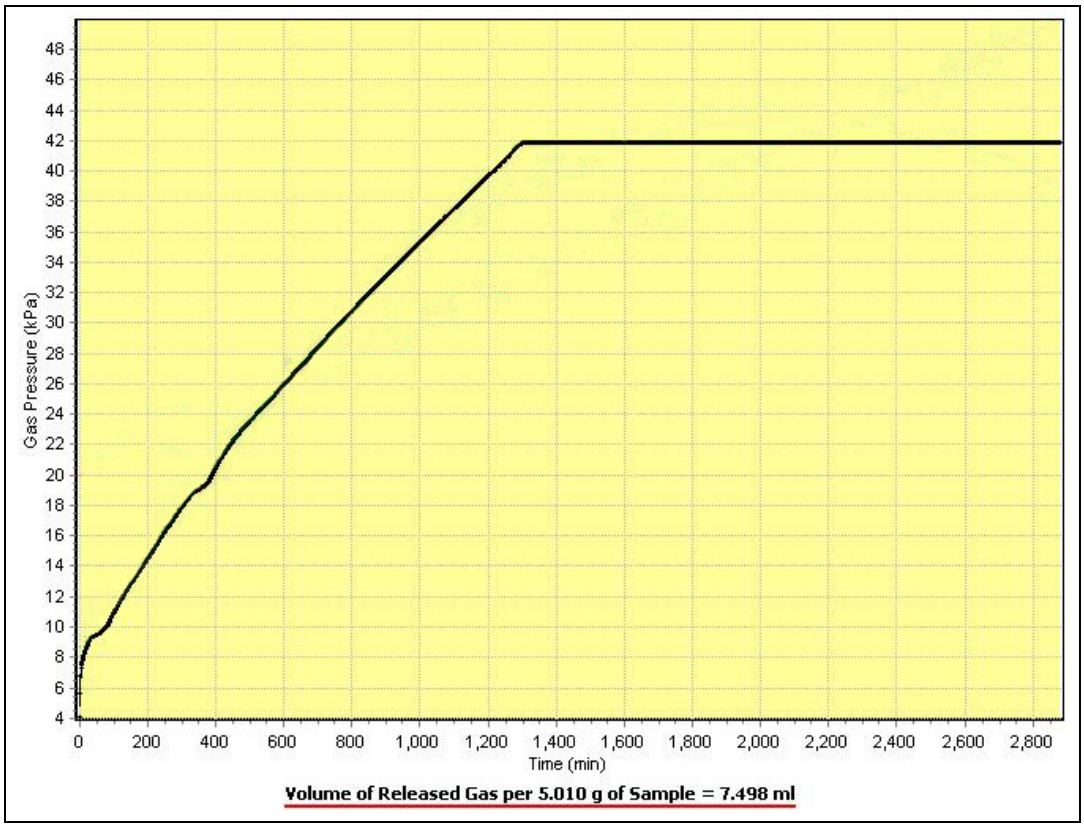

Figure A.2 Vacuum Thermal Stability Test Result for XLDB-2

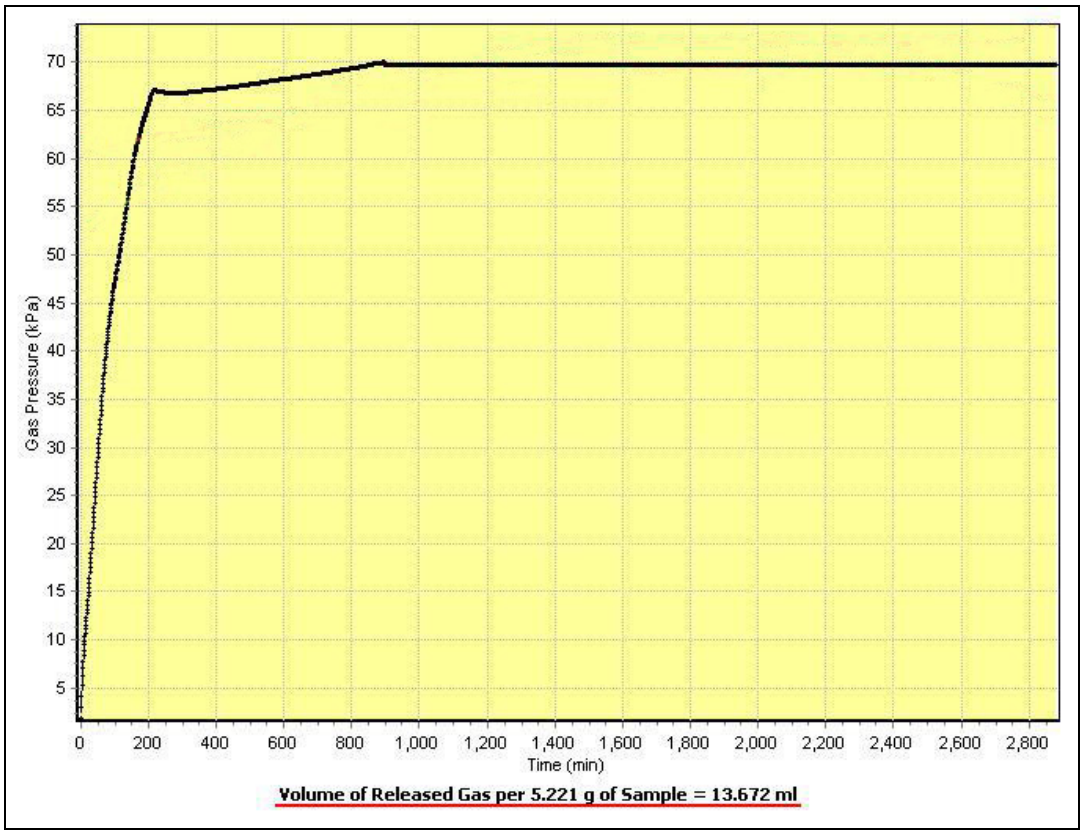

Figure A.3 Vacuum Thermal Stability Test Result for XLDB-3

APPENDIX B

LC-MS CHROMATOGRAMS OF PROPELLANT SAMPLES

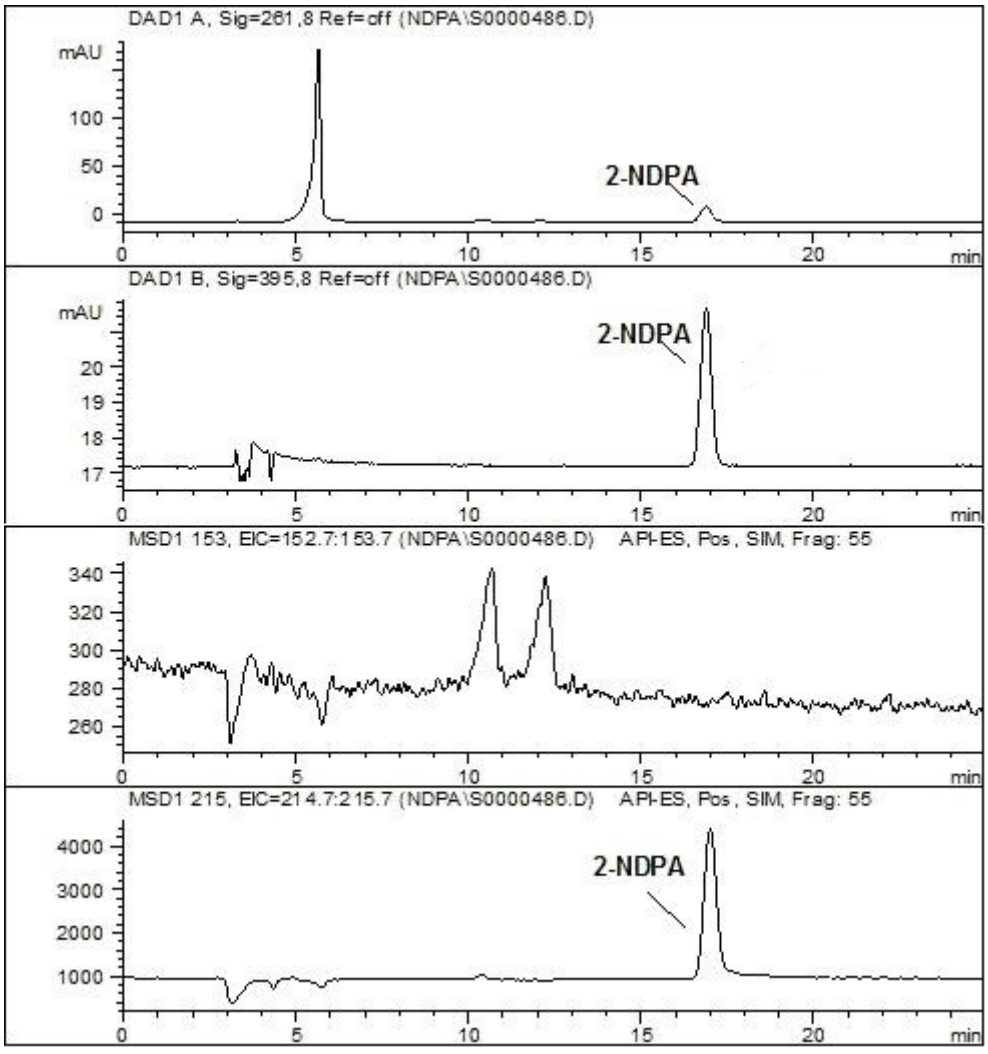

Figure A.4 Chromatograms for Unaged XLDB-1

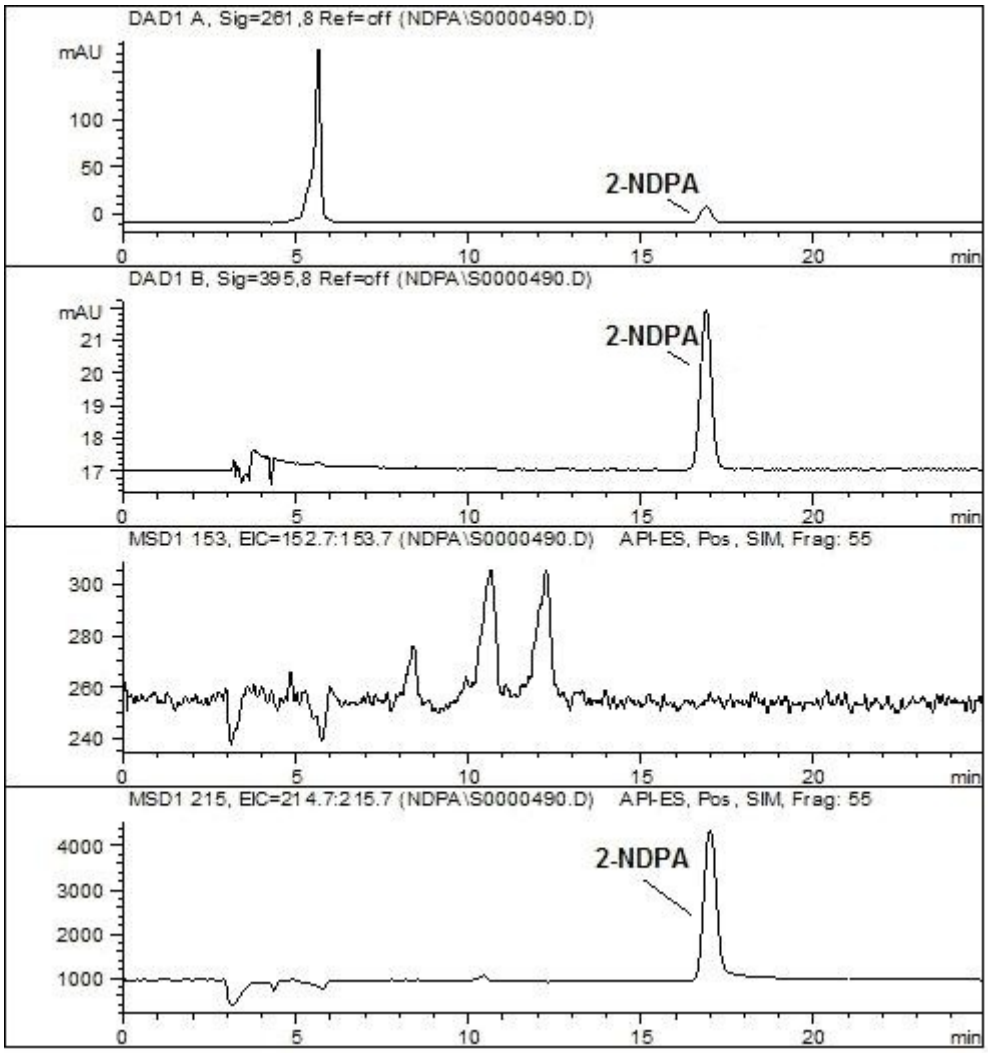

Figure A.5 Chromatograms for Unaged XLDB-2

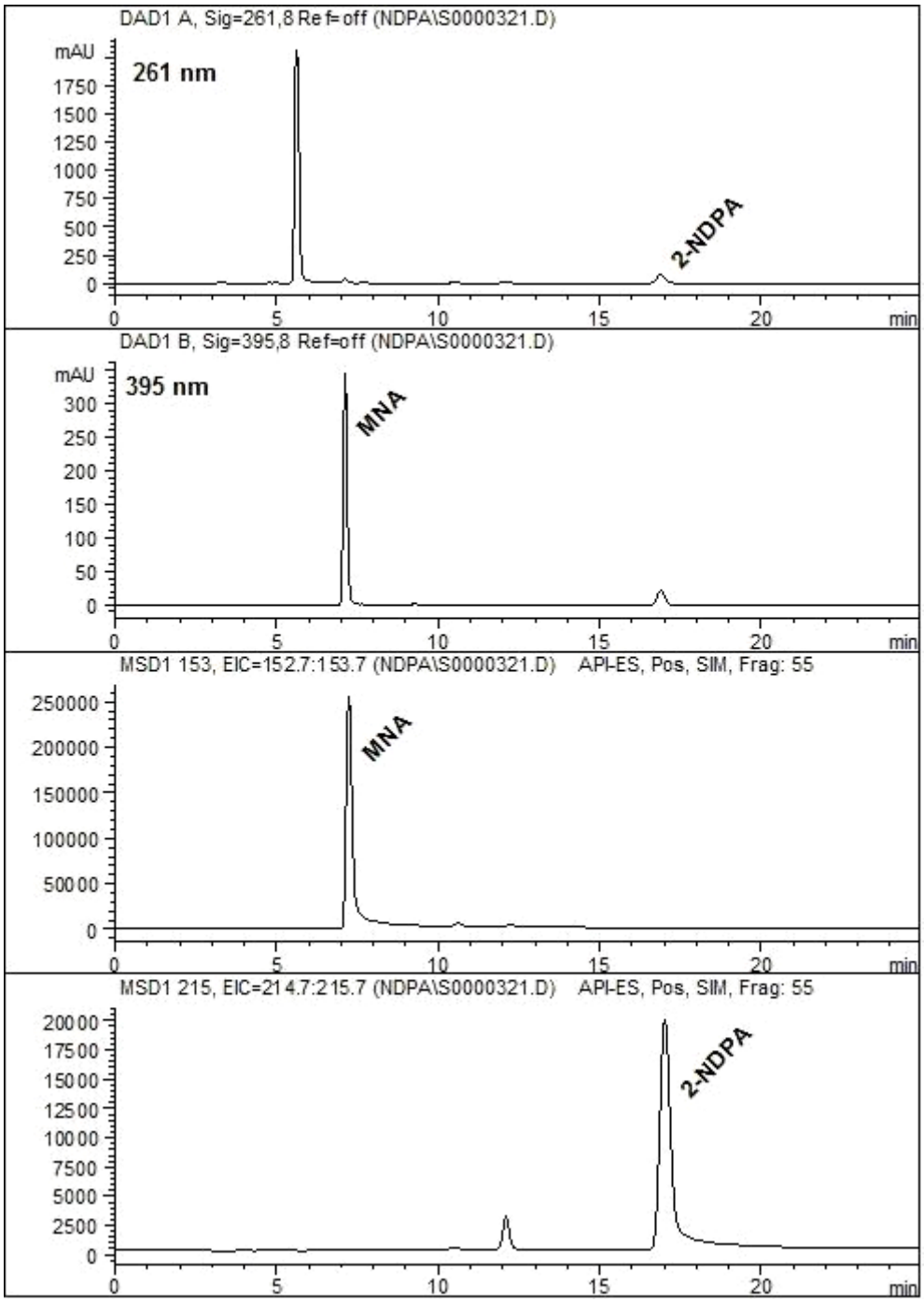

Figure A.6 Chromatograms for Unaged XLDB-3

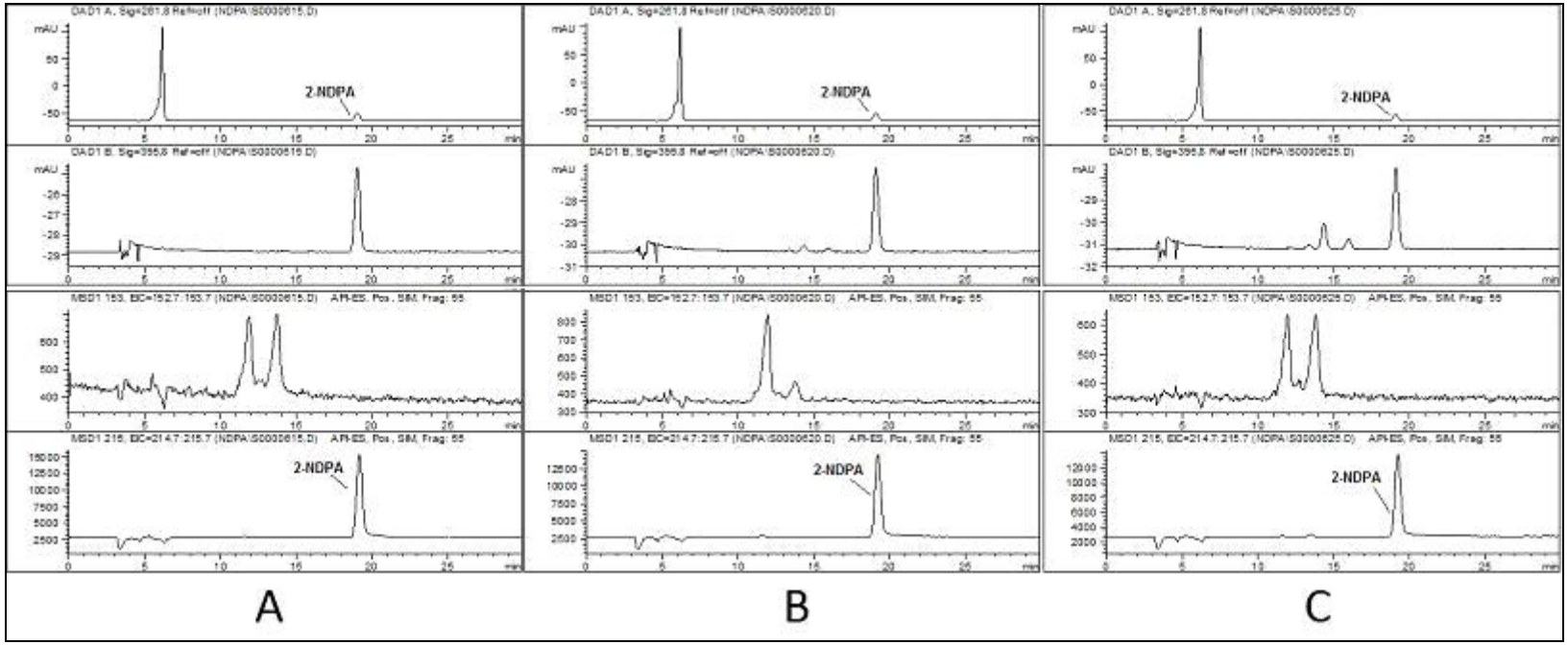

Figure A.7 Chromatograms for XLDB-1 Aged for 30 Days at (A) 45, (B) 55 and (C) 65°C

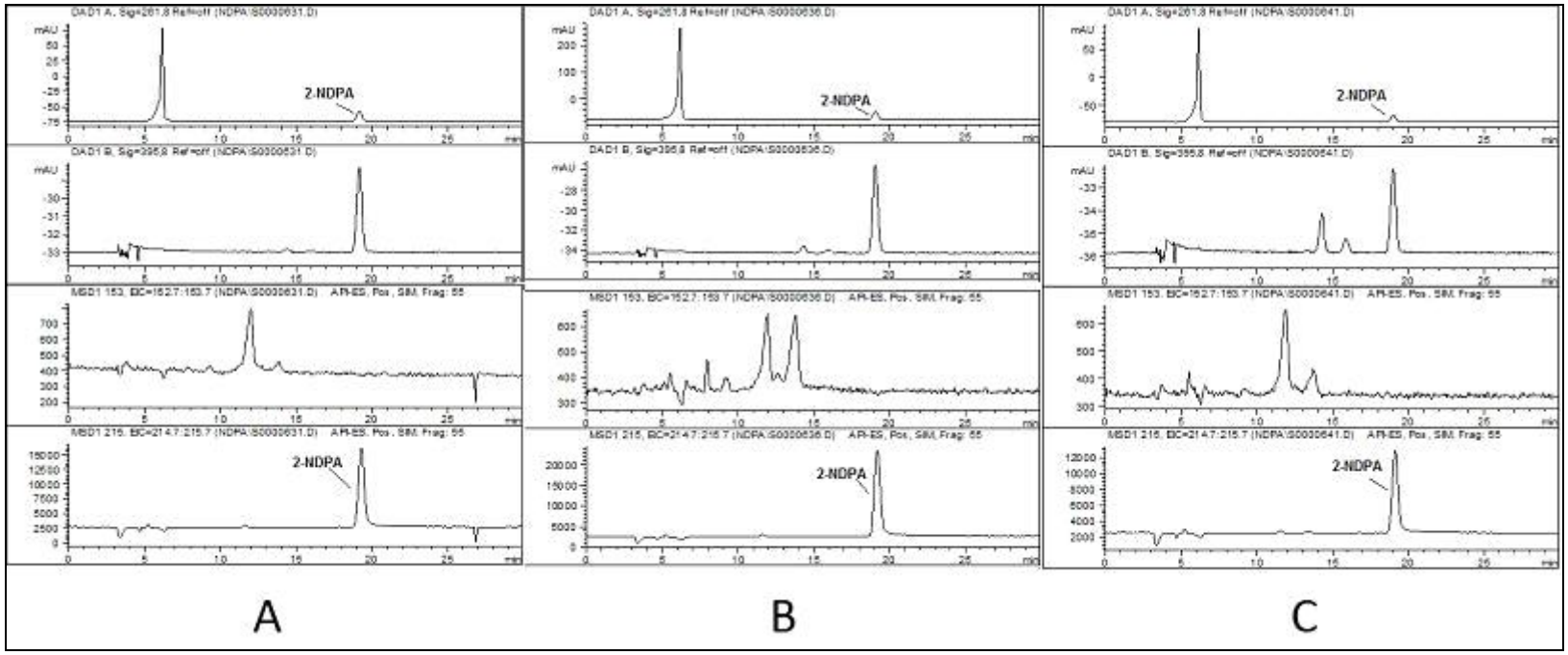

Figure A.8 Chromatograms for XLDB-2 Aged for 30 Days at (A) 45, (B) 55 and (C) 65°C

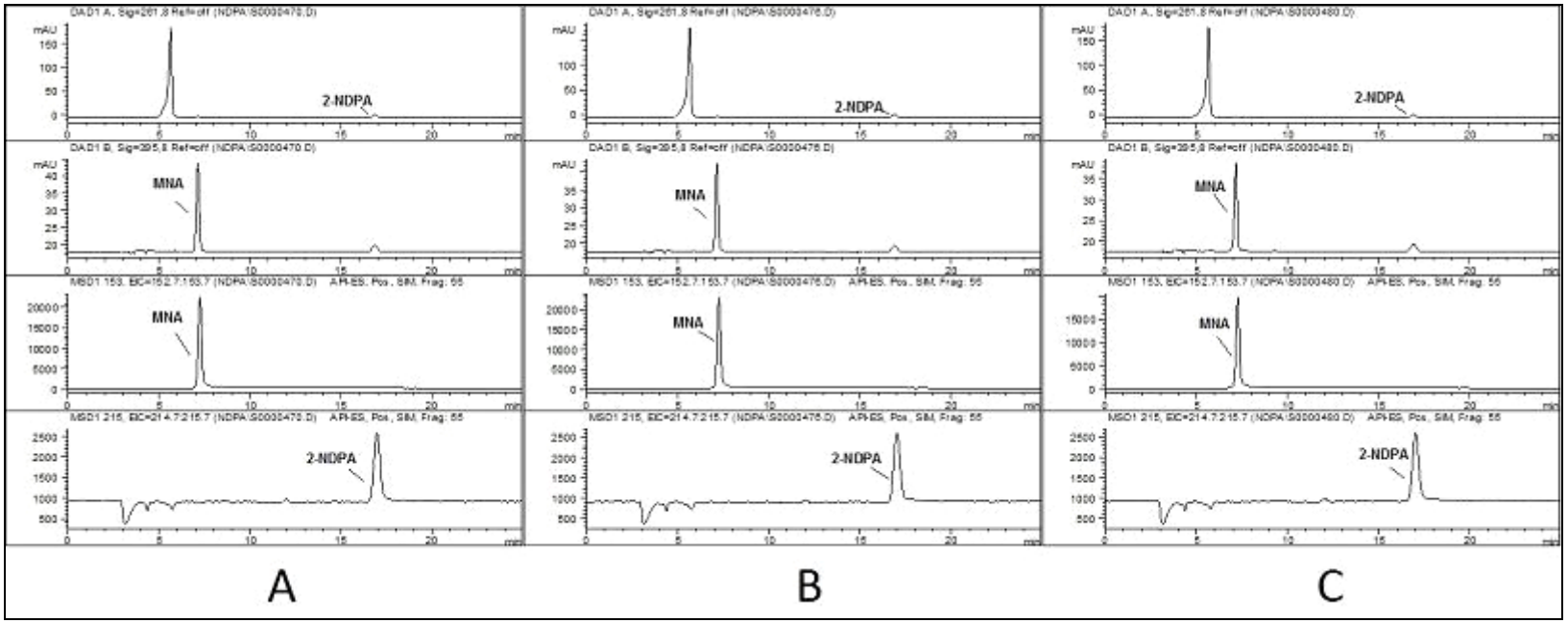

Figure A.9 Chromatograms for XLDB-3 Aged for 30 Days at (A) 45, (B) 55 and (C) 65°C

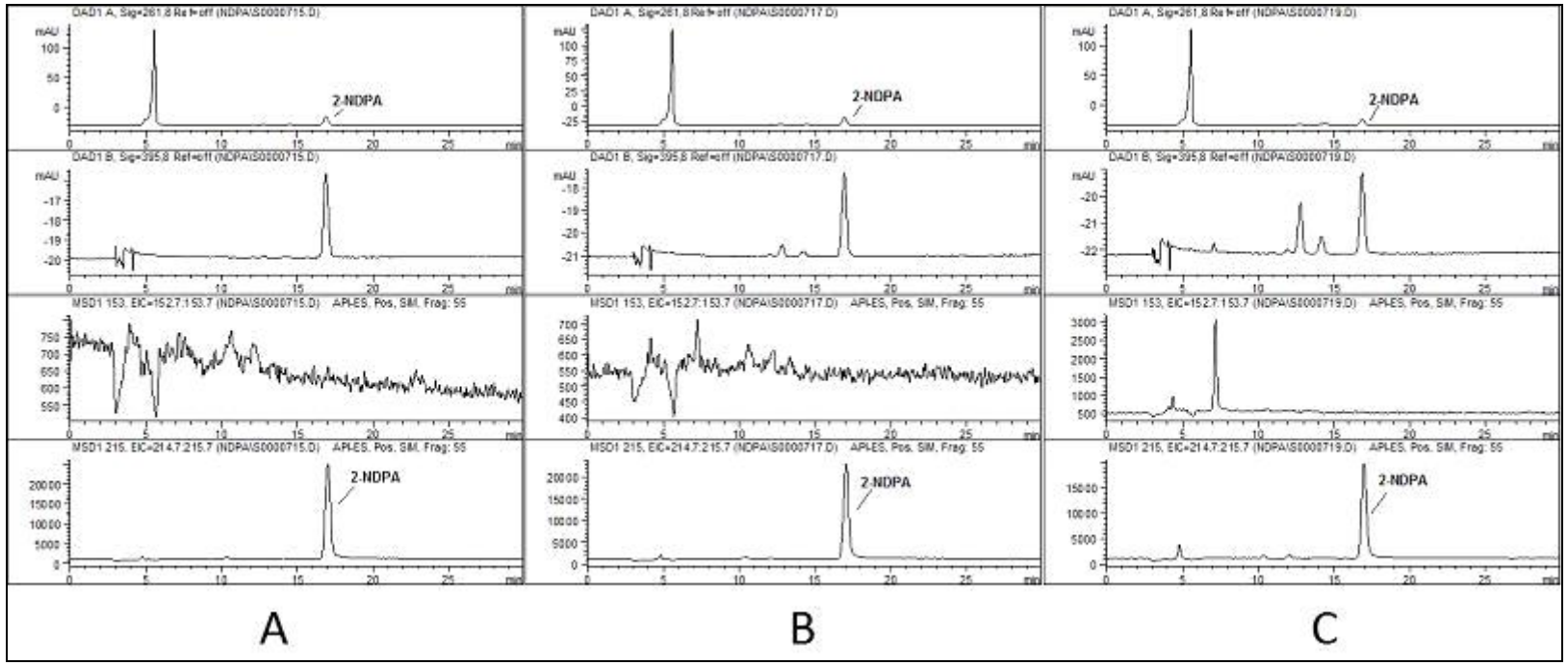

Figure A.10 Chromatograms for XLDB-1 Aged for 60 Days at (A) 45, (B) 55 and (C) 65°C

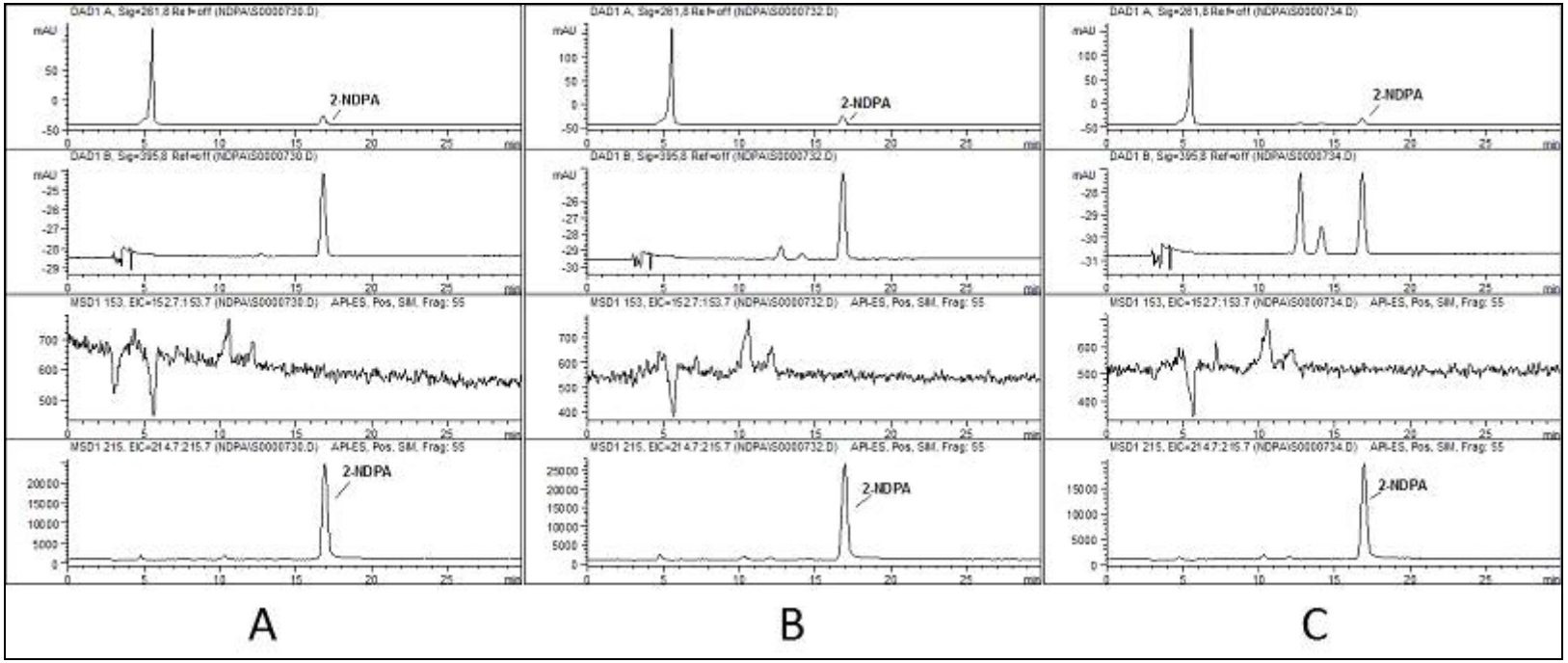

Figure A.11 Chromatograms for XLDB-2 Aged for 60 Days at (A) 45, (B) 55 and (C) 65°C

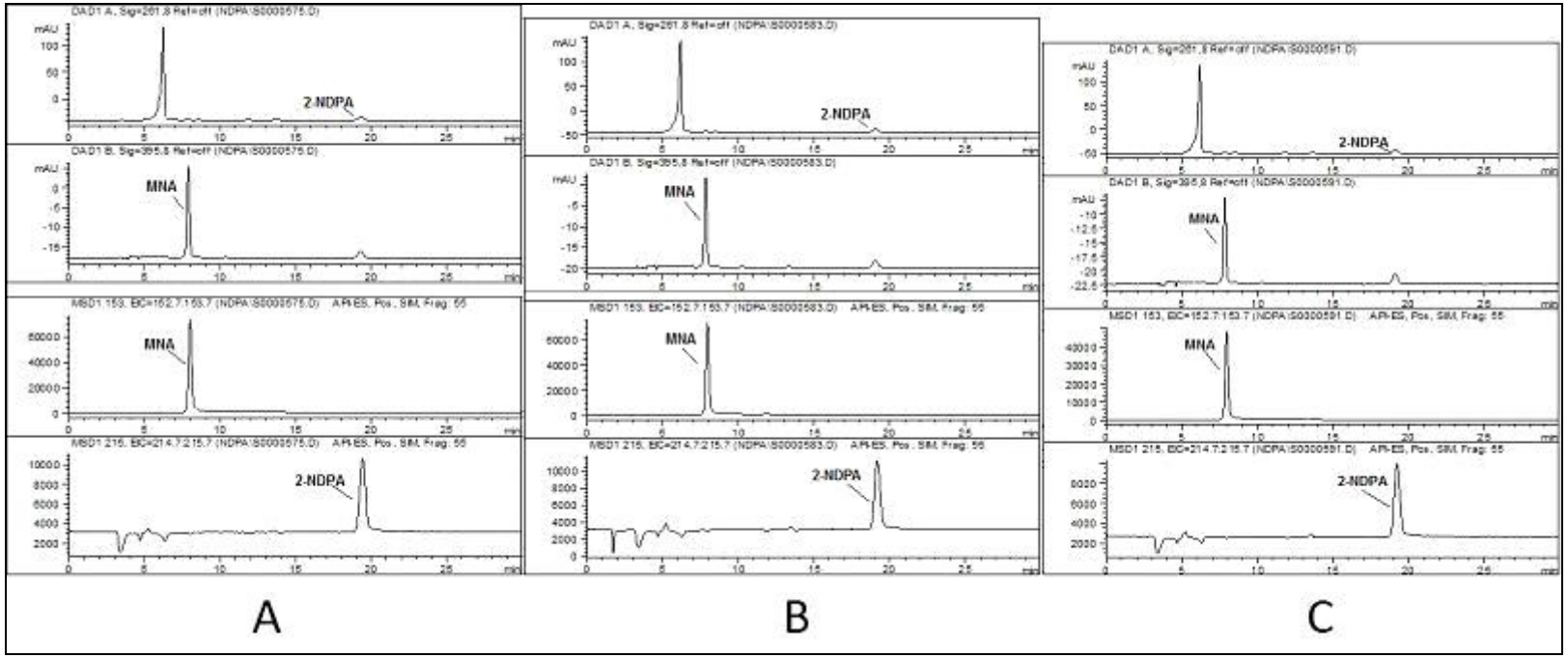

Figure A.12 Chromatograms for XLDB-3 Aged for 60 Days at (A) 45, (B) 55 and (C) 65°C

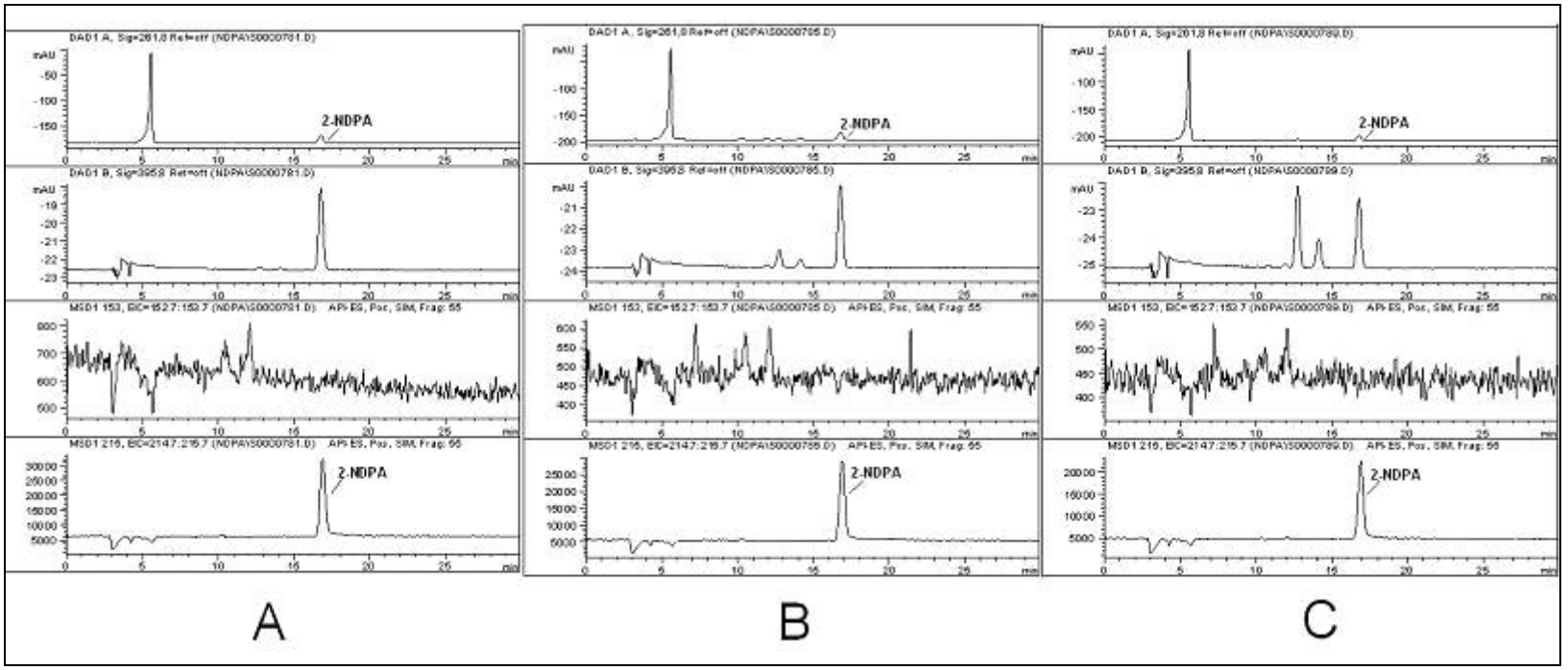

Figure A.13 Chromatograms for XLDB-1 Aged for 90 Days at (A) 45, (B) 55 and (C) 65°C

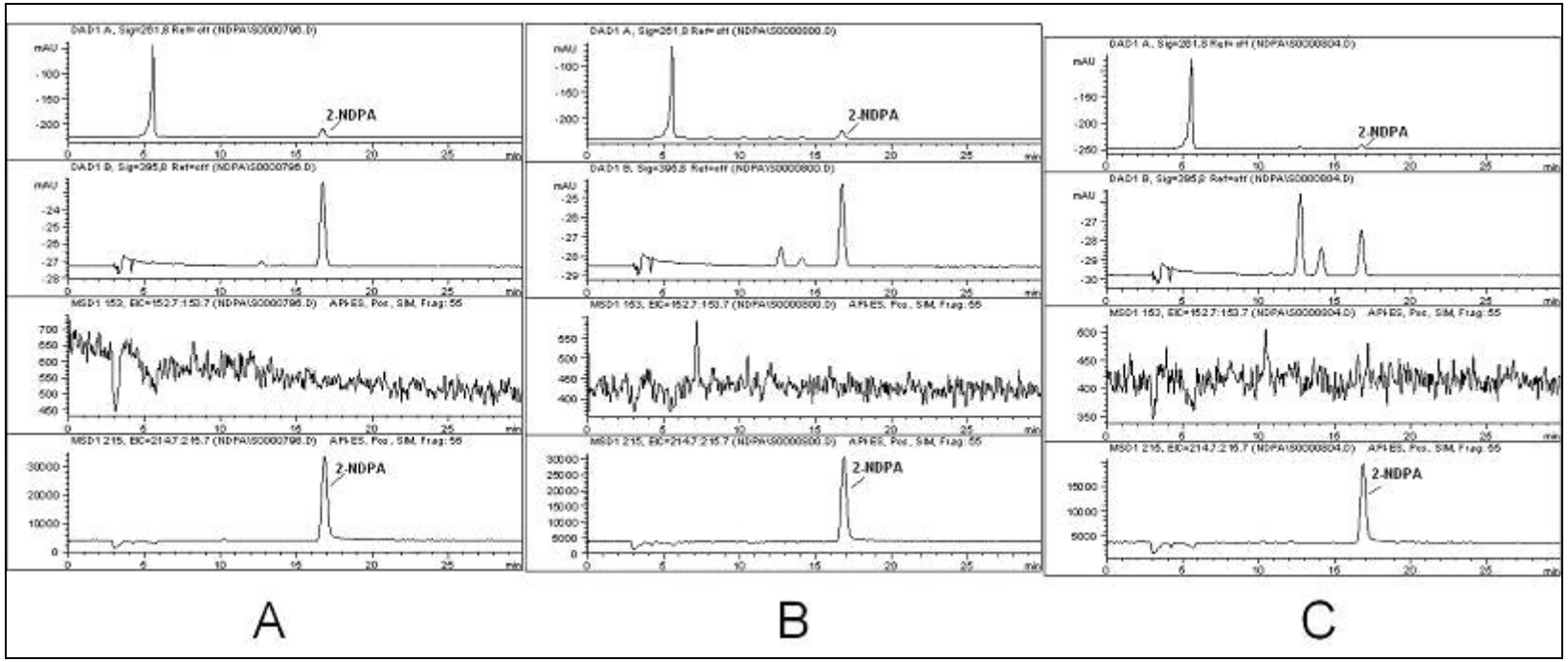

Figure A.14 Chromatograms for XLDB-2 Aged for 90 Days at (A) 45, (B) 55 and (C) 65°C

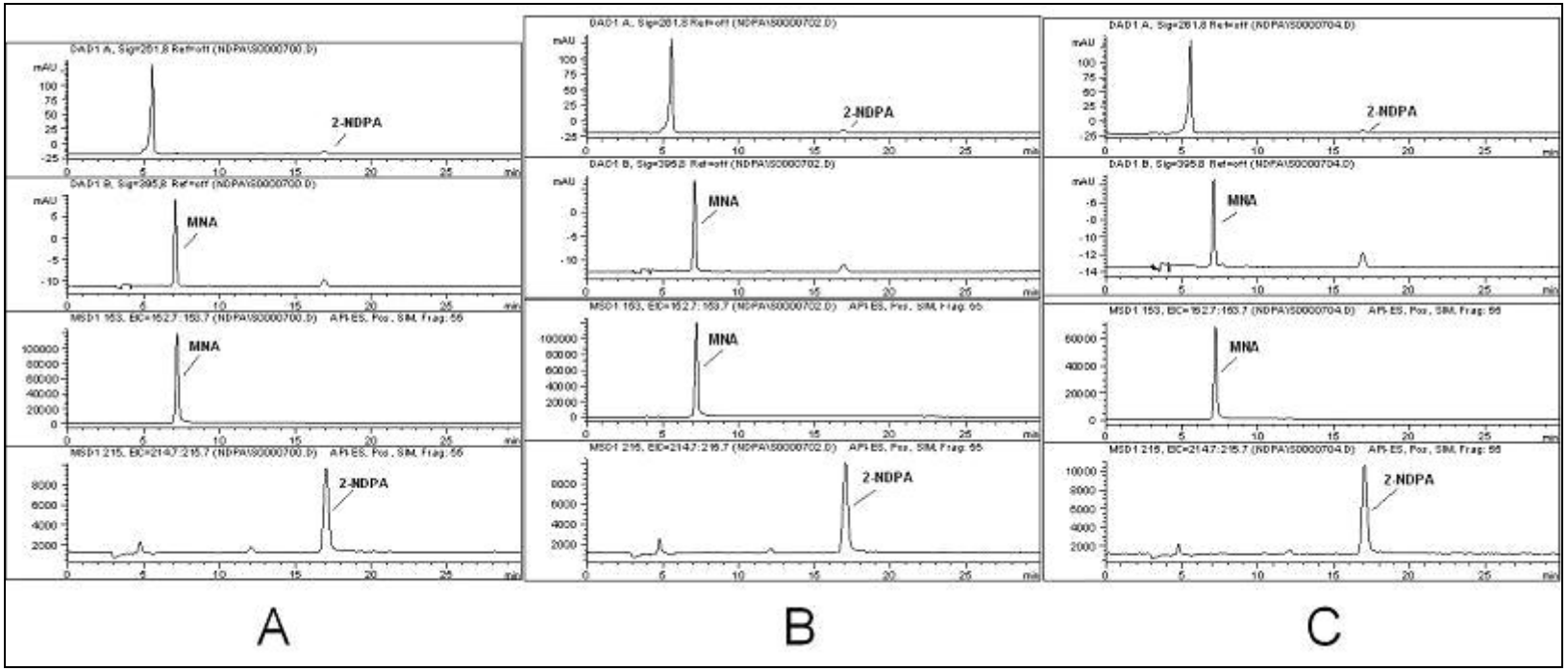

Figure A.15 Chromatograms for XLDB-3 Aged for 90 Days at (A) 45, (B) 55 and (C) 65°C

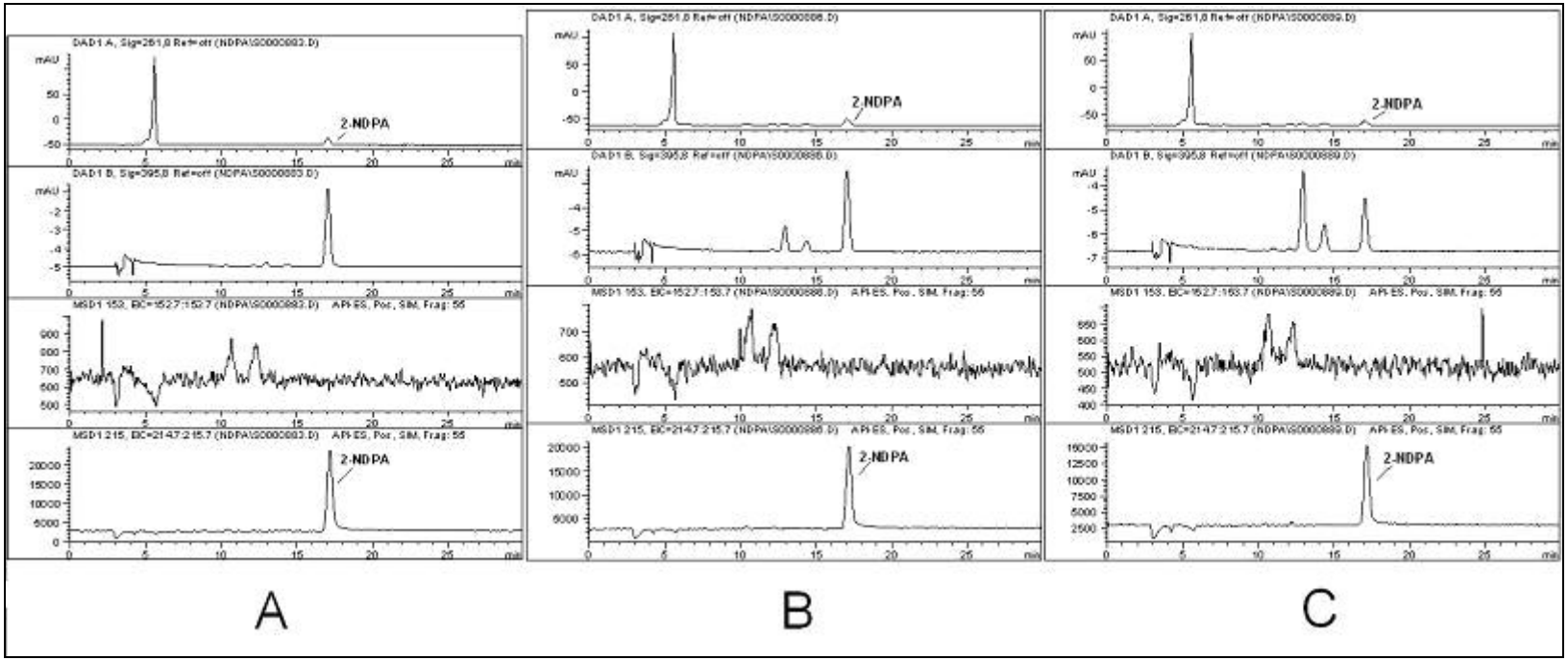

Figure A.16 Chromatograms for XLDB-1 Aged for 120 Days at (A) 45, (B) 55 and (C) 65°C

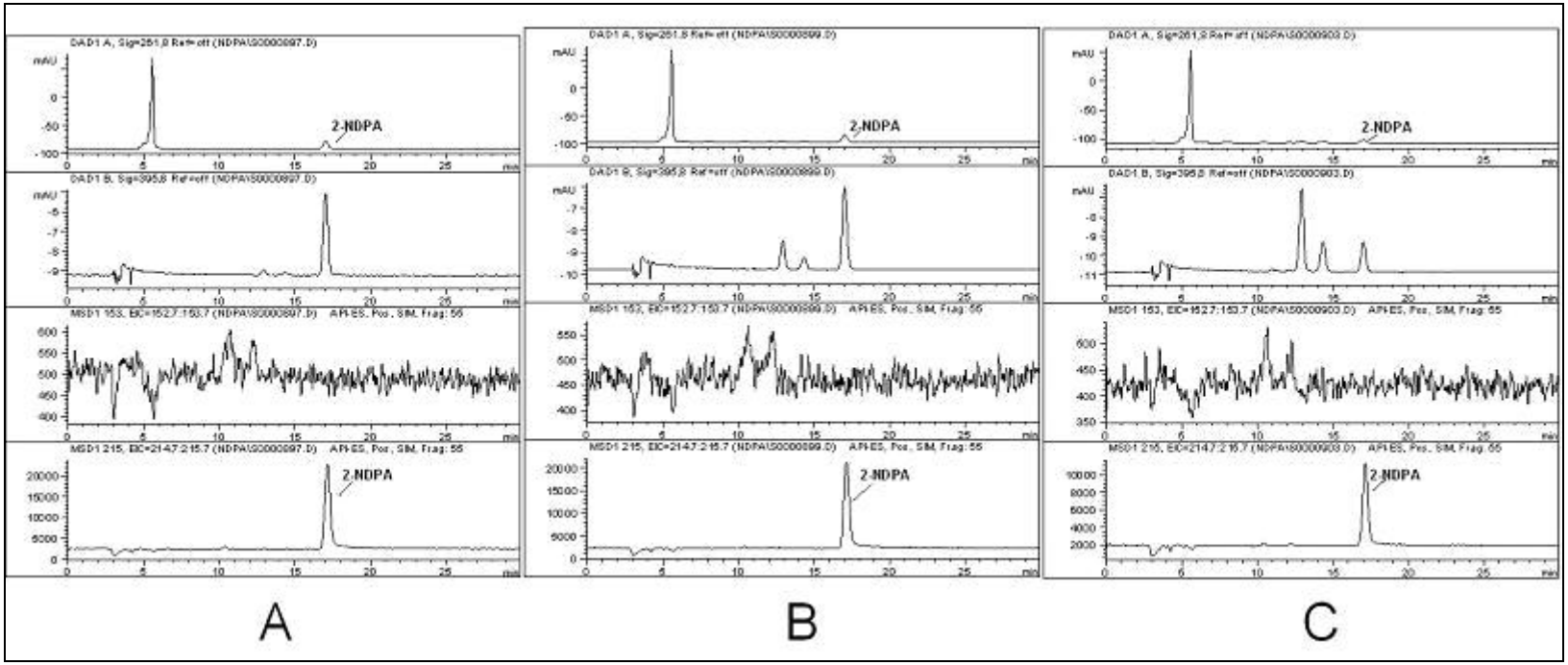

Figure A.17 Chromatograms for XLDB-2 Aged for 120 Days at (A) 45, (B) 55 and (C) 65°C

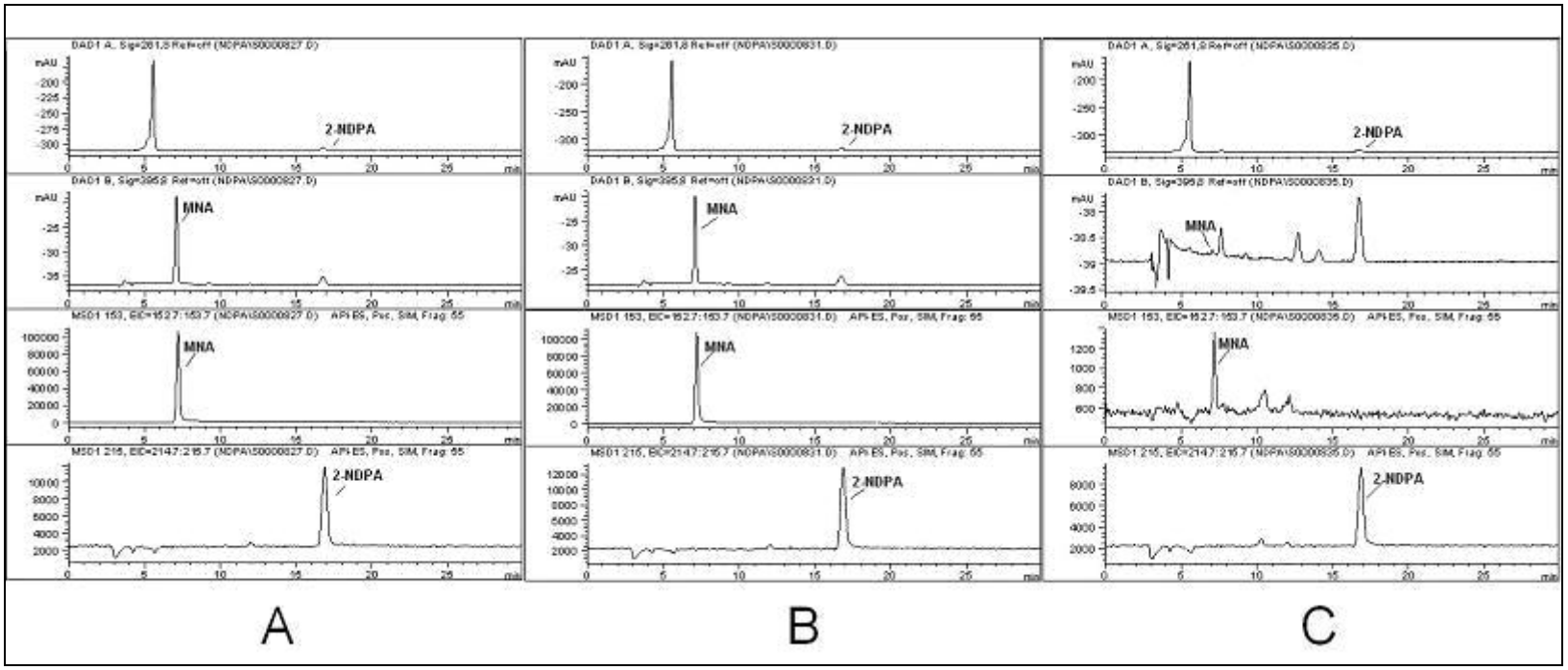

Figure A.18 Chromatograms for XLDB-3 Aged for 120 Days at (A) 45, (B) 55 and (C) 65°C

APPENDIX C

CONCENTRATION OF RESIDUAL STABILIZER FOR STORAGE AT ELEVATED TEMPERATURES

Table A.1 Concentration of Residual Stabilizer in XLDB-1 and XLDB-2 Propellants Aged at Elevated Temperatures

	Days:	**0**	**30**	**60**	**90**	**120**
XLDB-1		2-NDPA	2-NDPA	2-NDPA	2-NDPA	2-NDPA
Residual Stabilizer	45 °C	1.239	1.236	1.234	1.230	1.227
	55 °C		1.184	1.183	1.223	1.049
	65 °C		1.101	1.056	0.820	0.672
XLDB-2		2-NDPA	2-NDPA	2-NDPA	2-NDPA	2-NDPA
Residual Stabilizer	45 °C	1.243	1.240	1.220	1.234	1.225
	55 °C		1.200	1.208	1.185	1.127
	65 °C		1.079	0.949	0.761	0.507

Table A.2 Concentration of Residual Stabilizers in XLDB-3 Propellant Aged at Elevated Temperatures

	Days:	0		30		60		90		120	
XLDB-3		2-NDPA	MNA	2-NDPA	MNA	2-NDPA	MNA	2-NDPA	MNA	2-NDPA	MNA
Residual Stabilizer	45 °C	0.550	0.730	0.521	0.601	0.520	0.560	0.502	0.571	0.514	0.552
	55 °C			0.513	0.597	0.510	0.501	0.494	0.524	0.497	0.505
	65 °C			0.499	0.510	0.507	0.355	0.492	0.289	0.453	0.170

APPENDIX D

PLOTS FOR THE DETERMINATION OF RATE CONSTANTS AND BEST-FIT KINETIC MODELS

The experimental concentration data is used to plot x/a, ln(a/a-x) and x/[a(a-x)] against time, t, to determine the reaction rate constants for pseudo zero, pseudo first and pseudo second order reaction models, respectively. Here, x is the amount of stabilizer converted at time t, and a is the initial concentration of the stabilizer in wt. %. Linear fits are drawn to all plots and the formulas of the lines are obtained using MS EXCELL.

The slope of each line gives the reaction rate constant for the respective model. Also the R^2, coefficient of determination, values of the lines are obtained and this way the plot with the higher R^2 value is determined as the best fit. The plots are given in Figure A.19 - Figure A.45.

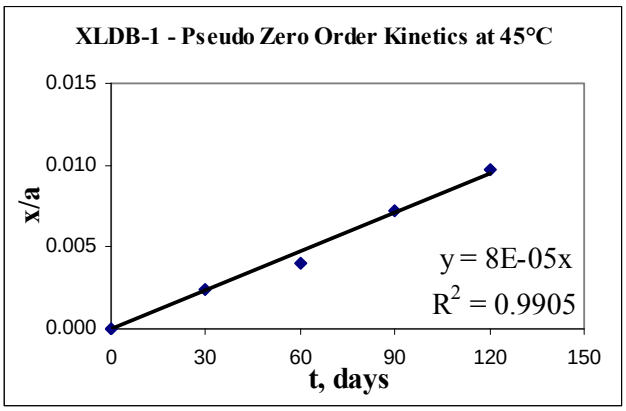

Figure A.19 Determination of Reaction Rate for the Pseudo Zero Order Depletion of 2-NDPA at 45°C for XLDB-1 Propellant

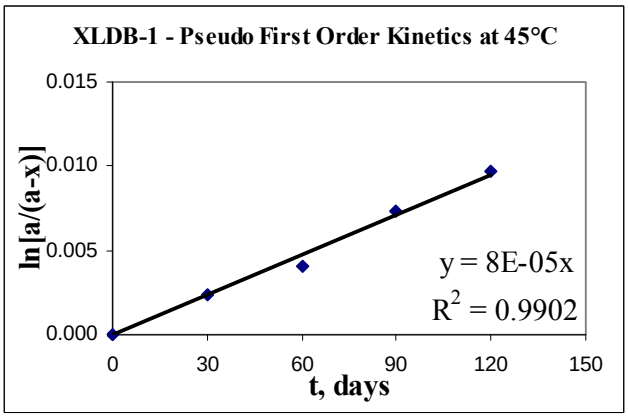

Figure A.20 Determination of Reaction Rate for the Pseudo First Order Depletion of 2-NDPA at 45°C for XLDB-1 Propellant

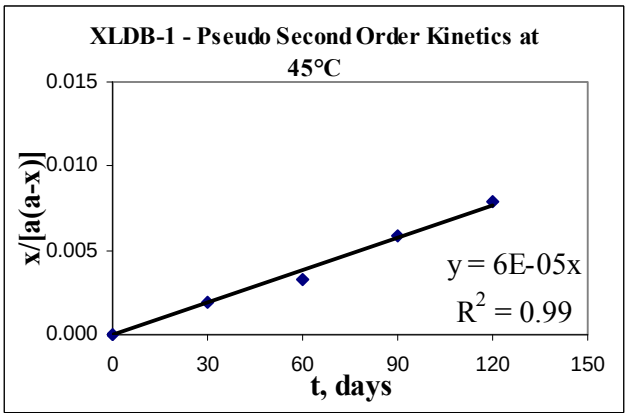

Figure A.21 Determination of Reaction Rate for the Pseudo Second Order Depletion of 2-NDPA at 45°C for XLDB-1 Propellant

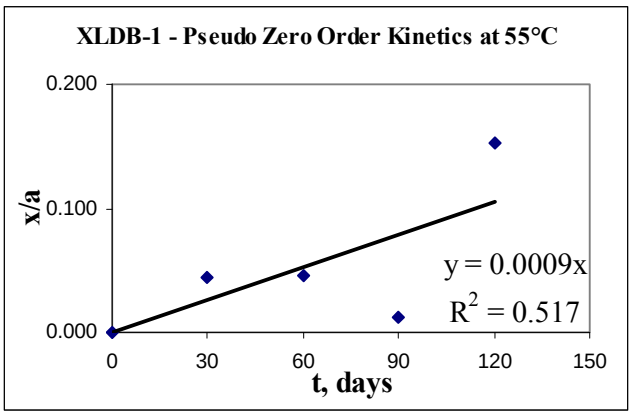

Figure A.22 Determination of Reaction Rate for the Pseudo Zero Order Depletion of 2-NDPA at 55°C for XLDB-1 Propellant

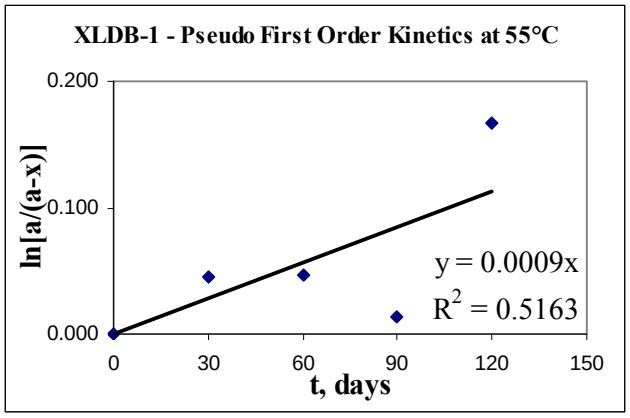

Figure A.23 Determination of Reaction Rate for the Pseudo First Order Depletion of 2-NDPA at 55°C for XLDB-1 Propellant

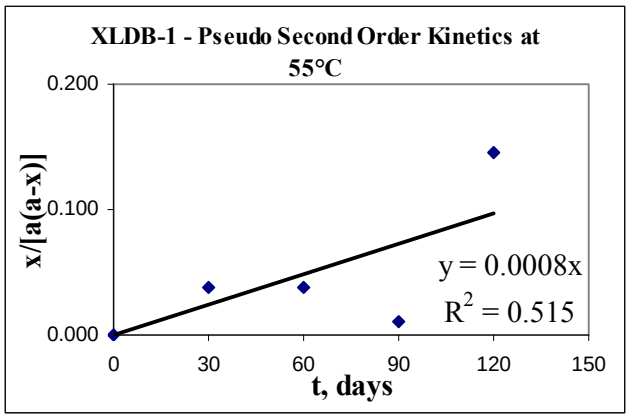

Figure A.24 Determination of Reaction Rate for the Pseudo Second Order Depletion of 2-NDPA at 55°C for XLDB-1 Propellant

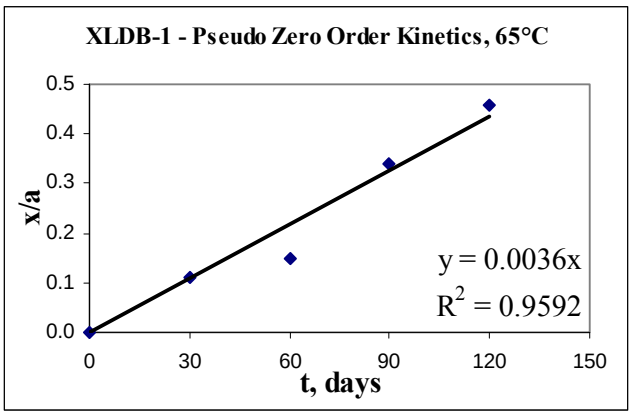

Figure A.25 Determination of Reaction Rate for the Pseudo Zero Order Depletion of 2-NDPA at 65°C for XLDB-1 Propellant

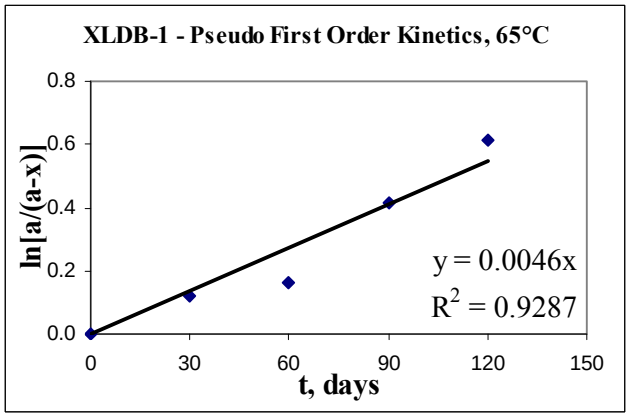

Figure A.26 Determination of Reaction Rate for the Pseudo First Order Depletion of 2-NDPA at 65°C for XLDB-1 Propellant

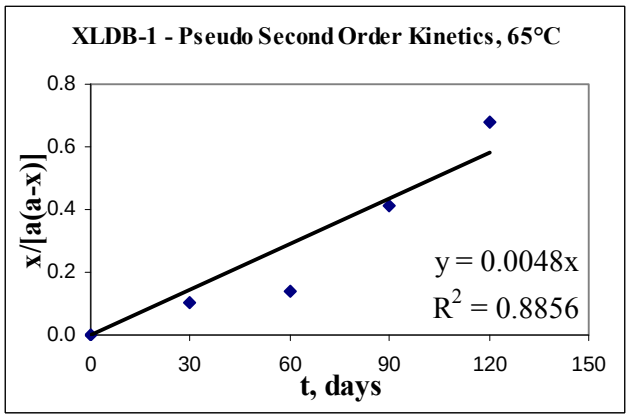

Figure A.27 Determination of Reaction Rate for the Pseudo Second Order Depletion of 2-NDPA at 65°C for XLDB-1 Propellant

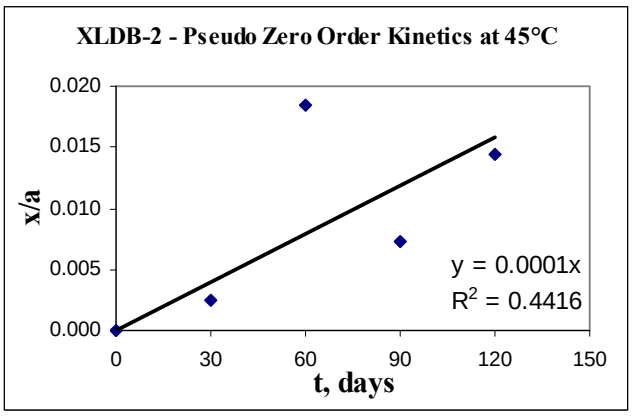

Figure A.28 Determination of Reaction Rate for the Pseudo Zero Order Depletion of 2-NDPA at 45°C for XLDB-2 Propellant

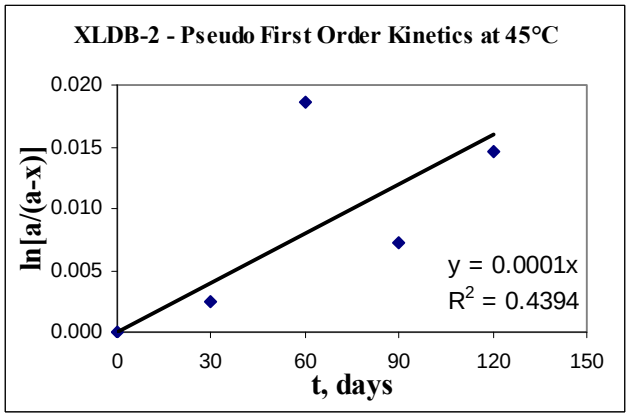

Figure A.29 Determination of Reaction Rate for the Pseudo First Order Depletion of 2-NDPA at 45°C for XLDB-2 Propellant

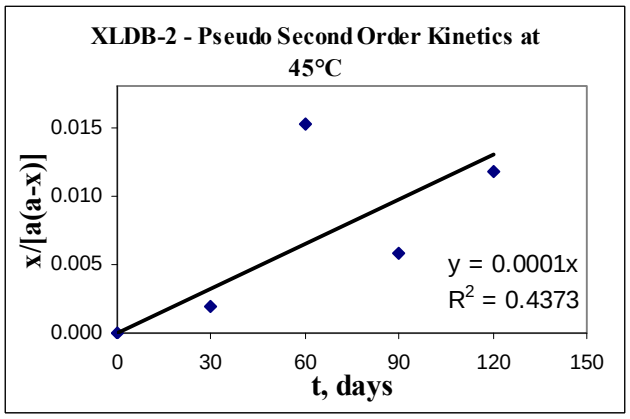

Figure A.30 Determination of Reaction Rate for the Pseudo Second Order Depletion of 2-NDPA at 45°C for XLDB-2 Propellant

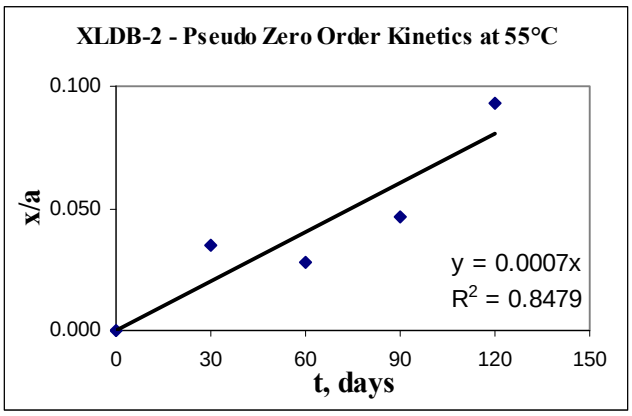

Figure A.31 Determination of Reaction Rate for the Pseudo Zero Order Depletion of 2-NDPA at 55°C for XLDB-2 Propellant

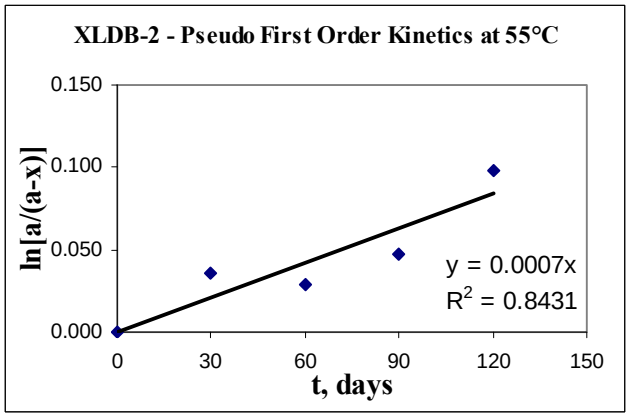

Figure A.32 Determination of Reaction Rate for the Pseudo First Order Depletion of 2-NDPA at 55°C for XLDB-2 Propellant

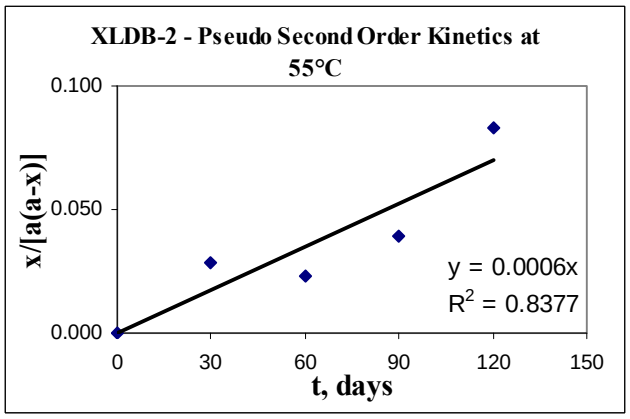

Figure A.33 Determination of Reaction Rate for the Pseudo Second Order Depletion of 2-NDPA at 55°C for XLDB-2 Propellant

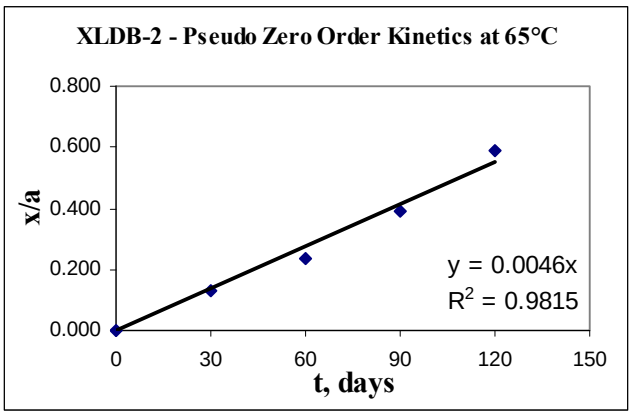

Figure A.34 Determination of Reaction Rate for the Pseudo Zero Order Depletion of 2-NDPA at 65°C for XLDB-2 Propellant

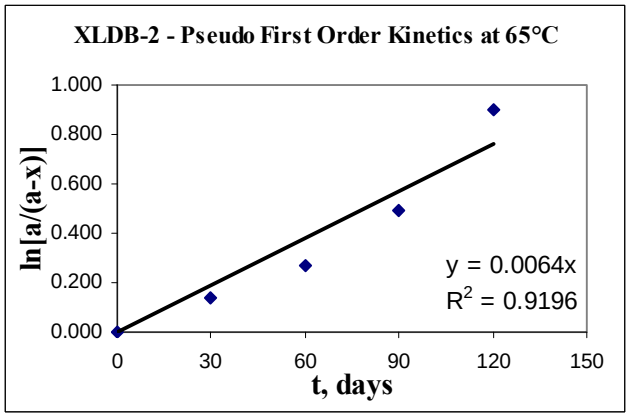

Figure A.35 Determination of Reaction Rate for the Pseudo First Order Depletion of 2-NDPA at 65°C for XLDB-2 Propellant

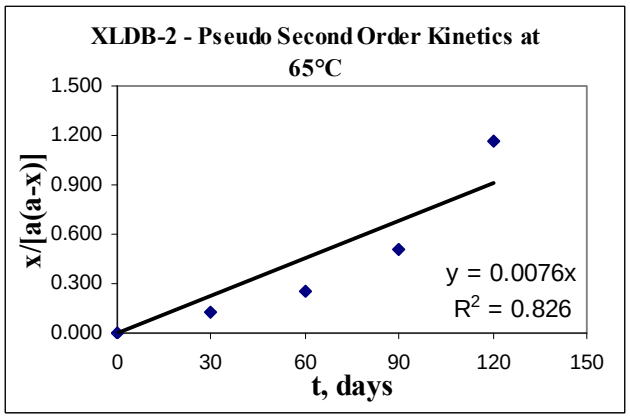

Figure A.36 Determination of Reaction Rate for the Pseudo Second Order Depletion of 2-NDPA at 65°C for XLDB-2 Propellant

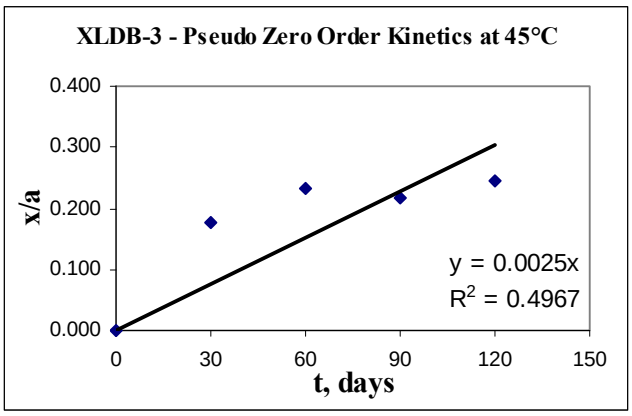

Figure A.37 Determination of Reaction Rate for the Pseudo Zero Order Depletion of MNA at 45°C for XLDB-3 Propellant

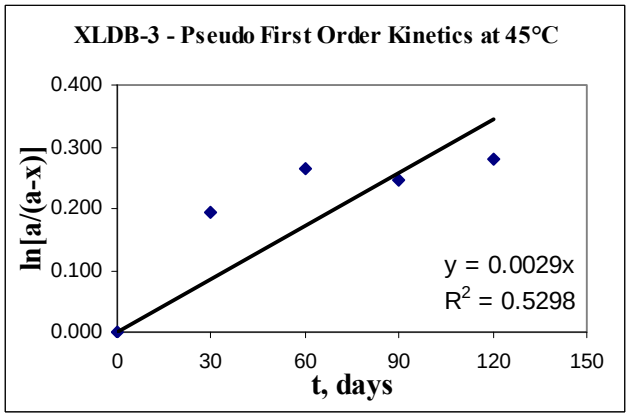

Figure A.38 Determination of Reaction Rate for the Pseudo First Order Depletion of MNA at 45°C for XLDB-3 Propellant

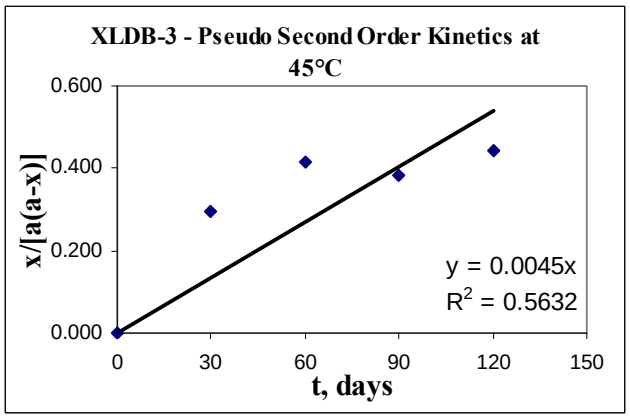

Figure A.39 Determination of Reaction Rate for the Pseudo Second Order Depletion of MNA at 45°C for XLDB-3 Propellant

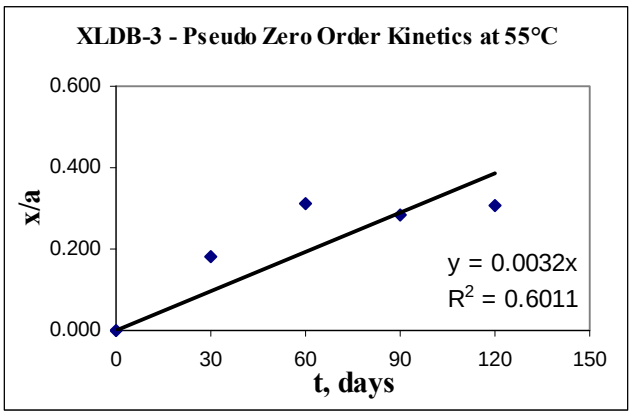

Figure A.40 Determination of Reaction Rate for the Pseudo Zero Order Depletion of MNA at 55°C for XLDB-3 Propellant

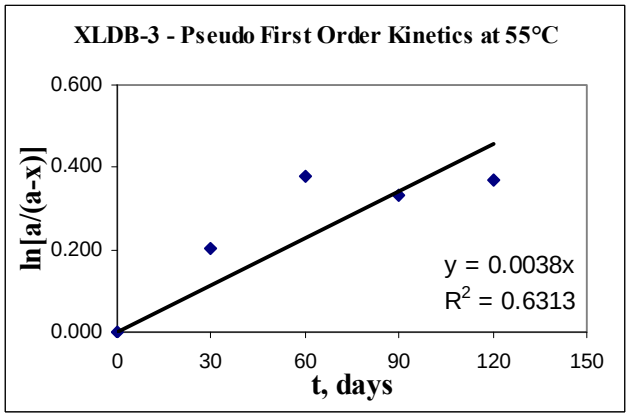

Figure A.41 Determination of Reaction Rate for the Pseudo First Order Depletion of MNA at 55°C for XLDB-3 Propellant

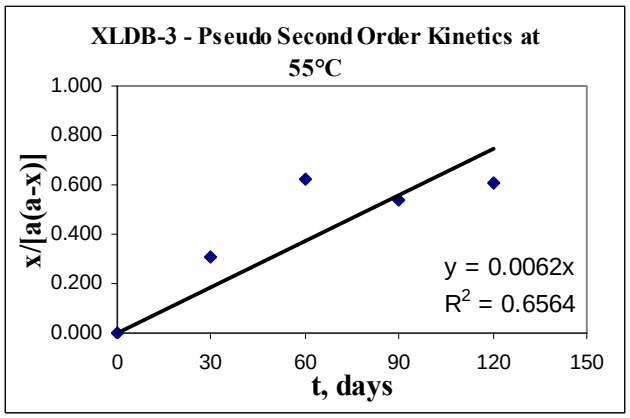

Figure A.42 Determination of Reaction Rate for the Pseudo Second Order Depletion of MNA at 55°C for XLDB-3 Propellant

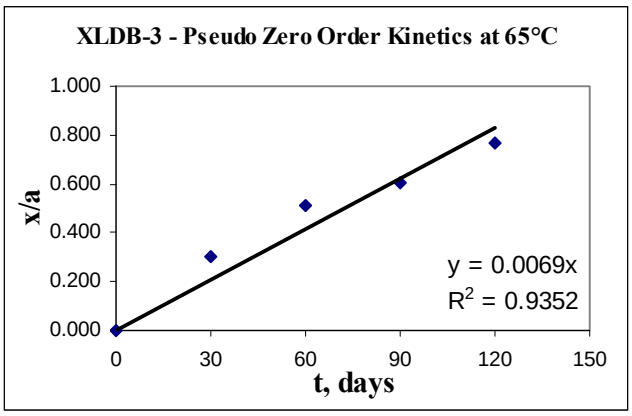

Figure A.43 Determination of Reaction Rate for the Pseudo Zero Order Depletion of MNA at 65°C for XLDB-3 Propellant

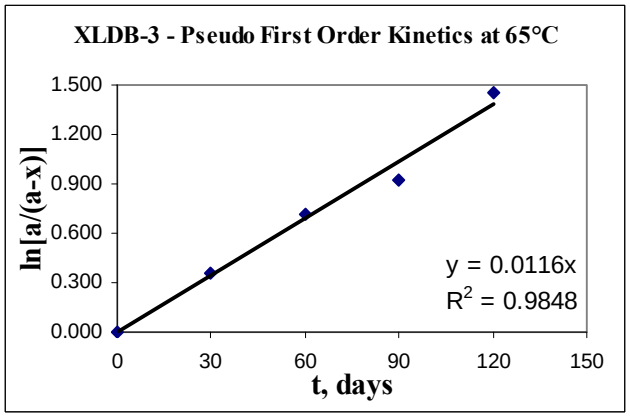

Figure A.44 Determination of Reaction Rate for the Pseudo First Order Depletion of MNA at 65°C for XLDB-3 Propellant

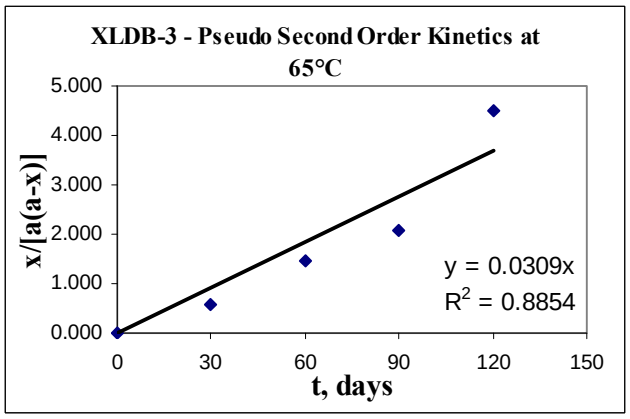

Figure A.45 Determination of Reaction Rate for the Pseudo Second Order Depletion of MNA at 65°C for XLDB-3 Propellant

APPENDIX E

MATHCAD SOFTWARE OUTPUT FOR BEST-FIT KINETIC MODELS

For the depletion of MNA in XLDB-3 propellant the following is assumed:

$$-\frac{d[A]}{dt} = k_0 + k_1[A] \tag{1.8}$$

By rearranging and integrating, the following is obtained:

$$[A] = -\frac{k_0}{k_1} + \left[\frac{k_0}{k_1} + a\right]\exp[-k_1 \cdot t] \tag{1.9}$$

Equation 1.9 is solved for k_0 and k_1, by the least squares fit method using MathCAD. The function called "expfit" was used with refined initial guesses 0.135, -0.012 and 0.595 for (k_0/k_1+a), $-k_1$ and $-k_0/k_1$, respectively. (Third parameter guess is -0.595 for the reaction at 65°C.) The output from the software is given in Figure A.46, Figure A.47 and Figure A.48, respectively for 45, 55 and 65°C.

$$time := \begin{pmatrix} 0 \\ 30 \\ 60 \\ 90 \\ 120 \end{pmatrix} \qquad conc := \begin{pmatrix} 0.730 \\ 0.601 \\ 0.560 \\ 0.571 \\ 0.552 \end{pmatrix}$$

$$guess := \begin{pmatrix} 0.135 \\ -0.012 \\ 0.595 \end{pmatrix} \qquad cfit := expfit(time, conc, guess)$$

$$cfit = \begin{pmatrix} 0.173 \\ -0.047 \\ 0.557 \end{pmatrix}$$

$a := cfit_0$

$b := cfit_1$

$c := cfit_2$

$m(x) := a \cdot e^{b \cdot x} + c$

$x := 0 .. 120$

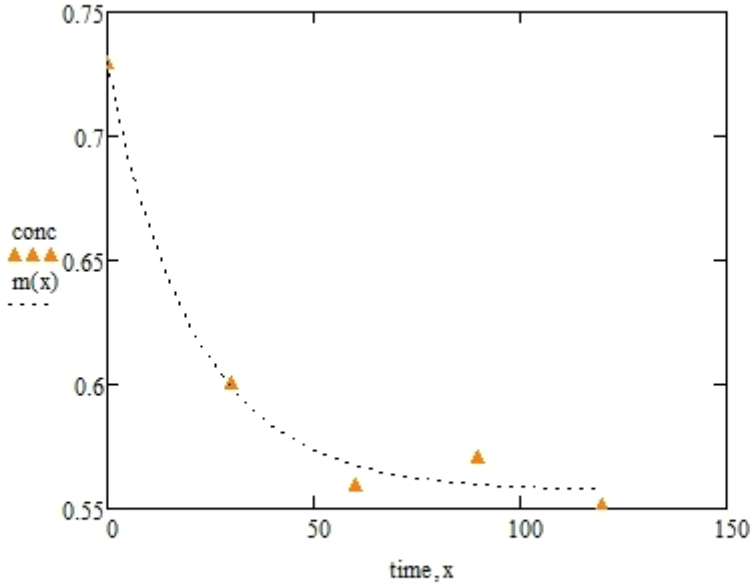

$k_1 := -b \qquad k_0 := -k_1 \cdot c$

$k_1 = 0.047 \qquad k_0 = -0.026 \qquad corr\left(conc, \overrightarrow{m(time)}\right)^2 = 0.99$

Figure A.46 Software Output for Shifting Order Kinetics at 45°C for XLDB-3

$$time := \begin{pmatrix} 0 \\ 30 \\ 60 \\ 90 \\ 120 \end{pmatrix} \qquad conc := \begin{pmatrix} 0.730 \\ 0.597 \\ 0.501 \\ 0.524 \\ 0.505 \end{pmatrix}$$

$$guess := \begin{pmatrix} 0.135 \\ -0.012 \\ 0.595 \end{pmatrix} \qquad cfit := expfit(time, conc, guess)$$

$$cfit = \begin{pmatrix} 0.233 \\ -0.034 \\ 0.499 \end{pmatrix}$$

$a := cfit_0$

$b := cfit_1$

$c := cfit_2$

$m(x) := a \cdot e^{b \cdot x} + c$

$x := 0 .. 120$

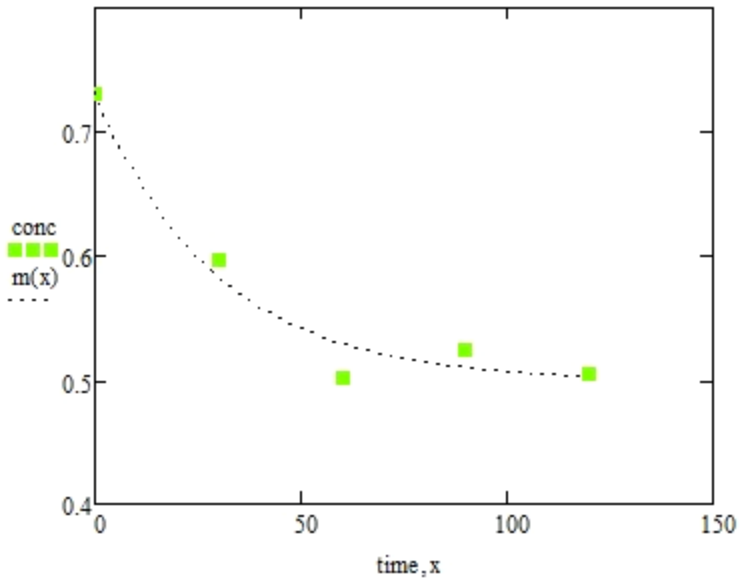

$k_1 := -b \qquad k_0 := -k_1 \cdot c \qquad corr\left(conc, \overrightarrow{m(time)}\right)^2 = 0.968$

$k_1 = 0.034 \qquad k_0 = -0.017$

Figure A.47 Software Output for Shifting Order Kinetics at 55°C for XLDB-3

$$time := \begin{pmatrix} 0 \\ 30 \\ 60 \\ 90 \\ 120 \end{pmatrix} \qquad conc := \begin{pmatrix} 0.730 \\ 0.510 \\ 0.355 \\ 0.289 \\ 0.170 \end{pmatrix}$$

$$guess := \begin{pmatrix} 0.135 \\ -0.012 \\ -0.595 \end{pmatrix} \qquad cfit := expfit(time, conc, guess)$$

$$cfit = \begin{pmatrix} 0.727 \\ -0.011 \\ -5.22 \times 10^{-4} \end{pmatrix}$$

$a := cfit_0$

$b := cfit_1$

$c := cfit_2$

$m(x) := a \cdot e^{b \cdot x} + c$

$x := 0 .. 120$

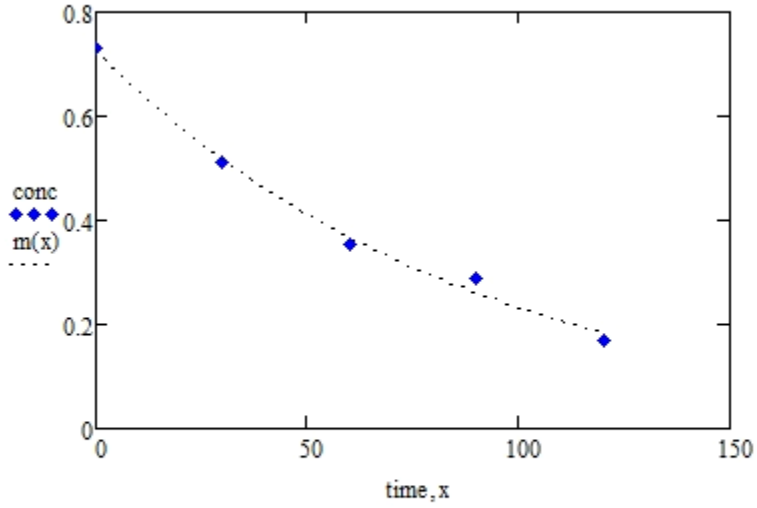

$k_1 := -b \qquad k_0 := -k_1 \cdot c \qquad corr\left(conc, \overrightarrow{m(time)}\right)^2 = 0.993$

$k_1 = 0.011 \qquad k_0 = 5.946 \times 10^{-6}$

Figure A.48 Software Output for Shifting Order Kinetics at 65°C for XLDB-3

Using pseudo zero, pseudo first and shifting order model equations, stabilizer concentration versus time plots were drawn and the coefficient of determination values were calculated using MathCAD. These values show the quality of the correlation between the model and the experimental data. Model equations are given in Table 4.5. The outputs of MathCAD software are given in Figure A.49 - Figure A.57.

Table 4.5 Kinetic Model Equations for the Depletion of Stabilizers

Propellant	**Stabilizer Concentration, *[A]* wt. %**	**Kinetics of the Depletion Reaction**
XLDB-1*	$a - k_0 \cdot a \cdot t$	Pseudo Zero Order
XLDB-2*		
XLDB-3**	$-\frac{k_0}{k_1} + \left[\frac{k_0}{k_1} + a\right] \exp[-k_1 \cdot t]$	Shifting Order
	$\exp(\ln a - k_1 \cdot t)$	Pseudo First Order

* Depletion of 2-NDPA

** Depletion of MNA

$$time := \begin{pmatrix} 0 \\ 30 \\ 60 \\ 90 \\ 120 \end{pmatrix} \qquad conc := \begin{pmatrix} 1.239 \\ 1.236 \\ 1.234 \\ 1.230 \\ 1.227 \end{pmatrix}$$

$$h(x) := 1.239 - (0.00008 \cdot 1.239 \cdot x)$$

$$x := 0 .. 120$$

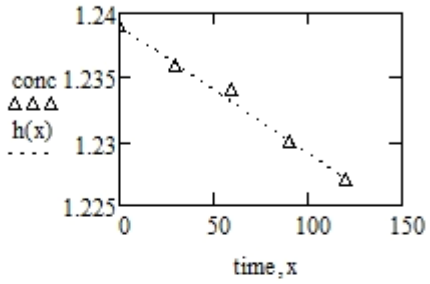

$$corr\left(conc, \overrightarrow{h(time)}\right)^2 = 0.991$$

$$g(x) := e^{(\ln(1.239) - 0.00008 \cdot x)}$$

$$x := 0 .. 120$$

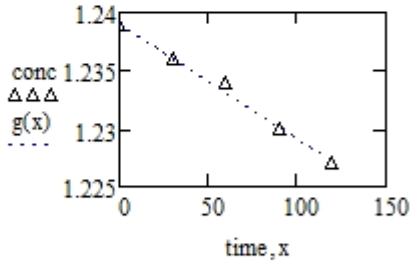

$$corr\left(conc, \overrightarrow{g(time)}\right)^2 = 0.991$$

$$f(x) := \frac{1}{\left(0.00006 \cdot x + \frac{1}{1.239}\right)}$$

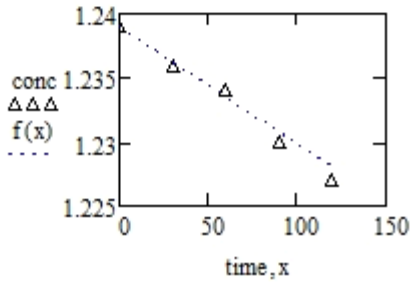

$$corr\left(conc, \overrightarrow{f(time)}\right)^2 = 0.991$$

Figure A.49 Software Output for Model Equations – XLDB-1, 45°C

$$time := \begin{pmatrix} 0 \\ 30 \\ 60 \\ 90 \\ 120 \end{pmatrix} \qquad conc := \begin{pmatrix} 1.239 \\ 1.184 \\ 1.183 \\ 1.223 \\ 1.049 \end{pmatrix}$$

$$h(x) := 1.239 - (0.0009 \cdot 1.239 \cdot x)$$

$$x := 0 .. 120$$

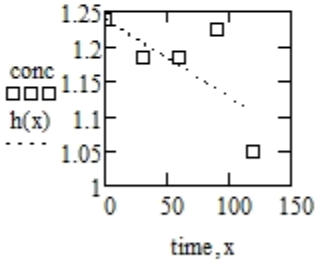

$$\text{corr}\left(conc, \overrightarrow{h(time)}\right)^2 = 0.519$$

$$g(x) := e^{(\ln(1.239) - 0.0009 \cdot x)}$$

$$x := 0 .. 120$$

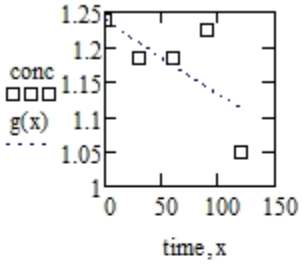

$$\text{corr}\left(conc, \overrightarrow{g(time)}\right)^2 = 0.511$$

$$f(x) := \frac{1}{\left(0.0008 \cdot x + \frac{1}{1.239}\right)}$$

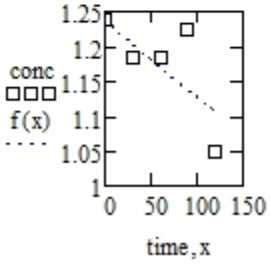

$$\text{corr}\left(conc, \overrightarrow{f(time)}\right)^2 = 0.502$$

Figure A.50 Software Output for Model Equations – XLDB-1, 55°C

$$time := \begin{pmatrix} 0 \\ 30 \\ 60 \\ 90 \\ 120 \end{pmatrix} \qquad conc := \begin{pmatrix} 1.239 \\ 1.101 \\ 1.056 \\ 0.820 \\ 0.672 \end{pmatrix}$$

$h(x) := 1.239 - (0.0036 \cdot 1.239 \cdot x)$

$x := 0 .. 120$

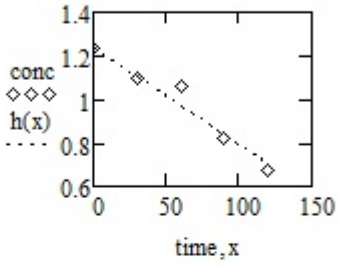

$$corr\left(conc, \overrightarrow{h(time)}\right)^2 = 0.963$$

$g(x) := e^{(\ln(1.239) - 0.0046 \cdot x)}$

$x := 0 .. 120$

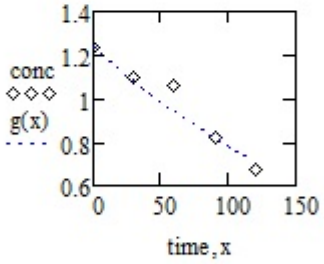

$$corr\left(conc, \overrightarrow{g(time)}\right)^2 = 0.937$$

$$f(x) := \frac{1}{\left(0.0048 \cdot x + \frac{1}{1.239}\right)}$$

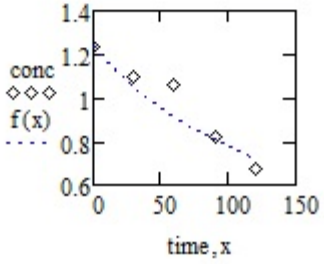

$$corr\left(conc, \overrightarrow{f(time)}\right)^2 = 0.903$$

Figure A.51 Software Output for Model Equations – XLDB-1, 65°C

$$time := \begin{pmatrix} 0 \\ 30 \\ 60 \\ 90 \\ 120 \end{pmatrix} \qquad conc := \begin{pmatrix} 1.243 \\ 1.240 \\ 1.220 \\ 1.234 \\ 1.225 \end{pmatrix}$$

$h(x) := 1.243 - (0.0001 \cdot 1.243 \cdot x)$

$x := 0 .. 120$

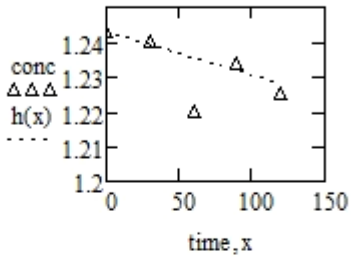

$$corr\left(conc, \overrightarrow{h(time)}\right)^2 = 0.463$$

$g(x) := e^{(\ln(1.243) - 0.0001 \cdot x)}$

$x := 0 .. 120$

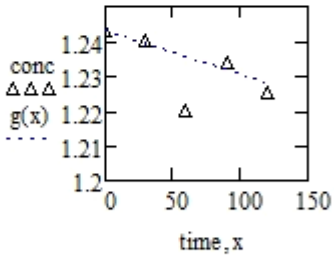

$$corr\left(conc, \overrightarrow{g(time)}\right)^2 = 0.463$$

$$f(x) := \frac{1}{\left(0.0001 \cdot x + \frac{1}{1.243}\right)}$$

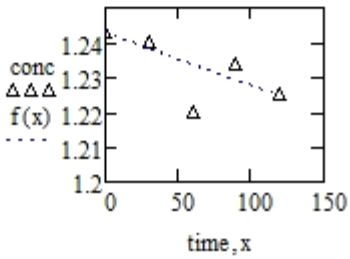

$$corr\left(conc, \overrightarrow{f(time)}\right)^2 = 0.465$$

Figure A.52 Software Output for Model Equations – XLDB-2, 45°C

$$time := \begin{pmatrix} 0 \\ 30 \\ 60 \\ 90 \\ 120 \end{pmatrix} \qquad conc := \begin{pmatrix} 1.243 \\ 1.200 \\ 1.208 \\ 1.185 \\ 1.127 \end{pmatrix}$$

$h(x) := 1.243 - (0.0007 \cdot 1.243 \cdot x)$

$x := 0 .. 120$

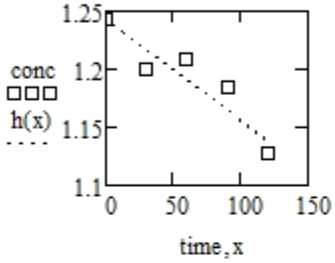

$$corr\left(conc, \overrightarrow{h(time)}\right)^2 = 0.848$$

$g(x) := e^{(\ln(1.243) - 0.0007 \cdot x)}$

$x := 0 .. 120$

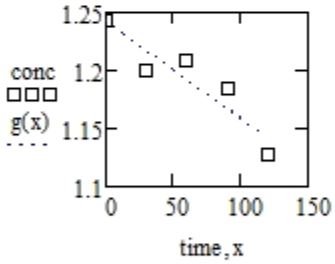

$$corr\left(conc, \overrightarrow{g(time)}\right)^2 = 0.844$$

$$f(x) := \frac{1}{\left(0.0006 \cdot x + \frac{1}{1.243}\right)}$$

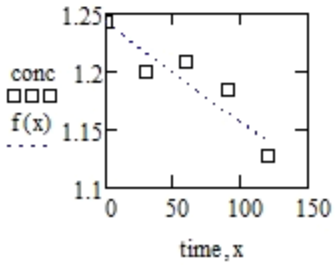

$$corr\left(conc, \overrightarrow{f(time)}\right)^2 = 0.839$$

Figure A.53 Software Output for Model Equations – XLDB-2, 55°C

$$\text{time} := \begin{pmatrix} 0 \\ 30 \\ 60 \\ 90 \\ 120 \end{pmatrix} \qquad \text{conc} := \begin{pmatrix} 1.243 \\ 1.079 \\ 0.949 \\ 0.761 \\ 0.507 \end{pmatrix}$$

$$h(x) := 1.243 - (0.0046 \cdot 1.243 \cdot x)$$

$$x := 0 .. 120$$

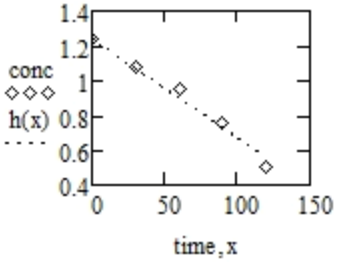

$$\text{corr}\left(\text{conc}, \overrightarrow{h(\text{time})}\right)^2 = 0.984$$

$$g(x) := e^{(\ln(1.243) - 0.0064 \cdot x)}$$

$$x := 0 .. 120$$

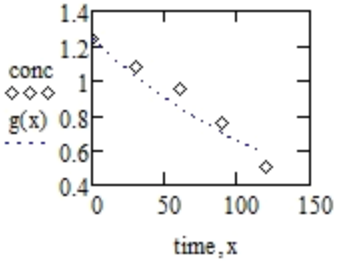

$$\text{corr}\left(\text{conc}, \overrightarrow{g(\text{time})}\right)^2 = 0.948$$

$$f(x) := \frac{1}{\left(0.0076 \cdot x + \frac{1}{1.243}\right)}$$

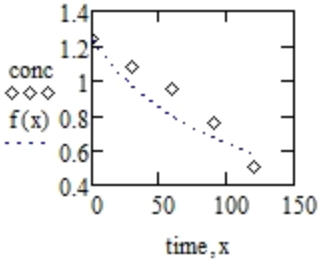

$$\text{corr}\left(\text{conc}, \overrightarrow{f(\text{time})}\right)^2 = 0.895$$

Figure A.54 Software Output for Model Equations – XLDB-2, 65°C

$$time := \begin{pmatrix} 0 \\ 30 \\ 60 \\ 90 \\ 120 \end{pmatrix} \qquad conc := \begin{pmatrix} 0.730 \\ 0.601 \\ 0.560 \\ 0.571 \\ 0.552 \end{pmatrix}$$

$h(x) := 0.730 - (0.0025 \cdot 0.730 \cdot x)$

$x := 0 .. 120$

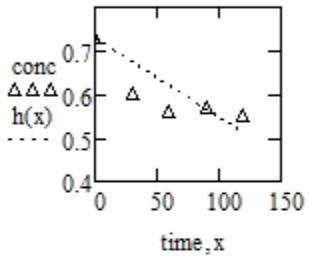

$$corr\left(conc, \overrightarrow{h(time)}\right)^2 = 0.69$$

$g(x) := e^{(\ln(0.730) - 0.0029 \cdot x)}$

$x := 0 .. 120$

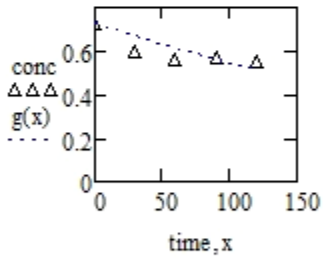

$$corr\left(conc, \overrightarrow{g(time)}\right)^2 = 0.731$$

$$f(x) := \frac{1}{\left(0.0045 \cdot x + \frac{1}{0.730}\right)}$$

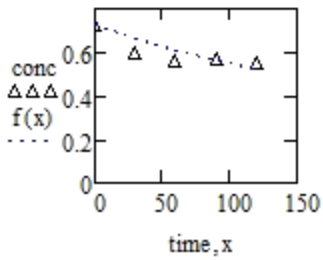

$$corr\left(conc, \overrightarrow{f(time)}\right)^2 = 0.769$$

Figure A.55 Software Output for Model Equations – XLDB-3, 45°C

$$time := \begin{pmatrix} 0 \\ 30 \\ 60 \\ 90 \\ 120 \end{pmatrix} \qquad conc := \begin{pmatrix} 0.730 \\ 0.597 \\ 0.501 \\ 0.524 \\ 0.505 \end{pmatrix}$$

$h(x) := 0.730 - (0.0032 \cdot 0.730 \cdot x)$

$x := 0..120$

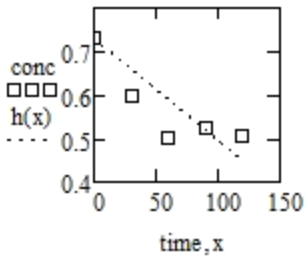

$$corr\left(conc, \overrightarrow{h(time)}\right)^2 = 0.731$$

$g(x) := e^{(\ln(0.730) - 0.0038 \cdot x)}$

$x := 0..120$

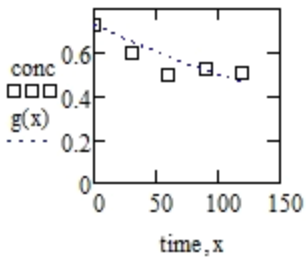

$$corr\left(conc, \overrightarrow{g(time)}\right)^2 = 0.784$$

$$f(x) := \frac{1}{\left(0.0062 \cdot x + \frac{1}{0.730}\right)}$$

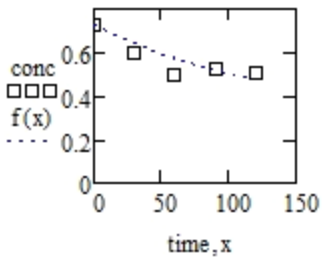

$$corr\left(conc, \overrightarrow{f(time)}\right)^2 = 0.829$$

Figure A.56 Software Output for Model Equations – XLDB-3, 55°C

$$\text{time} := \begin{pmatrix} 0 \\ 30 \\ 60 \\ 90 \\ 120 \end{pmatrix} \qquad \text{conc} := \begin{pmatrix} 0.730 \\ 0.510 \\ 0.355 \\ 0.289 \\ 0.170 \end{pmatrix}$$

$$h(x) := 0.730 - (0.0069 \cdot 0.730 \cdot x)$$

$$x := 0 .. 120$$

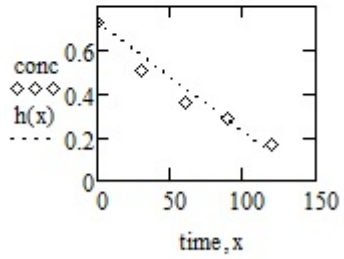

$$\text{corr}\left(\text{conc}, \overrightarrow{h(\text{time})}\right)^2 = 0.958$$

$$g(x) := e^{(\ln(0.730) - 0.0116 \cdot x)}$$

$$x := 0 .. 120$$

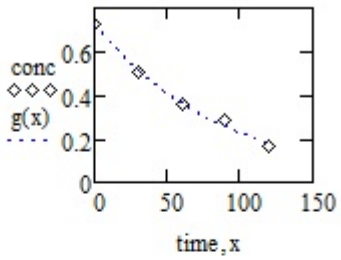

$$\text{corr}\left(\text{conc}, \overrightarrow{g(\text{time})}\right)^2 = 0.993$$

$$f(x) := \frac{1}{\left(0.0309 \cdot x + \frac{1}{0.730}\right)}$$

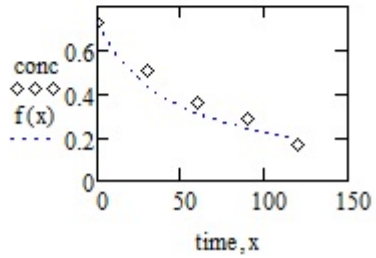

$$\text{corr}\left(\text{conc}, \overrightarrow{f(\text{time})}\right)^2 = 0.965$$

Figure A.57 Software Output for Model Equations – XLDB-3, 65°C

APPENDIX F

PLOTS FOR THE DETERMINATION OF KINETIC PARAMETERS – ARRHENIUS EQUATION

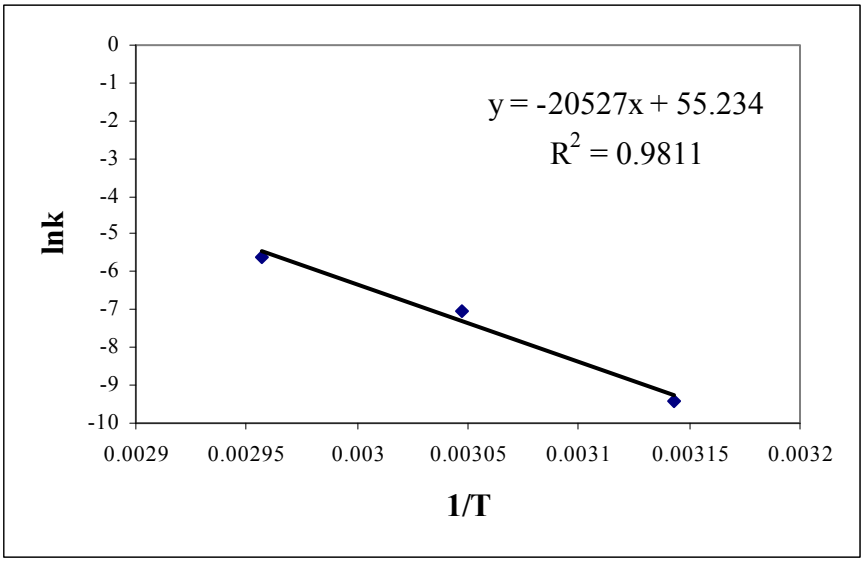

Figure A.58 Determination of Arrhenius Parameters for the Depletion of 2-NDPA in XLDB-1 – Pseudo Zero Order Kinetics

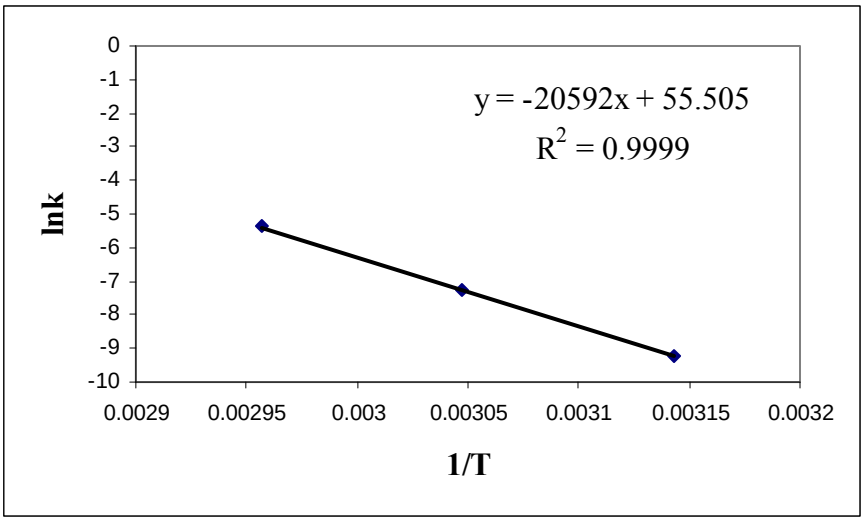

Figure A.59 Determination of Arrhenius Parameters for the Depletion of 2-NDPA in XLDB-2 – Pseudo Zero Order Kinetics

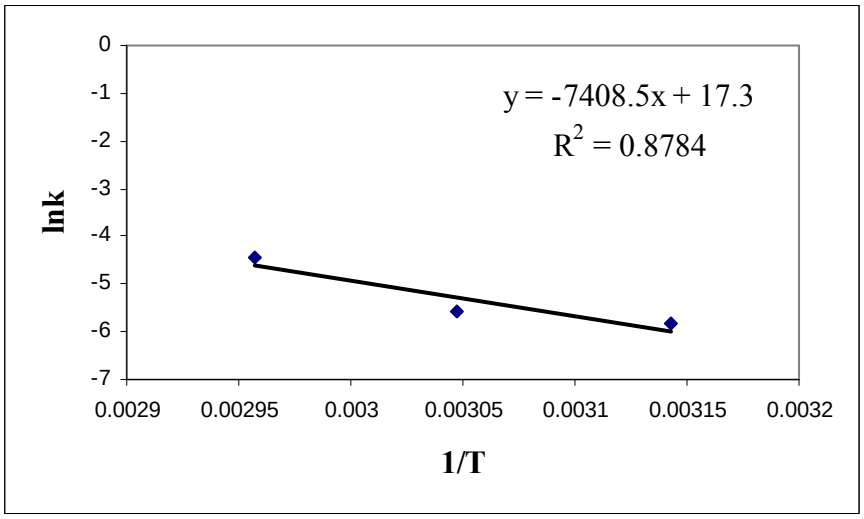

Figure A.60 Determination of Arrhenius Parameters for the Depletion of MNA in XLDB-3 – Pseudo First Order Kinetics

APPENDIX G

FTIR PLOTS

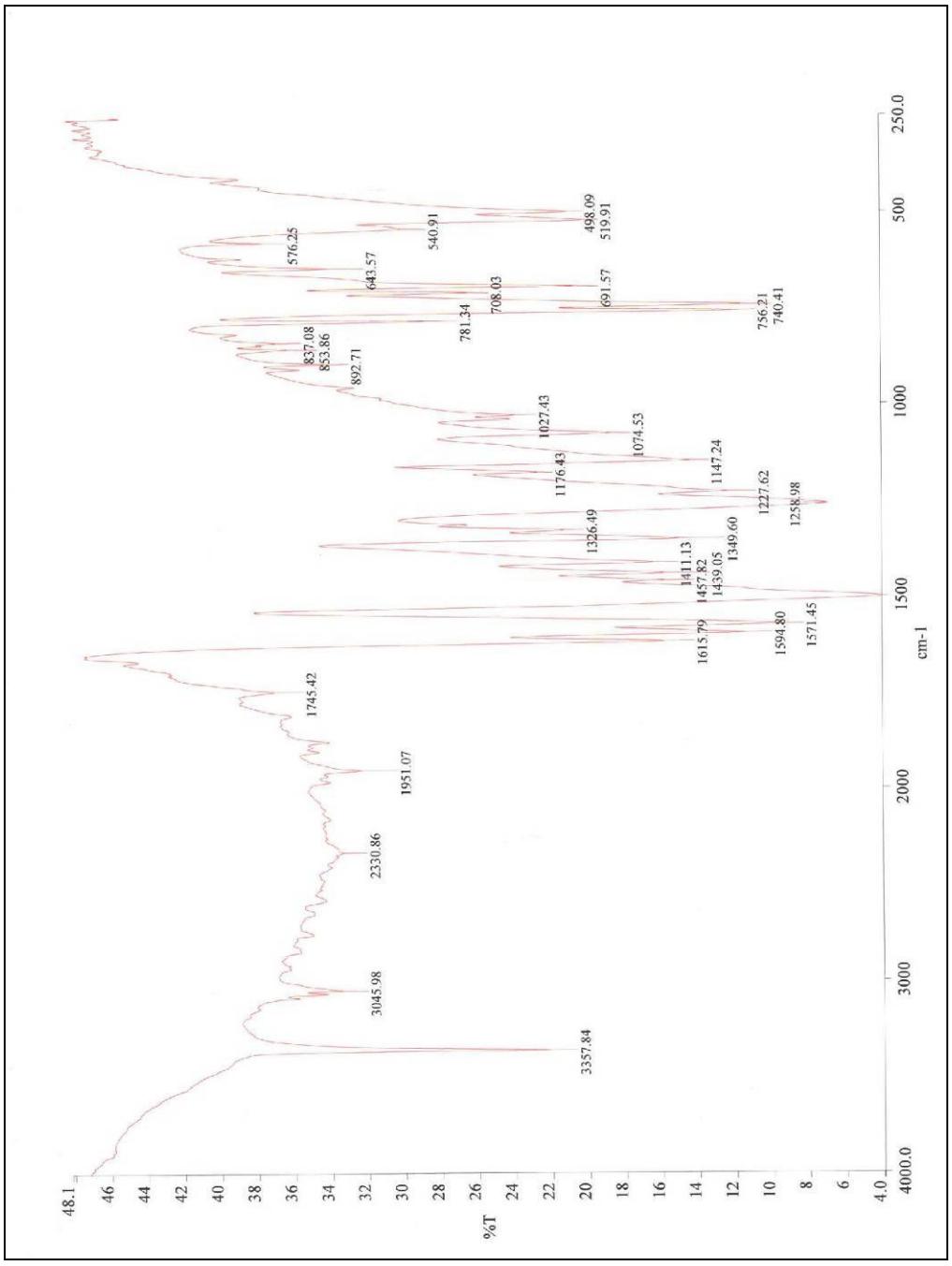

Figure A.61 FTIR Plot of 2-NDPA

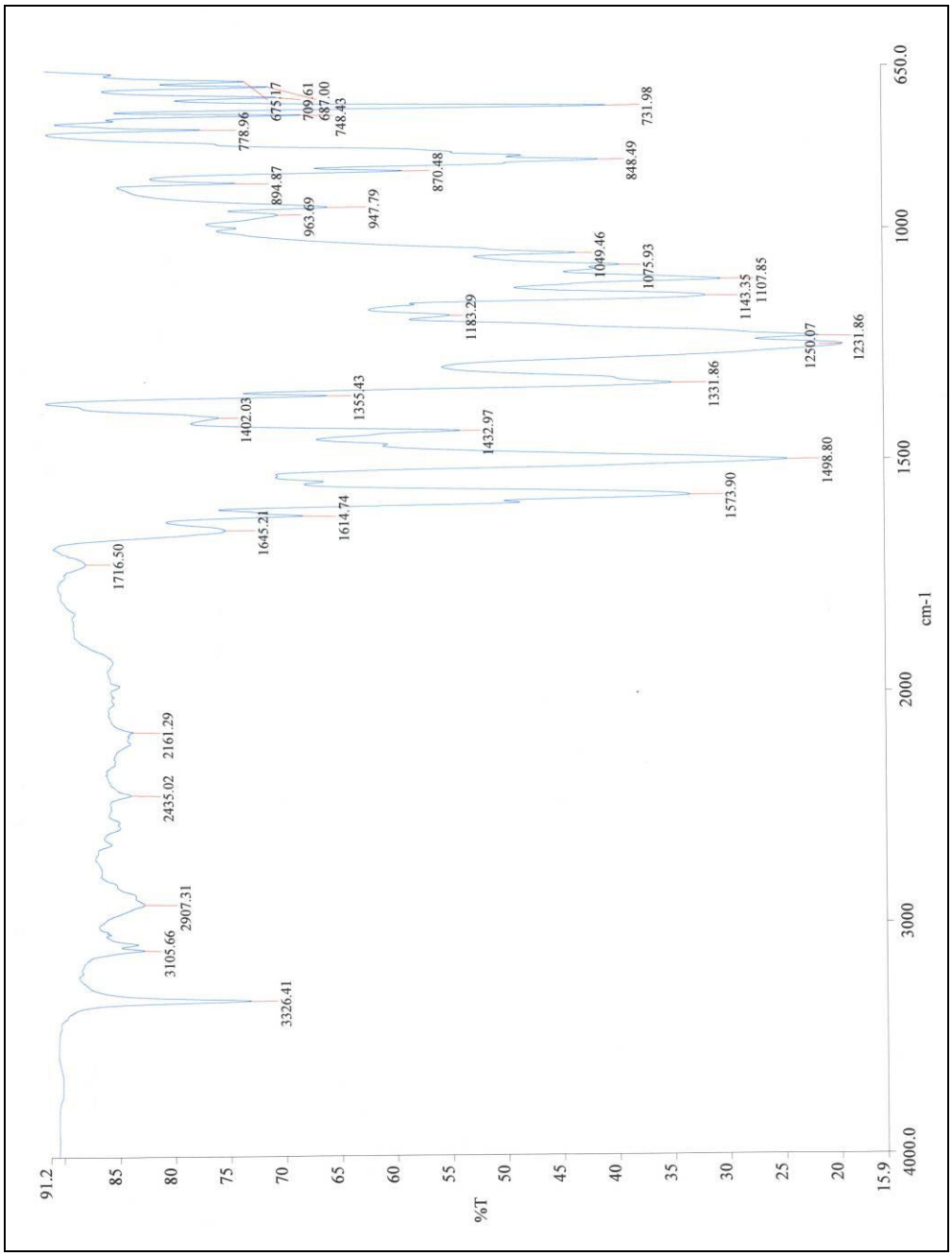

Figure A.62 FTIR Plot of Migrated Unknown Substance/s